EXPERIMENTAL INVESTIGATIONS OF PROPERTIES OF MAGNETOACTIVE POLYMERS

A Thesis

by

JAYADURGA IYER GANAPATHI

Submitted to the Office of Graduate Studies of
Texas A&M University
in partial fulfillment of the requirements for the degree of

MASTER OF SCIENCE

December 2010

Major Subject: Mechanical Engineering

EXPERIMENTAL INVESTIGATIONS OF PROPERTIES OF MAGNETOACTIVE POLYMERS

A Thesis

by

JAYADURGA IYER GANAPATHI

Submitted to the Office of Graduate Studies of
Texas A&M University
in partial fulfillment of the requirements for the degree of

MASTER OF SCIENCE

Approved by:

Chair of Committee,	Arun Srinivasa
Committee Members,	Terry Creasy
	Ramesh Talreja
Head of Department,	Dennis O'Neal

December 2010

Major Subject: Mechanical Engineering

ABSTRACT

Experimental Investigations of Properties of Magnetoactive Polymers. (December 2010)

Jayadurga Iyer Ganapathi,

B. Tech, Anna University

Chair of Advisory Committee: Dr. Arun Srinivasa

Dynamic responses of the MR Elastomers and MR gel have been studied carefully by various research groups. However, to understand completely the dynamic response of the material, it is important to have a clear understanding of quasi-static response of the material. Thus, for the current work, we have studied quasi-static response of the MR gel. For current setup, 27 samples were prepared using Septon, plasticizer and magnetic particles and were tested for 3 rounds over 3 different magnetic fields under plane strain compression. The results from plane strain compression show linear increase in the load taken with the increase in concentration of magnetic particles in absence of any magnetic field. The response characteristics under uniform magnetic field showed a huge leap in the load taken for particular deflection. To study the quasistatic respose, the material is assumed to behave like an isotropic hyperelastic response. Field dependent Neo-Hookean and field dependent Valanis Landel models have been fit to the data, and it was found that simple 1-term field dependent Valanis Landel model with power law coefficient as four agrees well with the shear modulus obtained from experiments. The shear modulus of MAP from the Valanis Landel and Neo Hookean model was assumed to be linearly dependent on the concentration of magnetic particles and magnetic field, and this matched the experimental data well.

To family, friends, teachers and The Almighty

ACKNOWLEDGMENTS

I would like to thank my advisor, Dr. Arun Srinivasa for guiding me patiently through this work and making me understand core concepts. I would thank him for his valuable advice and logical solutions for each my research issues and for understanding me through my tough times and being very co-operative. In short, I am grateful to him for helping me walk through this big learning curve of a Master's degree.I would like to thank my committee members, Dr. Terry Creasy, for being cooperative and extending his lab facilities to me and solving several machine related issues, and Dr. Ramesh Talreja, for his advice during the coursework on doing experiments and handling common issues during experiments.

I am grateful to my husband, parents and sister, for constantly motivating me throughout the process and for handling all other personal issues of mine thus enabling me to focus on my thesis work. I would like to thank my roommates and friends for maintaining a conducive environment. I would like to thank my research colleagues for healthy discussions on my research problems, concepts, good ideas, practical help in testing, capturing pictures and using Matlab. I wish to thank all the other people who have helped me. I extend my thanks to the Workshop Staff for giving useful tips for machining and for helping me machine my molds and fixtures. I thank my colleagues and my employer, at my part time work place, the College of Architecture, for handling situations at work for me during my absences and thanks to other friends who have helped me indirectly to be here. I thank The Almighty for everything!

TABLE OF CONTENTS

CHAPTER Page

LIST OF TABLES

LIST OF FIGURES

FIGURE Page

FIGURE Page

FIGURE Page

FIGURE Page

FIGURE Page

FIGURE Page

FIGURE Page

CHAPTER I

INTRODUCTION

Several class of polymers as elastomers, thermoplastics, thermosets, polymeric gels have been invented and studied carefully and hence have been put in to use for many applications. Elastomers in particular, have been used in many automobile applications such as mounts [1], seals [2], bushings [3] and many more applications [4]. They are primarily used to dampen noise [5], [6], [7], isolating vibrations [8], control structural compliance [9] in many of the applications. Recently, the ability to modify the properties of the polymers in response to external stimuli has opened new opportunities for applications of polymers. Thus, in the recent years, smart polymers such as thermo-responsive shape memory polymers, light active smart polymers, electroactive polymers [10], Magnetorheological (MR) fluids [11] and Magnetorheological elastomers, ionic gels [12] have become fields of major interest for researchers. The purpose of this study is to experimentally investigate the quasistatic response of one such "Smart Polymer"-a magnetic gel.

A. Overview of Smart Polymers

Many polymers have been invented that respond to several external stimuli as in temperature, light, electric field, magnetic field, several ions, pH [12]. In order to set the stage for the discussion of magnetic gels, we will first describe some well known smart polymers.

The journal model is *IEEE Transactions on Automatic Control.*

1. Thermo-responsive Smart Polymers

Shape Memory Polymers are a subclass of smart polymers that when deformed at a high temperature, have the ability to retain their deformed shape when cooled and then subsequently regain their shape when heated. The temperature at which most shape memory polymers are stimulated are around their glass transition temperature T_g. Above T_g, these polymers move from glassy(physically hard) to rubbery state(physically soft). Above the T_g, the polymers are rubbery in nature and hence soft and have a lower elastic modulus in comparison to its glassy state elastic modulus. These polymers show high deformation, low cost, low density, and potential biocompatibility and biodegradability and hence can be used for a wide variety of applications. Their applications mainly focused on temperature sensors, actuators and in medical areas, such as biodegradable sutures, actuators, catheters, and smart stents [12], [13], [14].

2. Light Active Smart Polymers

This class of smart polymers has the ability to change their shape in response to light or irradiation of a particular wavelength. These polymers require no temperature changes. Two strategies to introduce light sensitivity in polymers at the molecular level are to graft the polymers with photosensitive moieties or interpenetrating the permanent polymer network with olegomeric molecules having several photosensitive moieties reversibly forming a polymer network [12]. When photosensitive moities like azobenzene groups are linked to macromolecules, the interconversion between the two photoisomers can induce macroscopic changes in the polymeric material. When these azobenzene moieties are introduced in liquid crystalline elastomers, cis-trans isomerization triggers phase transition in the liquid crystalline elastomers reducing

the alignment order in them [15]. On the other hand, the introduction of photo reversible functional groups enables to achieve shape memory effect with light as an external stimulus. The common grafting photosensitive moieties are cinnamic acid or cinnamyliden acetic acid. These functional groups form covalent bonds with each other upon irradiation of suitable wavelength. When irradiated with different wavelength, the bonds are cleaved. During irradiation, cations are generated and back-reaction of these cations with anions occurs thermally in the dark. When these derivatives are introduced into polymers or gels and exposed to irradiation, they result in photo-generated charges and hence this variation leads to electrostatic repulsion and hence expansion and shrinkage [16].

3. Electroactive Smart Polymers

Electroactive polymers (EAPs) were developed as an attempt to make smart polymers to be used for actuation and vibration control in response to external electric stimuli. Several types of EAPs have been developed such as field-activated EAPs and Ionic EAPs [17]. Field-activated are driven by the Coulomb interaction (electrostatic force) produced by an electric field created between the coating electrodes on films or by charge on a local scale. Strain manifested from molecular, microscopic, or macroscopic phenomena, respond to an applied electric field. The applied electric field induces a molecular conformation change as the dipoles of the polymer molecules aligns with the field. Examples of this type of polymers include Ferroelectric polymers (PVDF), Dielectric EAPs (Silicone, Polyurethane)and Electrostrictive graft polymers (Modified co-polymer of PVDF) [17].

Ionic EAPs involves drifting or diffusion of ions i.e., application of voltage, either cause ions to move in or out of the gel or cations to move through the channel provided by the ions. Examples include Ionic gels (Polyvinyl alcohol) and Ionomeric polymer

composites (base ionomers) [17]. Electroactive Polymers have been successful for actuation applications. The underlying principle of operation [18] of dielectric EAP Actuators is that the polymer is sandwiched between two electrodes and voltage is applied to the setup. The voltage difference causes the polymer to compress and hence increase in area, as most elastomers are assumed to be incompressible. Thus the two modes of actuation makes it better compared to conventional electrostatic air gap actuators.

However, these polymers would require that the applied fields were in the order of kV/mm (typically of the order of 0-3 kV/mm to change shear stiffness of 20N/mm)to produce significant change in the response [17], [18], [19].

4. Magnetoactive Smart Polymers

Magnetoactive polymers (MAPs) have been developed in recent years motivated by magnetorheological fluids and electroactive elastomers, as a solution to the high voltage requirement problems of EAPs for applications. Magnetoactive polymers can be classified as either magnetoactive elastomers and magnetoactive gels. Magnetoactive elastomers comprise of magnetizable particles distributed in the elastomer matrix. Isotropic and Anisotropic Magnetoactive elastomers have also been developed and studied [20], [21], [22], [23]. Magnetoactive polymeric gel consists of magnetic particles dispersed in a continuous medium of swollen polymer network. In the gel, the magnetic particles are attached to the network by adhesive forces resulting in direct relation between magnetic and mechanical response of the polymeric gel. Magnetoactive polymers show large strain and very quick response[23], [24], [25], [26],[27], [28]. The ability for us to mold them to different shapes allows it to be used for wide range of applications. It has been used for industrial applications like vibration dampers, bushings, magnetic tapes, actuators, suspension devices and also for biomedical ap-

plications like soft actuators, artificial muscles, drug delivery system[23].

a. Magnetorheological Elastomers

Lokander and Stenberg [20] developed isotropic Magnetorheological elastomers. They used nitrile rubber, and other additives required for mixing and molding rubber. The iron particles were mixed into the rubber together with the vulcanization system in a Brabender mixer. All materials were vulcanized at 150°C for 30 min under a pressure of approximately 12 MPa. They prepared samples with both large irregularly shaped iron particles and carbonyl iron particles separately. They measured the dynamic shear modulus using Instron 8032 dynamic testing machine equipped with an electromagnet using a double lap shear specimen. The rubber segments were approximately $20 \times 15 \times 2$ mm, and sandwiched between brass plates. The rubber was fixed to the brass plates by a cyanoacrylate adhesive. They tested samples with 28% volume percentage of iron particles under 0T and 0.24T using the electromagnet. They also conducted density measurements, tensile strength and viscosity measurements. They found that the adhesive used influences the modulus of the samples largely at 0T measurements. Also they found large irregular iron particles used, showed greater MR Effect than carbonyl iron particles and in the similar manor they found that badly dispersed carbonyl iron particles that formed aggregates showed similar MR Effect as those of large irregularly dispersed iron particles. They found that the MR effect or tensile strength or strain at break increased and after a particular value of iron content, say 30% by volume of iron particles for their samples, that these properties started to deteriorate. They explained this behavior by a concept of Critical Particle Volume Concentration of iron content. Also they found that the rheological properties of the matrix material do not influence the MR effect.

Anisotropic Elastomers have been developed by Ginder et al. [21]. The MR

Elastomer was made of cis-polyisoprene or natural rubber. Natural rubber along with additives, crosslinking agents, plasticizers and 27% by volume of magnetizable particles such as carbonyl iron particles of 0.5 to 5 microns in size, were mixed in a conventional two roll mill and then molded into compression discs and cured at temperatures of 150 degree C in presence of magnetic field of flux density 0.5T. This resulted in particle alignment thus resulting in anisotropy. A double lap shear fixture was made and attached to a conventional servohydraulic testing machine. The storage modulus and loss modulus of the MR Elastomer specimens were measured as a function of strain amplitude and frequency. Magnetic Flux densities of 1.2T were generated by a C-frame electromagnet, which was driven with an operational amplifier. A sense coil was sparsely wound around the circumference of the sample. A fluxmeter was used to determine the average flux density from the voltage induced in the coil. The static magnetic properties of the samples were measured using a simple magnetic-induction based technique. The sample was held in one pair of identical but counter wound wire coils; the other coil is empty. The coils were then placed in the gap of the electromagnet and the applied field H was measured by Hall Effect Gaussmeter. The voltage generated in the coils when the field was applied was integrated and a signal proportional to the sample magnetization was obtained. Shear stress and shear strain loops were measured and it was shown there was a dramatic change in the stiffness of the material in presence of Magnetic field. It was also shown that these material generated significant magnetic stresses at a fixed strain and thus this type of smart elastomers respond to the magnetic field very quickly. They showed that the magnitude of modulus and loss tangent increased by 30% in presence of magnetic field for samples having 40% of volume in presence of 0.9T. They developed and studied a MR Elastomer bushing as a proof of concept of the possible application.

Deng and Gong [22] developed isotropic MR elastomers and further studied the vibration absorption of these MR Elastomers so that they could be used in applications. They also developed anisotropic MR Elastomers using silicone rubber and carbonyl iron particles. The ingredients are mixed in an agitator and then placed in vacuum to remove air from the mixture and then sealed in the aluminum molds and then placed in the magnetic field of 1T for 24hours. They measured shear modulus and loss modulus using a Dynamic mechanical Analyzer at 1.100T at various frequencies. They found that the shear modulus shows an increasing trend with magnetic field intensity. They also state that the slope that was increasing decreased with the increment in magnetic fields beyond certain magnetic field value. They explained this behavior as the magnetic saturation. As a step to study the vibration isolation of the MR Elastomer, they developed an adaptive tuned vibration absorber (ATVA) with a dynamic mass, static mass and smart spring elements of MR Elastomers. They calculated the shift frequency both theoretically and experimentally and found that they agree. It was found that the natural frequency of the system could be varied between 27.5Hz to 40Hz. According to them, an ATVA developed by them proved to work better than conventional tuned vibration damper.

Zrinyi et al., [23], [24], [25] have prepared both isotropic and anisotropic MR Elastomers. They prepared isotropic MR Elastomers using polydimethylsiloxane (PDMS), cross linking agents, catalyst, carbonyl iron and iron oxide as magnetic particles. The magnetic particles varied in size from 2.5 micron to 5 micron and they made samples with magnetic particles concentration varied between 10 to 30%. Both carbonyl iron and iron oxide particles were dispersed in PDMS and then mixed with other ingredients. The solution was transferred into a mould. The cross-linking reaction was carried out at ambient temperature for 4.5 hours. On the other hand anisotropic MR Elastomers were prepared by first mixing the magnetic particles with the polymer, the

cross-linking agent, and the catalyst and then stabilized the system in order to avoid aggregation and sedimentation of the solid particles. The mixture was subjected to 0.400T of uniform magnetic field which oriented the magnetic dipoles and when the particles were spaced closely enough, mutual particle interactions occurred. Then the mixture was crosslinked. According to them, during this process the iron particles arrange themselves in pearl chain form and then this form was locked by crosslinking the polymer. They tested both isotropic and anisotropic MR Elastomers in absence and presence of magnetic field. They showed that isotropic MR Elastomers showed a slight increase of elastic modulus by increasing the magnetic field. On the other hand anisotropic or oriented chains structured MR Elastomers exhibited much larger increase in modulus. This difference was seen at lower magnetic fields however at higher magnetic field this difference in modulus leveled off. It was shown that uniform magnetic field, parallel to particle alignment and perpendicular to deformation showed increase in modulus due to mutual interactions. These interactions grew stronger up to 0.150 T beyond which there was no increase. They concluded that parallel uniform magnetic field intensified the effect of the particle alignment. It was shown that higher concentrations of iron intensified mutual interactions and thus samples showed better mechanical properties.

b. Magnetorheological Gels

Zrinyi et al., [23], [24], [25], [26] made isotropic MR gel using Polyvinyl Alcohol (PVA) with glutardialdehyde (GDA) along with sol of magnetite. Isotropic or homogeneous MR gel was prepared by making a ferrofluid containing magnetite sol particles which in turn was prepared from FeCl2 and FeCl3 in aqueous solution. To counteract the van der Waals attraction and the attractive part of magnetic dipole interactions, colloidal stability was maintained by a small amount of HClO4 which induced peptization.

Then 8 wt% PVA solution and 1M GDA were used as the polymer along with the cross-linker. HCl was the initiator. The concentration of the magnetic particles in the gel was 1.2 wt%. After gelation the samples were kept in distilled water to remove the unreacted monomer. According to Zrinyi et al., in the ferrogel, the finely distributed magnetic particles attach to the flexible polymer network chains by adhesive forces. The solid particles, of colloidal size, serve as the elementary carriers of a magnetic moment. In the absence of an applied field the moments are randomly oriented, and thus the gel has no net magnetization. As soon as an external field is applied, the magnetic moments tend to align with the field to produce a bulk magnetic moment. As the strength of the field increases, all the particles eventually aligned their moments along the direction of the field, and as a result, the magnetization saturates. If the field is turned off, the magnetic dipole moments quickly randomize and thus the bulk magnetization is again reduced to zero. They assumed the magnetization of individual particles in the gel to be equal to the saturation magnetization of a pure ferromagnetic material (M_s), the magnetization of ferrogel (M) in the presence of an applied field can be described by the Langevin function. They used a Neo Hookean model to characterize the elastic response using so that, for the uniaxial compression mode, the nominal stress is given by

$$\sigma = G * (\lambda - \lambda^{-2}) \tag{1.1}$$

where σ is the nominal stress defined as the ratio of the equilibrium elastic force and the undeformed cross sectional area of the sample. The deformation ratio λ is the length, h (in the direction of the force) divided by the corresponding undeformed length, h_0. However, for polymer networks with magnetic particles G, the modulus of the system expressed as function of magnetic particle concentration as follows

$$G = G_0 * (1 + k_E \phi_m) \tag{1.2}$$

Here G_0 is the modulus of the gel without the magnetic particles. k_E is Einstein -Smallwood parameter and $k_E = 2.5$ theoretically for ideal network and ϕ_m represents volume fraction of the magnetic particles in the whole gel. Similarly they have stress-strain relations based on van der Waal's approach as

$$\sigma = G * (\lambda - \lambda^{-2}) * [\frac{1}{1 - \eta^{\frac{1}{2}}} - a^{\frac{1}{2}}] \tag{1.3}$$

$$\phi = \frac{1}{2}(\lambda^2 + \frac{2}{\lambda} - 3) \tag{1.4}$$

$$\eta = \frac{\phi}{\phi_{max}} \tag{1.5}$$

$$\phi_{max} = \frac{1}{2}(\lambda_m^2 + \frac{2}{\lambda_m} - 3) \tag{1.6}$$

where a is assumed to be global interactions between the chains of real network and λ_m represents maximal deformation ratio.

They tested the samples prepared in absence of magnetic field and in presence of magnetic fields. They found that in the absence of magnetic field, the response well matched van der Waal's Equations. In the presence of Magnetic field, they found that they were able to produce 40% strain and at a particular value of steady current used to generate magnetic field, there was an abrupt change in the shape. They explain this shape change theoretically and find that it closely matches the experimental observation which was the focus of their work.

Tony Pearce patented the idea of making elastomeric gels [29]. The patent de-

scribes the process of making a gelatinous elastomeric material, products made using this material. The invention describes in particular making of elastomeric gel using a triblock elastomer(A-B-A) and a plasticizer preferably mineral oil or combination of mineral oil and resin. The author prefers polystyrene - hydrogenated poly(isoprene - butadiene) - polystyrene for the A-B-A triblock co-polymer for the invention. He explains the chemistry behind triblock polymers. Polystyrene end groups are referred to as monoalkenylarene because of the chemical structure. The author says that monoalkenylarene molecules are attracted to each other by hydrophobic attraction, which is weaker than covalent bonding. The mid-block used for triblock copolymer is typically a aliphatic hydrocarbon with conjugated double bonds that provides greater stability to the molecule. Several monomers useful for the invention, like ethylene-butylene, butadiene, ethylene-propylene, isoprene-butadiene were investigated. Each of the mid-block investigated have different chemical structures and hence different physical characteristics. Hence in a chain, these mid-block monomers provide different types of interaction forces(hydrophobic interaction, hydrophilic, polar forces, van der Waals). The interaction of physical characteristics of the mid block plays a role in determining various attributes such as strength, elongation, elasticity, viscoelasticity, softness, tackiness and plasticizer retention. As the author interests were towards such attributes, he preferred (isoprene-butadiene) as his mid-block monomer for his invention.Thus the author believes that the triblock amorphous polymer form a three dimensional structure(due to attraction of end blocks and interaction between midblocks) with few loose ends in the network. The plasticizer improves workability, pliability and other properties based on plasticization theories. According to the author, all four theories of plasticizers (lubricity, gel mechanistic and free volume theory) state that addition of small plasticizer molecules that have greater affinity to the midblock component in comparison to the endblock components are preferred for

his invention. Based on the chemistry of the triblock polymers and plasticizers, the author uses Septon 4055 as the triblock polymer which has midblock polymer made of about 30% isoprene and 30% butadiene. The author uses both only mineral oil or mixture of mineral oil and resin for his invention.He uses paraffinic white mineral oil with a viscosity of 70-500 SUS at $100°F$(under brand name DUOPRIME 90 or TUFFLO) for pure mineral oil plasticizers. For mineral oil mixture as plasticizer he uses 37.5% paraffinic mineral oil with 150 SUS and 62.5% resin (WINGTACK by Goodyea). The author also uses detackifiers, antioxidants, flame retardants, colorants for elastomeric gel with specific requirements. He has made elastomeric gel with plasticizer and elastomer ratio varying between 1.5 : 1 to 25:1. He states that gel with oil: elastomer ratios of 2.5:1 to 8:1 are most preferable for applications.The author has made the elastomeric gel by different methods mainly classified as melt blending and solvent blending. In melt blending manufacturing process, the elastomer, plasticizer and additives are mixed and heated together while agitating the mixture during heating. Then the compound is cooled to get the gel. The author prefers $260°F$ to $290°F$ for ten minutes or lesser. Stirring, agitation, or high shearing forces are preferred to get homogeneous mixture. The author states that either injection molding or extrusion could be used, however the author has used a 35:1 L by D ratio, twin screw extruder. In Solvent blending, plasticier and additives are added to the elastomer dissolved in a solvent and after the process, the solvent is removed. He has also used fomaing method to manufacture the gel. He has made five samples of each type of elastomeric gel and tested them for percentage elongation and tensile strength as per ASTM D412 using a Model QC-II-30XS-B Electronic Tensile tester. Each of the samples were O-shaped rings with an outer diameter od 0.500 inch and inner diameter of 0.375 inch. He also measured percentage oil bleed of three disk shaped samples of material of 3cm diameter and 6.5 mm thickness. It is seen from

the results that the oil:elastomer ratio of 3:1 to 5:1 show greater strength at failure. However with high oil:elastomer ratio like 8:1, the elongation at break properties are improved while the strength at failure decreases. It is also seen that higher viscosity mineral oil gives lesser oil bleed as preferred in applications. It was shown that properties(elongation at break, tensile strength, reduced oil bleed and comparable softness) of the elastomeric gel made with Septon 4055 was improved in comparison to Chen's invention of elastomeric gel [30] using of KRATON G 1651 (an SEBS coploymer). The author believes this from the NMR analysis results that the superior physical properties of SEPTON 4055 is due to the length of the midblock side chains.

Motivated by the MR Elastomers and gel concept for the vibration applications Janarthanan [27] prepared a MR gel at Texas A&M University and studied its magnetic field response characteristics. He used thermoplastic elastomer, Septon (A-B-A triblock polymer, wherein A represents a crystalline polymer such as a polystyrene, monoalkenylarene and B is an elastomeric polymer such as hydrogenated polybutadiene and polyethylene), mineral oil and magnetic particles. He prepared the sample by heating the polymer to preheated oil. At 350° Fahrenheit, polymer melted to blend with the oil and then nearly 28 to 32% of iron particles 30-40 micron in size were added to the mixture and heated. Throughout the process the ingredients were mixed intermittently to get a uniform mixture. When the sample had heated and mixed well, the polymer gel was poured on to the mold of the required shape. He demonstrated few working mechanisms like a peristaltic pump, a diaphragm pumping system. A simple setup to study the response of MAP in pulsating field was made. Using this setup, study was made to measure displacement as a function of material thickness, frequency of input signal and amplitude of input signal. Also a crude lumped parameter model was fit frequency response of MAP. Since it was first of this class of polymer, all the work was done with the intention to prove that MAP could

be prepared using Septon and that the response of the polymer was interesting to further do a careful study.

Motivated by the work of Janarthanan [27], Rao et al., [28] studied the functional behavior of a particular type of magnetorheological gels under dynamic and static shear conditions in the presence of a magnetic field through experimental investigations. They prepared samples using the procedure followed by Janarthanan in his work [27]. They used Septon 8006, mineral oil and carbonyl iron particles of size between 2 to 10 microns for their sample preparation. They made samples without magnetic particles and found the optimum ratio between the polymer and oil has to be 1:4. They prepared samples with various proportions like 10%, 30%, 50%, and 70% by weight of carbonyl iron particles mixed with a constant ratio 1:4 of copolymer to mineral oil gel matrix mass fractions. They maintained 200 Degree C during sample preparation to prevent agglomeration of the particles. The mixture is then cured at room temperature and then cut into small rectangular magnetic gel strips of 20 mm 20 mm 3 mm for use in the mechanical characterization tests. This magnetic gel strip is then sandwiched between two non-magnetizable thin plates and adhesively bonded to them using a cyanoacrylate adhesive. Most of the experiments have been conducted experiments using dynamic mechanical analyzer (DMA) testing machines for identifying the dynamic characteristics of MR elastomers. DMA has been developed with the underlying assumption that material being tested will undergo small linear deformations. The authors state that one of the main drawbacks of using DMA for the elastomers is that, elastomers undergo large nonlinear deformations and it is difficult to get uniform magnetic field with DMA. They assume that material is characterized under static loading conditions by a Neo-Hookean model with a magnetic field dependent shear modulus. The authors believe that with this assumption, the shear stress is directly proportional to the amount of shear even for finite deforma-

tions. Similarly, under dynamical conditions, they assumed that the shear stress is dependent on the shear rate. Thus to study the response of large deformations in presence of magnetic field, a simple free decay apparatus was developed as shown in Fig. 1.

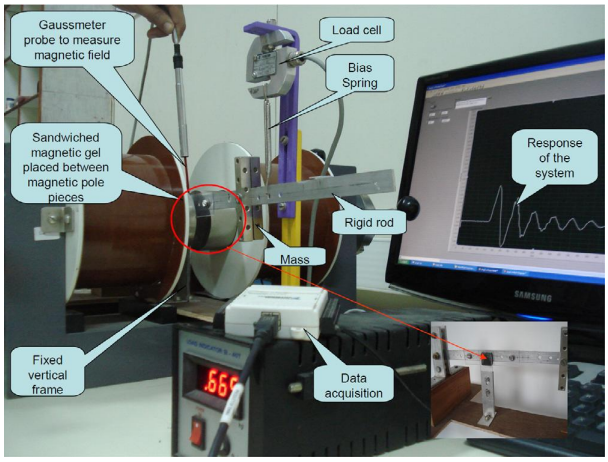

Fig. 1. Magneto-Mechanical Coupled Free Decay Testing Instrument on Magnetic Gel under Shear Mode Oscillation. Included with permission from the authors [28]

They determined the natural frequency and damping ratio of gels using the changes in dynamic properties of an oscillating rod in the system. To do the same, they first measured the dynamic characteristics of the free oscillating rod, without the magnetic gel specimen attached to the rod. The spring and the mass cause the rod starts to oscillate and the response of the system is measured using a load cell. Initial excitation dies down due to air friction and other damping conditions. Then the magnetic gel is placed appropriately in the system that allows a shear mode vibration of the gel sample. After the sample is mounted in equilibrium position, the gel is excited so that the shear oscillations and a fresh response measurement are made on the system. The same test procedure is repeated under various magnetic fields in the range of 0 -0.7 T for different gels prepared. A very simple model involving just two parameters has been developed by them. They found a significant increase in storage

modulus of up to 59%, under the influence of a magnetic field. They more specifically found, an optimal mass fraction of about 50% of the magnetic particles can be used over a range of 0-0.4 T of magnetic field and concluded at that particular magnetic field and concentration to show the best results in vibration control applications. They also found that no significant change in the damping ratio is observed under various magnitudes of the magnetic field. They believed it is an important observation in the context of the application.

B. Hypothesis

From the literature reviewed, it has been clear that dynamic response of the MR Elastomers and MR gel have been studied carefully by various research groups. However, we believe that to completely understand the dynamic response of the material, it is important to have a clear understanding of quasi-static response of the material. Thus we propose to study the quasi-static response of the MR gel. The hypothesis underlying the proposed work is that Magnetic fields can change the quasistatic response characteristics of MR Gels and that this can be measured. This is fundamentally different from the studies such as the ones by Zrinyi et al. [23] - [26] where the change in shape due to a magnetic field gradient was studied. It is generally accepted that, in a uniform magnetic field, there will be no force on the magnetic particles and hence no change in shape [27] however, we hypothesize that properties such as elastic moduli do in fact change in the presence of a magnetic field. While this effect is little understood, we propose to take a first step by quantifying this change if it indeed exists. Specifically, we hypothesize that under uniform magnetic fields, the magnetic gel will behave like an incompressible soft rubbery material whose material parameters such as shear modulus etc are functions of magnetic particle concentration

and applied magnetic field.

C. Objectives of Current Work and Scope

Most applications of polymer in particular elastomers use them in compression mode, primary objective of the current work is to study the quasistatic response of MAP under compression. Both uniaxial and plane strain compression tests give a good insight of the polymer's behavior. However, plane strain compression tests are preferred over uniaxial compression tests for the current work because the focus of the work is to study quasistatic response and not shape changes. Current work thus involves sample preparation and testing the samples. Samples of different concentration are made. Also several batches of a sample concentration. Samples of different geometries mainly rectangular and disc shaped would be made. For current setup, 27 samples were prepared, 3 samples would be tested under uniaxial compression for 3 rounds and 3 samples of disc geometry would be tested under uniaxial compression. 21 samples would be tested for 3 rounds over 3 magnetic fields under plane strain compression. To study the behavior of MAP in presence of magnetic field it is required that appropriate setup for conducting tests in presence of magnetic field is ready. Almost all literature about MR materials uses an electromagnet set up for testing or an electromagnet is integrated with the design of the testing equipment.For the current work, a simpler technique is proposed where large permanent magnets of different known strengths will be used. The principal advantage of such an approach is the ability to study small samples and a guaranteed magnetic field strength. The dimensions of permanent magnets and the sample were chosen such that there would a uniform magnetic field experienced when the sample is placed between the magnets and tested. After the experimental setup is ready and experiments are found to be

repeatable, the effect of concentration of magnetic particles and the effect of magnetic field on the response of the gel would be studied. Effect of magnetic field would be studied by conducting tests on the sample in presence of magnets of various strengths. On successful experimental investigation, the response of MAP would be compared with isotropic rubber like elastic models whose parameters are functions of magnetic field and concentration of magnetic particles. A schematic representation of objective is shown in Fig. 2.

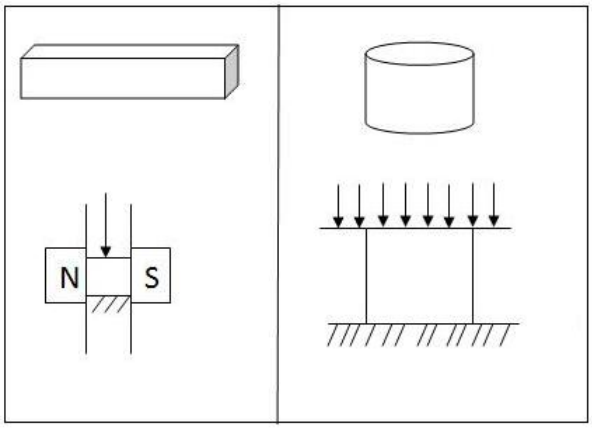

Fig. 2. Schematic Diagram of Objective of Current Work

Most literature has made anisotropic samples, however, current work is restricted to isotropic samples preparation. Current work would focus on quasistatic response and hence studying viscous response of the material out of the scope. This work focuses on characterizing MAP's response under uniform magnetic field. This is a fairly new variety of polymers and it is necessary to study this material under simple test conditions. Introducing non-uniform magnetic field and conducting tests would lead to shape changes in the material. Currently, quantifying the three dimensional shape change would be a challenging task.

CHAPTER II

EXPERIMENTAL INVESTIGATIONS OF MAGNETOACTIVE POLYMERS

Experimental Investigations have been conducted to test the underlying hypothesis that magnetic fields can change the quasistatic response characteristics of MR Gels. Details of material preparation and testing are presented here.

A. Materials

Magnetoactive polymeric gel comprises of a polymer, a plasticizer and magnetic particles.

1. Polymer

The polymer used for the current work is a thermoplastic elastomer copolymer (trade name Septon). Septon is a series of high performance thermoplastic elastomers developed by Kuraray Co. LTD. This polymer has also been used by a few authors mentioned in the literature, [27], [28] to make polymeric gel filled with magnetic particles. All the grades of Septon are well known for their mechanical properties, heat resistance, chemical resistance, low temperature properties, low toxicity, good weatherability. This is a series of triblock polymers of A-B-A type (as shown in Fig. 3) where hydrogenated styrene forms end-block polymer and the mid-block polymer is a thermoplastic elastomer. This thermoplastic elastomer is either b-poly(ethylene/propylene) or b-poly(ethylene/propylene)-b or b-poly(ethylene/butylene)-b or b-poly(ethylene-ethylene/propylene)-b. From the structure point of view, Polystyrene serves as a hard block and the elastomer as a soft block in the co-polymer. Polystyrene blocks function to form a network as they have greater affinity to other polystyrene blocks thus keeping the elastomer network in place. The elastomeric portion has a good

affinity to additives like oil which is a desirable property for the preparation of MAP. Samples for the current work make use of Septon 8006 grade having a structure as Polystyrene-b-poly(ethylene/butylene)-b-polystyrene as shown in Fig. 3

2. Plasticizer

From the literature, plasticizer used for the preparation of polymeric gel is either mineral oil or a mixture of mineral oil with other plasticizers. Mineral oil bonds are believed to be attracted to the mid-block polymer thus allowing sliding between the mid-block polymer relatively easy. Mineral oil being readily available in large quantities at a reasonable price makes it a preferred choice of plasticizer for MAP. Paraffinic white mineral oil, Animed is used for sample preparation in this work.

3. Magnetic Particles

The most widely used magnetic particles are Ferric or Ferrite particles or solution of $FeCl_2$ or water atomized iron particles or carbonyl iron particles. For the current work, both water atomized iron particles and carbonyl iron particles have been used. Atomet Grade 75, Water Atomized Iron particles(WAIP) were procured from Quebec Metal Powders Canada having particles of size 50-70 μm and a purity greater than 99.4% Fe along with trace amounts of C, S, Mn and other elements. Carbonyl Iron Powder(CIP), developed by BASF in 1925, is a thermal decomposition of pentacarbonyl iron. Several grades of CIP are avialable from hard to soft based on the end applications. For the current work, soft CIP grade is used having a particle size varying between 4 to 10 μm with a polycristalline structure. Its purity is about 99.8% Fe content and a low C, N, and O content. This grade is known for its magnetization properties and has been for MR Fluids.

4. Other Possible Additives

Other additives that could be added are antioxidants to improve its weathering and ageing properties. A detackifier could be added if tackiness is not desired.

B. Requirements for Material Preparation

The tools and apparatus required for sample preparation are explained below.

1. Mold

Compression molding is used to prepare consistent geometry samples for the current work. In this technique, the sample is first heated and then poured in an open mold cavity. Then the top plate is pressed against the mold using pressure. The sample is allowed to cool to get the configuration of the mold cavity. The mold for current work is made from aluminum metal blocks with a precision machined cavity of 10mm width samples. A rectangular steel plate with suitable thickness is used for the top plate of compression molding. A picture of the molds is as shown in Fig. 4.

2. Apparatus Required

Apparatus required for the preparation of samples include hot plate, beaker, stirrer, scissor, thermocouple or infra red temperature reader and a scientific weigh scale. Any scientific hot plate that could reach and hold the temperatures in the range of 300 to 400° C is preferred. The hot plate used for current work is a GE Hot Plate with a rated power of 1000 watts. It was chosen for its rapid heating and consistent performance and fully adjustable temperature control. Its solid die-cast heating plate provides an even temperature distribution. A beaker and stirrer for holding and heating the required quantities of the sample uniformly. An infra red temperature

reader is used to check for any anomalies in the temperature reached by the hot plate during the process. A scientific weighing scale is necessary to weigh the samples precisely. Samples are finally trimmed to required dimensions using scissors.

C. Requirements for Material Testing

Instron 5567 electromechanical system was used for material testing in the current setup. This machine has load frames, designed to apply load to the test specimen and a system to record the displacement of the cross-head. The cross-head moves up to apply tensile load and moves down to apply compressive load on the specimen. Setting test parameters, operating the system, collecting and analyzing test data is done through Bluehill, a software program provided by Instron. The machine has a load cell of 5kN. This machine has wedge grips. The Bluehill Software has additional test settings of cyclic loading and unloading. The system has provision to conduct both load controlled or displacement controlled tests. Compression fixtures made mainly has a top and a bottom platen using polycarbonate thick sheets. Each of the platen has a flat surface for compressing the specimen and an extruded portion that would enable it to be attached to the grips of Instron(as shown in Fig. 5) The dimensions of the platen are fixed to ensure that a homogeneous deformation of the specimen could be maintained and maximum width of the extrusion is matched to that of the grips of Instron. Plane Strain condition is achieved in the current experimental setup by placing two plates to the sides of the bottom platen(as shown in Fig. 6). The dimensions of the width of the platen are fixed based on the magnetic domain distance of the magnets to be used for testing. Two thin plates are attached to both sides of the bottom platen by bolt and nuts. To prevent the cantilever bending, two holes are drilled on the top corners of the thin plates and then would be loosely bolt.

Plane strain compression fixtures were machined from aluminum blocks, to ensure that platens do not interfere or get affected by magnetic field.

1. Magnets

Permanent magnets are used to produce magnetic field. Several neodymium, ceramic and aluminum magnets, purchased from Master Magnetic Inc. of different geometries. A Gaussmeter was used to measure the magnetic field between the pair of magnets held at outer sides of two plates. Neodymium magnets(NB50502N) of dimensions 2" × 0.5" × .5". Ceramic magnets(CB702NMAG) of dimensions 2" × 1" × 0.5".

2. Other Instruments

Other Instruments that would be required during the course of work are a vernier caliper, scale, markers, mechanical tools.

D. Material Preparation

Process used to prepare the sample has been referred as melt blending by one of the authors in the literature [29]. Current work is aimed at making the sample using a simpler technique. The process initially followed to make samples was the same as followed by Janarathanan[27]. In this process, the polymer, mineral oil and magnetic particles are weighed using a scientific digital scale. The convention used in the current work expresses the ingredient concentration as percentage by weight ratio of Mineral Oil:Polymer:Magnetic Particles. Polymer and magnetic particles required for the sample preparation are held in sheet of paper. The difference in weight of paper before and after adding polymer gives weight of the polymer taken for sample preparation. Similarly, magnetic particles are taken. For mineral oil, the procedure

followed is the same except for that the weight of oil is measured from the difference in weight of beaker. Initially all the procedure of sample preparation was done using water atomized iron particles. Then the beaker with the mineral oil is heated for 4-5 minutes and the polymer is then added to the heated oil. Once the polymer melts and forms a clear viscous liquid, iron particles are added to the melt. That is why it is appropriately referred as melt blending. The hot mixture is then poured on to the molds fabricated and the top plate is pressed against the mixture in the bottom mold. This gives the sample the required shape.

Repeatability is an important aspect of performing experiments. Hence for every sample concentration, three batches were prepared. Initially the concentrations chosen to work were varied with both Septon and magnetic particle proportion. Few samples with different proportions of Oil, Septon and WAIP were tried to establish proof of concept. The proportions that were successfully made in initial attempts are summarized in table I.

A sample is said to be repeatable if the sample of a particular concentration and different batches of same concentration, shows same response characteristics under similar testing conditions. In other words, a specimen should take the same load each time it is deformed to a fixed value. However,with the initial samples of concentrations as listed in Table II, a larger spread was found in the response.

Then the preparation steps were repeated with increased time and low heat settings with the underlying assumption that sufficient time is required to heat the mixture uniformly. To understand the cause for problem, the microstructure was observed under an optical microscope. It was noticed that most of the specimens had bubbles and few portions of unmelted polymer as shown in the Fig. 8.

A closer look at the samples through the microscope helped in identifying the likely solution to the problem of large spread in the data. Metallic particles were cold

due to which islands were formed. To rectify this, we decided to heat the powder with the fluid before adding. Henceforth, it was decided that samples require better mixing and uniform heating which was achieved by adding the magnetic particles prior to addition of polymer.Also it has been followed that a low heat setting of the hot plate would be maintained during the entire mixing process till the polymer melts to form a viscous liquid. From the literature reviewed, it had been seen that most research groups have used carbonyl iron particles as the magnetic particles. Thus carbonyl iron particles(CIP) purchased from BASF was used to make samples. An attempt to study the effect of size of iron particles on the response of MAP has been done by comparing the response characteristics of MAP with WAIP and CIP. Proportions that were made with CIP as magnetic particles for MAP are listed in Table III. The procedure for MAP Sample preparation can be summarized as below:-

- Required quantities of Polymer, Mineral oil and Magnetic particles are precisely measured and kept ready prior to the preparation. All other required apparatus are kept clean and ready to use.

- Oil is preheated for 4-5 minutes in the beaker on the hotplate at medium heat. At this stage the temperature of the hotplate rapidly increases from room temperature to 60 to 80°C.

- Now the magnetic particles are added to the heated oil and stirred well. This takes about 2-3 minutes and the temperature of the hot plate continues to rapidly increases to 130-150°C.

- When the magnetic particles have mixed well with the oil, polymer is added to the mixture. Polymer, an inhomogeneous white powder tries to absorb all the oil. During this process the temperature of the hot plate raises from 150 °C to

nearly 240-260°C.

- At this stage, reduce the heat setting to low heat and continue stirring the mixture.The polymer being mixed forms a highly viscous solid. Thorough mixing is done to ensure that the polymer does not agglomerate. The temperature of the hot plate reduces to approximately 150°C. This is continued, till the polymer begins to melt to form a viscous liquid.

- The polymer is mixed well to form a homogeneous viscous liquid and then is ready to be poured to the mold. In many cases, when the proportion of magnetic particles is more, then the polymer melts to form a viscous gel which is then taken with the stirrer and dropped in the mold.

- The top plate of the mold is pressed against the gel and allowed to cool. After cooling, excess polymer is trimmed to the required dimensions.

- As it is difficult to visually classify MAP samples into their concentration, it is a good practice to label the samples prepared soon after the preparation to avoid confusion at a later point of time.

- It is to be noted that even after careful preparation of the sample, there are some surface irregularities or defects introduced. Examples include incomplete mold filling, trimming.

E. Material Testing

MAP Samples prepared were tested using Instron 5567. Required dimensions for the specimens are attributed to the molding process. Two modes of testing were done viz uniaxial compression and plane strain compression.

1. Compression Testing Procedure

Compression test procedure aims to determine compression stiffness of the material. Two types of uniaxial compression tests are possible using Instron. One is load controlled and other is the displacement controlled test. Displacement controlled tests have been conducted for the current work. The set of steps to be followed to conduct the test are listed below

- Test specimens are molded and cut to the required length using scissors. Test specimens of approximately $25mm \times 10mm \times 6mm$ were used. These dimensions are fixed by plane strain compression test to be conducted on the same specimen.
- The test is conducted at normal atmospheric conditions.
- The compression fixtures are attached to the grips of Instron. Care is taken that the platens are flat and there is no inclination to the platens and that the platens do not touch each other resulting in impact loading and machine to fail as shown in Fig. 9
- The dimensions of the specimen are measured using a vernier caliper.
- Tweezers are used to hold the specimens owing to their dimensions and place them within the boundaries of the marking. The buttons on the control panel of the machine are used to move the crosshead up or down. Using the buttons, the top platen is brought to touch the top surface of the sample without compressing it.
- Using the provided software(Bluehill Inc.) inputs are fed to the system.
  - Compression Test Profiler is used as the test profile. SI units are used for recording and calculations.

- Then a brief description of the sample is fed to software so that it is convenient to recognize the data looking at the load versus deflection plot. The details like the sample number, batch number, timestamp, composition, ratio, dimensions of that particular specimen, loading rate and test description.
- One of the most important step in testing o feed the control parameters. At this step, the exact profile of the test is given. One of the suitable test profile amongst Absolute Ramp, Relative Ramp, Triangle and Hold is selected. It is to be noted that, Triangle profile could be used for tests have loading followed by unloading to be done. Hold profile is used for stress relaxation kind of tests. Absolute Ramp is used to move the crosshead by feeding absolute displacement values. Then, the type of test as either load controlled or displacement controlled is specified. For the current work, displacement controlled test is specified. Then the end point for displacement, strain rate, number of cycles are given for both the loading and unloading. The end condition to stop the test in case the test does not work fine is also given. For current work, absolute ramp profile is chosen and end point is specified as 3mm for compression during loading and 0mm for compression during unloading is specified. To study the quasistatic response, the strain rate is kept very low. The strain rate indicates the rate at which the crosshead moves to compress or unload as is given as 1mm/min (strain rate of approximately 0.00277 s^{-1}) for current work.
- Parameter for graph plotted during testing can be given. For the current work, compressive load vs compression is chosen to be plotted and stored as .pdf format. Then results are exported in .RAW format (or comma

separated txt/csv file).

2. Plane Strain Compression Procedure

Plane strain compression (or pure shear) tests are preferred to uniaxial compression since the width of the specimen through which the magnetic field flows can be controlled so that there is no influence of the lateral spreading of the sample on the magnetic flux. It is thus decided that plane strain compression tests would be conducted to study the quasistatic response in absence and presence of magnetic field.

Plane Strain fixtures were fabricated using aluminum blocks as show in Fig. 10. It mainly has a bottom(part A as shown in Fig 10) and top platen (part B as shown in Fig 10) of width 10mm and plates (part C as showin Fig. 10) attached to two ends of bottom platen to constrain the deformation of the specimen in that direction. The procedure followed is similar to uniaxial compression. The two platens are attached to the grips with their surfaces parallel to each other. This is ensured by marking parallel lines on the platens to be attached to the grips of Instron machine. Grease or oil is applied to the sides of the top platen and inner faces of the two plates to eliminate dry friction and to prevent the polymer from sticking to the confining aluminum sheets. The separation between the two inner sides of top and bottom platen is maintained as 8mm. The crosshead would now move by 6mm during loading and move back to 0mm during unloading. All other parameters are prescribed exactly as the compression test. Since the separation between the two side plates is just around 10mm, tweezers are used to handle the specimen. To place the specimen at exactly same position as any other specimen being tested, the specimen is pushed in by a known distance of 30 mm using a wooden stick.

3. Plane Strain Compression with Magnetic Field

One of the primary objective of the current work is to study the quasistatic response of this polymer in presence of magnetic field. Magnetic field was introduced by the permanent magnets. Two permanent magnets of same dimensions were held apart(part E shown in Fig. 11) on the plates. It is expected that there would be some magnetic flux leakage and entire magnetic flux would not flow through the specimen being tested. A circuit analogy (Refer Appendix A) is used for the current work to channel magnetic field lines through the sample and to understand the behavior of the sample under uniform magnetic field. Details about this is found in . To avoid flux leakage and channel the magnetic field lines through the specimen, the magnetic circuit loop should be closed. To do this steel plates are attached to magnets by magnetic attractive force. These two parallel steel plates are interconnected by another steel plate by magnetic attraction. This channels the magnetic lines through the specimen as shown in Fig. 12. The test is conducted as explained in uniaxial compression.

The current work is aimed at making MAP samples and studying its quasi-static response. For the final results to be reliable it is necessary that the results obtained are reproducible. To achieve this condition, it is necessary to make repeatable samples and repeatable test results for a sample and sample concentration. Initial samples showed greater spread in the response. It was thought that the specimens tested had undergone nonhomogeneous deformation. So to ensure tests result into homogeneous deformation a thin layer of oil was applied to the top and bottom surface of the specimen. It was always seen that the surface of the samples tested were highly uneven. Surface evenness could be achieved, if the samples were prepared well in the mold or cut evenly with a blade. However it is believed that surface irregularities

would not affect the result to a great extent. Another major reason that was thought to be cause of increased spread in the response, was the geometry of the sample. So disc shaped samples were made and tested under uniaxial compression. Results were compared with uniaxial compression test results of rectangular shaped samples. It was found that geometry did not have a major effect on the specimen. The specimens used in the current work are soft and have surface irregularities on one side and thus it was not possible to touch and start the test at the same point of the specimen each time. This was carefully removed by maintaining a fixed distance between the platens which is feasible. Thus an invariance in the test could be attained to study the variance in the material.

4. Limitation of Experimental Setup

Tests were conducted with a non magnetic sample but with the magnets attached to study the effects of the presence of the magnets on the frictional response. It was observed that up to a strain of about 40% there was little effect of the presence of the magnet. Above 40 strain, it was observed that there seemed to be a strong effect of the magents on the frictional response. These tests enabled us to verify that (1) upot 40% strain, the presence of the magnets and the force of attaction between the poles of the magnet did not substantially affect the response of the material, above 40% strain the results of the test are unreliable since the friction has a large effect.

After ensuring that repeatability to an acceptable limit, tests were run to study the effect of concentration and magnetic field. Each test was repeated three times to remove any unaccounted effects.

CHAPTER III

RESULTS AND DISCUSSIONS

Experiments have been done following the procedures described in the previous chapter. In order to verify the underlying hypothesis of the current work, several tests as summarized in the table have been conducted. The covention used in the current work is specimens of particular concentration, referred as **SampleNo** like S24, S26 S29, S30 and S31. The details of the concentration is given in Table II and Table III. Batches refer to making the sample of a particular concentration at different time and are referred as B1, B2, B3 or BA, BB, BC and so on in the order in which they were prepared. Typically a specimen is referred with a Sample Number and a Batch Number, for example S26 B2, S26 B3 and so on. For current setup, 27 samples were tested, 21 of them tested for 3 rounds over 3 magnetic fields under plane strain compression. 3 samples were tested under uniaxial compression for 3 rounds and 3 samples of disc geometry were tested under uniaxial compression. Summary of the experiments done are listed in Table IV.

A. Data Processing

The data from the tests are recorded in .RAW format (or comma separated txt/csv file). In order to process the data and plot graphs it is necessary to retrieve data from the .RAW files. For the current work, data has been exported to a spreadsheet and after calculating values from the data, it is processed using Matlab and plotted using Tecplot software.

Data is processed using following steps :-

- Instron records Time Step, Extension, Load, calculated Compressive Load, cal-

culated Compression,calculated True Stress, calculated True Strain and many other values. However, only Time step, Extension and Load will be used from the .RAW data. Data in columnar format can be seen by exporting .RAW data to a spreadsheet.

- Additional rows and columns other than Time step, Extension and Load are deleted. The Actual Load, Stress and Strain calculations are to be done using this raw data.

- As mentioned in the previous chapter, the samples prepared have surface irregularities. Following the decision to maintain a fixed separation distance between inner sides of the platen, the dept or thickness of the specimen will be calculated from the data recorded.For plane strain compression test runs, the samples thickness varied between 6 to 7 mm, the separation distance between the inner side of the platen was maintained to be 8 mm. Actual Depth or thickness = 8 - (Value of Compression where Loading begins).

- The load values recorded by the system are influenced by static friction and device noise until the top platen displaces to touch the top surface of the sample. The load value due to static friction is reached within 10 timesteps. This load value is then seen to oscillate due to noise in the system. From Instron machine specifications and careful study of data recorded, it is seen that this load value oscillates between 0.01N to maximum of 1N(Friction also being responsible for additional noise). Thus, the process followed for current work to select the point from where loading begins is as follows

  - The time step corresponding to last appearance of the significant(mantissa) load value due to the friction load along with noise, during loading is taken.

  - The load value of the next timestep is chosen as the starting point of loading for that particular test data.
  - Actual Load value for that data set is calculated as Actual Load = Load - Load due to friction and noise i.e. $ActualLoad = CurrentLoad - StartingPointLoad$.

- Stress is calculated as $Stress = Load/Area$. The length and width dimensions of the specimen measured using vernier caliper are used for cross section area calculations. The Load here refers to Actual Load calculated in the previous step.

- Strain is calculated as $Strain = \frac{(Extension - StartingPointExtension)}{(8 - StartingPointCompression)}$. StartingPointExtension refers to extension value corresponding to starting point load. StartingPointCompression is the negative value of starting point compression. For the denominator, negative value of extension is used because it is being subtracted from an absolute value of 8.

- Once stress strain calculations are done, the sheet is saved and the stress strain values are copied to another sheet where all such stress strain values are consolidated. Furthermore, the mean of each round of stress and strain for a batch is calculated and averaged response of all batches for a particular sample concentration.

- When all the excel sheets are consolidated, the data is exported to Matlab for further comparison and calculation standard deviation and then exported to text file as vectors that are tab separated. This processed vector information is plotted using TecPlot. All the figures plotting raw data are shown in Appendix F

B. Repeatability

Repeatability of experiments or reproducibility of results is a key aspect in an experimental investigation. This section discusses, efforts taken to lower spread in the response of the material tested under compression are stated.

1. Effect of Specimen Geometry

Several parameters were believed to be the cause for the large spread in the data initially recorded. One of them was geometry of the specimen. It was thought that the rectangular specimens were small to introduce dimensional effect issue leading to repeatability problem. This as verified by making larger disc shaped samples and testing them. It was found that geometry did not have an influence. This is because the effect of sample dimensions are taken care while calculating stress and strain. This can be seen in Fig. 13. The key factor that helped to get reproducible responses that the starting point of the test should be kept fixed. This is done by maintaining a fixed distance between the platens.

2. Influence of Test Setup

It was found that careful preparation of the samples gave lesser deviation from the average value. This is shown in the Fig. 14. The plot part (a) shows the comparison of stress versus strain for different batches for different rounds of test in uniaxial compression mode. Plot part (b) shows Mean stress strain plot of different rounds of the same test performed on the same specimen. It is seen that different batches of the same concentration of MAP show repeatability under both uniaxial and plane strain compression mode. It is seen from Fig. 15 that responses of the samples with same concentration of magnetic iron particles, show greater uniformity in uniaxial

compression mode when compared to its response under plane strain compression. This is seen because of the limitation of plane strain compression setup, mainly the lateral surface constraints, as discussed. This is clearly seen in plot part c.

3. Effect of Size of Magnetic Particles

It is known that size of iron particles would influence the response of MAP under compression. However, this belief had to be verified and it was necessary to quantify the difference. Hence,batches of samples with same concentration of iron particles but different sized iron particles were tested. The size of the iron particles of WAIP are between 50 to 70 microns and that of CIP are between 5 to 10 microns. These batches were tested in absence of magnetic field and presence of magnetic field as shown in Fig. 16 and in Fig. 17. From the graphs it is seen that 20% CIP and WAIP response overlap and that of samples with 50% CIP shows slightly higher stress values than samples with 50% of WAIP. Thus it could be said that at 0T there is no significant effect of the size of iron particles at 0T. However, in the presence of a small magnetic field of 0.19T, samples with smaller sized iron particles that is samples with 20% or 50% CIP take greater loads. It is seen that the stress value reached by samples with 50% CIP is 0.07MPa and that reached by 50% WAIP is 0.04 MPa at strain 35% as seen in Fig. 18. This agrees to our belief and all the further experiments would use CIP as its magnetic particles.

C. Effect of Concentration of Magnetic Particles

Experiments to study quasistatic response of MAP samples with different concentrations of magnetic particles have been conducted. Samples with 0%, 5%, 20%, 35% and 50% have been made and tested under different magnetic fields of 0T, 0.19T and

0.47T. For all the samples, proportion of Mineral Oil : Polymer is maintained to be 4:1. The responses of the experiments are shown in Fig. 19. Each of the figure have a two subfigures associated, the first subfigure shows the mean of 3 rounds of each batch of sample that has been tested. The second subfigure represents the mean of mean of all batches and all runs for that particular sample concentration. It is mostly referred as averaged data of the sample, and for all the plots, standard deviation is shown on this averaged data plot.

It is seen that loads taken by the samples increase with the increase in the concentration of magnetic particles as see n in Fig. 20 and Fig. 21. This agrees with with the general understanding that samples with greater magnetic particles would take greater load values.

D. Effect of Magnetic Field

All the specimens have been tested at 3 magnetic fields, 0T,0.19T and 0.47T. The plots obtained from the data are shown in the Fig. 22 to Fig. 26. It is seen that Magnetic field has a significant effect on the stiffness of the material. Each of the figure have a two subfigures associated it. The first subfigure shows the mean of 3 rounds of each batch of sample that has been tested. The second subfigure represents the mean of mean of all batches and all runs for that particular sample concentration. It is mostly referred as averaged data of the sample, and for all the plots, standard deviation is shown on this averaged data plot.

To summarize the effect of concentration and magnetic particles, values of stress taken by the averaged data of each sample at 35% strain is plotted in Fig 27. It is seen that Fig 27 that samples with higher concentration of iron particles take greater load even in absence of magnetic field. In the absence of increase in the stress

undergone by samples with 50% iron particles shows nearly 70% in comparison with samples without magnetic fillers. This response characteristic is as expected. The explanation for this effect lies in the fact that iron has greater strength and greater the iron particle content, greater would be the load withstanding capacity of the MAP gel. However, an optimum proportion can only be added owing to uniform material preparatio ability. It is seen that a linear trendline fits the plot at 0T, thus giving an idea of the trend in increase with concentration. It is expected that there would not be greater change in stress taken or load withstanding capacity as the tests were conducted with uniform magnetic field. However, the response obtained during the experiemental investiagtion shows nearly 250% increase in the stress taken for 35% strain. This amount of increased load withstanding capacity shows that there is significant increase in the stiffness of material. However, the explanation for this phenomenon is still unknown.

From the all the plots shown, standard deviations up to 25 to 30% are seen. However, it is to be noted that the standard deviation is over a small sample seet size. It is seen from Fig. 28, the ratio of standard deviation to mean increases with the increased concentration of iron particles and magnetic field. This increase in standard deviation can be attributed to small sample size, manual preparation of samples. In spite of a standard deviation being around 25-30%, the primary observation of increased load withstanding capacity or increased stiffness still holds good.

From the discussions, above, effort has been made to quantify the response using simple calculations. To quantify the response and make predictions about the material, developing a model would become necessary. For the current work, comparison to existing isotropic elastomer models has been done.

CHAPTER IV

MODEL

A systematic analysis has been done to fit isotropic hyperelastic model to the experimental data based on the assumption that this could be done. From the literature, it is seen that many research groups have used Neo-Hookean model to fit their experimental data. For the current work, we have compared between the parameter values obtained by fitting Neo-Hookean, and the Valanis-Landel model to elucidate to what extent - a Neo-Hookean model wold be sufficient to describe this material, as assumed by other authors.

A. Hyperelastic Models

Considering body B with a reference configuration κ_R being deformed and takes a configuration κ_t at time t. Second order tensors are denoted in upper boldface, vectors by lower boldface. For two vectors, $\mathbf{a}$, $\mathbf{b}$ belonging to $\Re$, their tensor product acting on a vector $\mathbf{c}$ is $(\mathbf{a} \otimes \mathbf{b})\mathbf{c} = (\mathbf{b} \cdot \mathbf{c})\mathbf{a}$ for $\mathbf{c}$ belonging to $\Re$. The inner product is defined as $\mathbf{A} : \mathbf{B} = tr(\mathbf{A}^T\mathbf{B})$. For this body, $\mathbf{F}$, a second order tensor,is used to denote the gradient of deformation, $\mathbf{C} = \mathbf{F}^T\mathbf{F}$ is used to denote right Cauchy Green strain tensor, $\mathbf{B} = \mathbf{F}\mathbf{F}^\mathbf{T}$ is used to denote left Cauchy Green strain tensor. In this relation, $\mathbf{F}^T$ denotes the transpose of $\mathbf{F}$. First Piola Kirchhoff stress or nominal stress, $\mathbf{P}$, represents engineering stress. Cauchy Stress or true stress is denoted using $\mathbf{T}$.

A hyperelastic or Green elastic material is a model for a material that purely elastic and its constitutive relation is characterized by a strain energy density function, W. In other words, a material for which a strain energy function exists and whose stress is derived from this strain energy function is called as Hyperelastic material[31]. For the present model, under uniform magnetic fields, we will assume that the response

of the material is describable solely in terms of an isotropic hyperelastic function $W(\mathbf{F}\mathbf{F}^T, B, c)$ where B is the magnitude of magnetic flux and c is the concentration of the magnetic particles. W can be expressed in terms of invariants $\mathbf{I}_1, \mathbf{I}_2, \mathbf{I}_3$ in the form $W(\mathbf{I}_1, \mathbf{I}_2, \mathbf{I}_3, B, c)$. The invariants in terms of principal stretches $\lambda_1, \lambda_2, \lambda_3$ of $\mathbf{U}$ are given as

$\mathbf{I}_1 = tr(\mathbf{B}) = \lambda_1^2 + \lambda_2^2 + \lambda_3^2$

$\mathbf{I}_2 = \frac{1}{2}((tr(\mathbf{B}))^2 - tr(\mathbf{B}^2)) = (\lambda_1\lambda_2)^2 + (\lambda_2\lambda_3)^2 + (\lambda_3\lambda_1)^2$

$\mathbf{I}_3 = det\mathbf{B} = (\lambda_1\lambda_2\lambda_3)^2$

The principal stretch ratios λ_i can be related to the experimental values of engineering strain for both uniaxial compression and plane strain compression as $\lambda_i = (1 + \epsilon_i)$, where ϵ refers to the strain calculated from the data recorded in the experiments. Stress response in terms of strain energy density is given as

$$\mathbf{P} = \mathbf{F} \cdot \frac{\partial W}{\partial F} \tag{4.1}$$

And Cauchy Stress

$$\mathbf{T} = \frac{1}{det\mathbf{F}} \frac{\partial W}{\partial \mathbf{F}} \cdot \mathbf{F}^T \tag{4.2}$$

Elastomers are generally considered as incompressible material. For incompressible material,

$$det(\mathbf{F}) = \mathbf{I} \tag{4.3}$$

.

The current work uses plane strain compression condition. Thus, the deformation for the current work can be expressed as $\mathbf{x} = \lambda_1\mathbf{X}$, $\mathbf{y} = \lambda_2\mathbf{Y}$, $\mathbf{z} = \mathbf{Z}$, where **x, y, z** belong to deformed configuration at time t and **X, Y, Z** belong to reference configuration or to undeformed state in the current work. Hence the deformation

gradient looks like

$$\mathbf{F} = \begin{bmatrix} \lambda_1 & 0 & 0 \\ 0 & \lambda_2 & 0 \\ 0 & 0 & 1 \end{bmatrix} \tag{4.4}$$

Assuming that this MAP behaves as an incompressible material, from equation 4.3, it can be found that $\lambda_2 = 1/\lambda_1$. Substituting the eigen values of $\mathbf{F}$ or stretch ratios, $\mathbf{B}$ can be written as

$$\mathbf{B} = \begin{bmatrix} \lambda_1^2 & 0 & 0 \\ 0 & \frac{1}{\lambda_1^2} & 0 \\ 0 & 0 & 1 \end{bmatrix} \tag{4.5}$$

The strain energy density function W is of the form $(\mathbf{I}_1, \mathbf{I}_2) as \mathbf{I}_3 = 1$. For such incompressible materials, the Cauchy stress is then expressed as

$$\mathbf{T} = 2\frac{\partial W}{\partial \mathbf{I}_1}\mathbf{B} - 2\frac{\partial W}{\partial \mathbf{I}_2}\mathbf{B}^{-1} - p\mathbf{I} \tag{4.6}$$

For isotropic materials, the principal stresses can be written in terms of the stretch ratios as

$$T_i = 2\lambda_i^2\frac{\partial W}{\partial I_1} - 2\frac{1}{\lambda_i^2}\frac{\partial W}{\partial I_2} - p \tag{4.7}$$

1. Field Dependent Neo-Hookean Model

The Neo-Hookean model was proposed by Rivlin [32]. This model was developed based on concepts of cross-linking of elastomers. Elastomers are crosslinked polymer networks and on application of force or when tried to deform, initially, the polymer chains move past each other but restore back to their origin position because of crosslinks. Typically the Neo-Hookean model fit the data well within 20 to 25% strain for rubbery materials that were tested by Treloar and Rivlin and Saunders.

The strain energy density function for incompressible material is given a form as

$$W = C_1(\mathbf{I}_1 - 3) \tag{4.8}$$

The Cauchy stress for incompressible Neo-Hookean material could be expressed as

$$\mathbf{T} = -p\mathbf{I} + 2C_1\mathbf{B} \tag{4.9}$$

Substituting values of $\mathbf{B}$ from equation 4.5 into 4.9,

$$\mathbf{T}_{11} = -p\mathbf{I} + 2C_1\lambda_1^2 \tag{4.10}$$

$$\mathbf{T}_{22} = -p\mathbf{I} + \frac{2C_1}{\lambda_1^2} \tag{4.11}$$

However, since the sample is allowed to expand freely in the second direction, there is no stress in that direction. Hence $\mathbf{T}_{22} = 0$. Substituting this in equation 4.11, the value of $p = \frac{2C_1}{\lambda_1^2}$. Substituting this value of p in equation 4.10 that

$$\mathbf{T}_{11} = 2C_1\lambda_1^2 - \frac{2C_1}{\lambda_1^2} = \mu(\lambda_1^2 - \frac{1}{\lambda_1^2}) \tag{4.12}$$

where $\mu = 2C_1$ and this is a function of the particle concentration and the magnetic field.

2. Field Dependent Valanis-Landel Model

Valanis Landel [33] developed a model that could be used over large strains and parameters could be derived from experiments. According to them, the strain energy density function of the material need not be expressed in terms of strain invariants. A necessary and sufficient function that W will pertain to isotropic elastic material is that it merely needs to be a symmetric function of stretch ratios.

$$W = w(\lambda_1, \lambda_2, \lambda_3) \tag{4.13}$$

such that $w(\lambda_i, \lambda_j, \lambda_k)_{i\neq j, j\neq k, k\neq i}$ remains invariant with any permutation of i, j, k. Valanis and Landel assumed a "separable" form for W of the form

$$W = w(\lambda_1) + w(\lambda_2) + w(\lambda_3) \tag{4.14}$$

As per VL Model,the Cauchy stress is given as

$$T_i = \lambda_i w'(\lambda_i) - p \tag{4.15}$$

To use Valanis Landel Model, some form of strain energy function should be assumed that is separable. For this Ogden's [31] strain energy function was chosen. This strain energy has the form

$$W = \sum_{p=1}^{N} \mu_p(\lambda_1^{\alpha_p} + \lambda_2^{\alpha_p} + \lambda_3^{\alpha_p} - 3)/\alpha_p \tag{4.16}$$

According to Ogden, for λ values less than 1.2, N=1 is sufficient to model the response or in other words, one term Valanis Landel Model would be sufficient to model the response. Therefore, the strain energy density function takes the form

$$W = \frac{\mu\lambda_1^{\alpha}}{\alpha} + \frac{\mu\lambda_2^{\alpha}}{\alpha} + \frac{\mu\lambda_3^{\alpha}}{\alpha} - \frac{3}{\alpha} \tag{4.17}$$

where μ and α are functions of magnetic field and concentration of magnetic particles.

Using this strain energy density function, the Cauchy stress can be given as

$$\mathbf{T}_{11} = \lambda_1\mu\lambda_1^{\alpha-1} - p \tag{4.18}$$

$$\mathbf{T}_{22} = \lambda_1 \mu \lambda_2^{\alpha-1} - p \tag{4.19}$$

For plane strain compression, the sample is allowed to move freely in the second direction and hence there would be no stress in that direction. Hence when equation 4.19 is set to zero, p is calculated to be $p = -\mu\lambda_2^{\alpha-1}$. From equation 4.3, it is found that $\lambda_2 = 1/\lambda_1$. Substituting the value of p, λ_2 in equation 4.18, the expression for Cauchy Stress for Valanis Landel Model for current work is derived to be

$$\mathbf{T}_{11} = \mu(\lambda_1^{\alpha} - \frac{1}{\lambda_1^{\alpha}}) \tag{4.20}$$

B. Fitting Model to Experimental Data

The results obtained from the experiments conducted are plotted. The Cauchy stress relations for the Neo-Hookean(NH) and Valanis Landel(VL) models derived are used to fit the data. Valanis Landel Model has two parameters namely μ and α. For the current work, both parameters are taken to be functions of concentration of iron particles and magnetic field. Similarly μ parameter for Neo-Hookean model is taken to be a function of concentration of iron particles and magnetic field. Since two parameters are unknown for Valanis Landel model, *nlinfit* function available in Matlab is used to plot the stress relation of VL Model.

The plots obtained for fitting models for different concentrations of magnetic particles at different magnetic fields have been plotted and few of them are shown below from Fig. 29 to Fig. 31. All other plots can be seen in Appendix G.

The plots (Fig. 32 and 33) show the variation of VL parameter (μ * α) which represents the shear modulus[31] of the material for the current system as a function of magnetic field and concentration of magnetic particles. Similarly, the variation of

NH model parameter (μ * α, which has a value 2) as function of magnetic field and concentration of magnetic particles are shown in Fig. 32 and Fig. 33 From the plots, it is seen that parameters obtained from Valanis Landel model fit experimental data well and that this nice fit was possible when the value of α mostly varies between 4 and 5 as seen in Table V. Valanis-Landel Model with $\alpha = 4$ would be a good starting point for developing a rigorous model. To support this observation, VL 1-term model with $\alpha = 4$ was fit again to determine the goodness of fit and all the plots are shown in Appendix H. From the residue values, r obtained by fitting the experimental data with nlinfit function the R^2 value is calculated using $R^2 = 1 - (sum(r^2)/sum((stress - mean(stress))^2))$. The values obtained for R^2 vary between 0.98 to 0.99. To obtain a typical form of shear modulus for the current work, effect of concentration is determined by plotting shear modulus as a function of concentration of magnetic particles. It is seen that the response curve of variation of shear modulus at 0T is linear. It is then assumed that the effect of magnetic field which is in turn a function of concentration of magnetic particles is linear. Then the form of the shear modulus as a function of concentration of magnetic particles and magnetic field looks like

$$\mu_{shearmodulus} = \alpha_0 + \alpha_1 C + mCB \tag{4.21}$$

where B is magnetic field, C is the concentration of magnetic particles. α_0 and α_1 are obtained from constant and slope of a linear curve fit at $B = 0T$ i.e. $\mu_{concwithoutmagnetic} = 0.0004C + 0.0189$. To find the effect of magnetic field, the effect of concentration obtained at 0T is subtracted and then the initial shear modulus

assumes a form as shown in equation 4.22

$$\begin{aligned} \mu_{concwithmagnetic} &= \mu_{shearmodulus} - \mu_{concwithoutmagnetic} \\ \mu_{concwithmagnetic} &= mCB \end{aligned} \tag{4.22}$$

Equation 4.22, could be solved by minimizing the error in equation 4.22 as shown in equation 4.23.

$$Error = (\sum \mu_{concwithmagnetic} - m \sum BC) \tag{4.23}$$

The minimization of error in the shear modulus could be solved using Least Square Fit as shown in equations 4.24 to get values of m as 0.001655.

$$\begin{aligned} (\tfrac{\partial \mu_{concwithmagnetic}}{\partial m}) = (\sum \mu_{concwithmagnetic} - m \sum BC)^2 = 0 \\ 2(\sum \mu_{concwithmagnetic} - m \sum BC)(BC) = 0 \\ \sum \mu_{concwithmagnetic} BC - m \sum (BC)^2 = 0 \\ m = \tfrac{\sum \mu_{concwithmagnetic} BC}{\sum (BC)^2} \end{aligned} \tag{4.24}$$

The final form of shear modulus is given by equation 4.25 where C is given as % concentration

$$\mu_{shearmodulus} = (0.0189 + 0.0004C + 0.00165BC) \tag{4.25}$$

To non-dimensionalize equation 4.25 where μ is divided by constant value μ_0 and C is given as a fraction and not %

$$\frac{\mu_{shearmodulus}}{\mu_0} = (1 + 2.1164C + 8.7566BC) \tag{4.26}$$

where $\mu_0 = 0.0189$

Similarly a form for shear modulus for Neo Hookean Model is obtained as

$$\mu_{nhshearmodulus} = (0.0218 + 0.0004C + 0.001891BC) \tag{4.27}$$

Fig. 34 compares the values of Shear Modulus obtained for VL Model and NH Model from Shear Modulus Form and Experiments. It is seen that the form for Shear Modulus by assumption of linear dependence on concentration of magnetic particles and magnetic field predicts values for shear modulus matching shear modulus obtained from experiments. This statement is further supported by Fig. 35 where comparison of VL Model using calculated shear modulus values and experimental data is shown. It is seen that the VL Model with power law coefficient as 4 and shear modulus value calculated from Shear Modulus form predicts the response for MAP as a close match to experimental investigations. All the figures comparing Averaged Experimental Data, VL and NH Model using calculated Shear Modulus for individual concentrations and magnetic field are shown in Appendix I. It is seen that the Model Plots using computed shear modulus values to agree well with averaged experimental data at higher magnetic fields at all concentrations however there is some larger variation at lower magnetic fields.

It is also seen that when 1 term Valanis Landel Model with power law coefficient as 4, maintains the simplicity as a Neo Hookean Model. This is because the strain energy function of a Neo Hookean Model looks like $W = C_1(tr(\mathbf{B}) - 3)$ and using this strain energy density function the Cauchy stress tensor is expressed as $\mathbf{T} = \mu(\lambda_1^2 - \lambda_1^{-2})$ where 2 is the power law co-efficient. Similarly for a 1-term Valanis Landel Model with power law coefficient as 4, the strain energy density function would look as shown in equation 4.28

$$W = C_1(tr(\mathbf{B}^2) - 3) \tag{4.28}$$

Hence the Cauchy stress tensor would have a form as shown in equation 4.29

$$\mathbf{T} = \mu tr(\mathbf{B}^2) - p\mathbf{I} \tag{4.29}$$

where μ is a function of concentration of magnetic particles and magnetic field. It is also seen that NH Model prediction matches closely to experimental data until 20% strain.

CHAPTER V

CONCLUSIONS

A. Summary

Experimental investigations were conducted to understand the quasistatic response of Magnetoactive polymers. To conduct experiments, Samples with 0%, 5%, 20%, 35% and 50% magnetic particles were prepared and three batches of each was prepared. Samples of both rectangular and disc shaped geometries were prepared. Sampes were prepared with different sized iron particles ranging between 5 to 10 μm and 50-70 μm were prepared. Tests were conducted over 21 samples for 3 rounds over 3 different magnetic fields to study the effect of concentration of magnetic particles and magnetic field on the specimen. Also effect of size of magnetic particles, geometry of the specimen and concentration of magnetic particles were studied. It was seen that geometry of the specimens did not show any significant difference in the stress response of these polymers. Specimens filled with different sized magnetic particles were tested and tests verified general belief that samples with finer sized iron particles took greater loads for same deformation. It was seen that concentration of magnetic particles had great influence on the response of this material. It was observed that samples with greater concentration of iron particles showed 70% increase in the load taken when compared with theircounterparts without magnetic fillers. It is belived that there is a linear dependence on the concentration of magnetic particles. Current work agrees well with this belief. Tests were performed under uniform magnetic field at 0T, 0.19T and 0.47T. It is expected that the response characteristics would not change to a large extent owing to uniform magnetic field. However, the stress response characteristics of the material is interesting and it has shown up to 250%

increase in stress taken for strains lesser than 40%. Comparison with isotropic rubber like models like Neo-Hookean and Valanis Landel have been done. It was seen that Neo-Hookean model assumption holds good only below 20 to 25% strains. If the application requires greater strains, however, Neo-hookean model would not be able to predict the response completely. For such applications where strains lesser than 50%, 1 term Valanis Landel model seems to a good choice of model to represent the material behavior.

B. Conclusions

An interesting variable stiffness material, in the presence of magnetic field, has been investigated. The stress response under compression for this material is found to be linearly dependent on concentration of magnetic particles at 0T (as seen in Fig. 27). The 1-term field dependent Valanis Landel was found to represent the response of the material well (as seen in plots of Appendix G). It is also seen that the 1-term field dependent Valanis Landel Model's power law coefficient(α) is independent of both concentration of magnetic particles and magnetic field. The 1-term field dependent Valanis Landel model with power law coefficient as 4 is seen to represent the material response well for all particle concentrations and magnetic fields tested(as seen in the plots of Appendix H, with $R^2 \approx 0.98$. It is assumed that the shear modulus of MAP to be linearly dependent on the concentration of magnetic particles and magnetic field and a simple form having dependence of both concentration of magnetic particles and magnetic field variables ($\mu_{shearmodulus} = \alpha_0 + \alpha_1 C + mCB$) is assumed where α_0, α_1, m are constants. It is seen the assumption of shear modulus dependence on magnetic field holds good irrespective of the magnetic field tested with as seen in Fig. 32. It is however seen that the assumption of linear dependence of concentration

is far approximate (as seen in Fig. 33 and plots in Appendix I) and further tests with same samples and different concentration of samples are required to make definite conclusions.

C. Future Work

Current work was limited to study of quasistatic response of the material. The viscous response of this material could be further studied to understand its dynamic and time-dependent properties. Currently, as the material has been investigated for quasistatic response, uniform magnetic fields were used to study the response characteristics. With the current work's contribution further extension to study the material response under non-uniform magnetic field could be carried on. Also only isotropic samples were prepared and tested which could be extended to anisotropy. Although, the current set up could be used reliably only up to 40% strains and and better set ups and sample dimesnions could be worked on to study the effect under larger strains. The theory has been currently investigated from the hyperelastic perspective and requires to be extended to viscoelastic models to use this material for applications.

REFERENCES

[1] RR Koons, "Production and quality-control of elastomer mounts," *Rubber Age*, vol. 105, pp. 55–56, 1973.

[2] B Morgan, "Elastomer bearing seals in oil-lubricated automobile transmissions," *Ball Bearing Journal*, vol. 188, pp. 27–28, 1976.

[3] LG Soderhol, "Natural rubber bushings pivot radius arms of utility vehicle," *Design News*, vol. 26, pp. 48–49, 1971.

[4] J Lesage, "Elastomers in the oil and automotive industries," *Revue De L'Institut Francais Du Petrole*, vol. 48, pp. 383–411, Jul-Aug 1993.

[5] EI Rivin and BS Lee, "Experimental-study of load-deflection and creep characteristics of compressed rubber components for vibration control devices," *Journal of Mechanical Design*, vol. 116, pp. 539–549, Jun 1994.

[6] M Abdulhadi, "Stiffness and damping coefficients of rubber," *Ingenieur Archiv*, vol. 55, pp. 421–427, 1985.

[7] DE Newland and HEM Hunt, "Isolation of buildings from ground vibration - a review of recent progress," *in Proc of the Institution of Mechanical Engineers Part C-Journal of Mechanical Engineering Science*, vol. 205, pp. 39–52, 1991.

[8] A Stevenson, "Use of rubber for vibration isolation," *Plastics & Rubber International*, vol. 7, pp. 68, 1982.

[9] GB Warburton, "Natural-rubber for earthquake protection of buildings and vibration isolation," *in Proc of the International-Conference on Earthquake Engineering & Structural Dynamics*, vol. 12, pp. 104–110, 1984.

[10] Aleksandra M. Vinogradov, "Accomplishments and future trends in the field of electroactive polymers - art. no. 69270m," in *Electroactive Polymer Actuators and Devices (EAPAD) 2008*. SPIE; Amer Soc Mech Engineers; Intelligent Mat Forum; Jet Propuls Lab; Natl Sci Fdn, Mar 2008.

[11] J Wang and G Meng, "Magnetorheological fluid devices: Principles, characteristics and applications in mechanical engineering," *In Proceedings of the Institution of Mechanical Engineers Part L-Journal of Materials-Design and Applications*, vol. 215, pp. 165–174, 2001.

[12] Harper Meng and Jinlian Hu, "A brief review of stimulus-active polymers responsive to thermal, light, magnetic, electric, and water/solvent stimuli," *Journal of Intelligent Material Systems and Structures*, vol. 21, pp. 859–885, Jun 2010.

[13] A Lendlein and S Kelch, "Shape-memory polymers," *Angewandte Chemie-International Edition*, vol. 41, pp. 2034–2057, 2002.

[14] C. Liu, H. Qin, and P. T. Mather, "Review of progress in shape-memory polymers," *Journal of Materials Chemistry*, vol. 17, pp. 1543–1558, Mar 2007.

[15] T Ikeda, M Nakano, YL Yu, O Tsutsumi, and A Kanazawa, "Anisotropic bending and unbending behavior of azobenzene liquid-crystalline gels by light exposure," *Advanced Materials*, vol. 15, pp. 201–205, Feb 2003.

[16] Marc Behl and Andreas Lendlein, "Actively moving polymers," *Soft Matter*, vol. 3, pp. 58–67, Oct 2007.

[17] Yoseph Bar-Cohen and Qiming Zhang, "Electroactive polymer actuators and sensors," *MRS Bulletin*, vol. 33, pp. 173–181, Mar 2008.

[18] Ailish O'Halloran, Fergal O'malley, and Peter Mchugh, "A review on dielectric elastomer actuators, technology, applications, and challenges," *Journal of Applied Physics*, vol. 104, pp. 1–11, Oct 2008.

[19] M.E. Nichols, J.M. Ginder, L.D. Elie, and R.A. Pett Electrorheological elastomers useful as variable stiffness articles, US Patent 5,607,996, Nov 1997.

[20] M Lokander and B Stenberg, "Performance of isotropic magnetorheological rubber materials," *Polymer Testing*, vol. 22, pp. 245–251, May 2003.

[21] JM Ginder, ME Nichols, LD Elie, and JL Tardiff, "Magnetorheological elastomers: Properties and applications," in *Smart Structures and Materials 1999: Smart Materials Technologies*. SPIE; Soc Exptl Mech; Amer Soc Mech Engineers; BFGoodrich Aerosp; Def Adv Res Projects Agcy; US Army Res Off; USAF Res Lab; Ceram Soc Japan; Intelligent Mat Forum, Japan, Mar 1999.

[22] Hua-Xia Deng and Xing-Long Gong, "Application of magnetorheological elastomer to vibration absorber," *Communications in Nonlinear Science and Numerical Simulation*, vol. 13, pp. 1938–1947, Nov 2008.

[23] Genoveva Filipcsei, Ildiko Csetneki, Andras Szilagyi, and Miklos Zrinyi, "Magnetic field-responsive smart polymer composites," in *Oligomers Polymer Composties Molecular Imprinting*, pp. 137–189. 2007.

[24] Z Varga, G Filipcsei, A Szilagyi, and M Zrinyi, "Electric and magnetic field-structured smart composites," *Macromolecular Symposia*, vol. 227, pp. 123–133, Jul 2005.

[25] Z Varga, G Filipcsei, and M Zrinyi, "Smart composites with controlled anisotropy," *Polymer*, vol. 46, pp. 123–133, Aug 2005.

[26] M Zrinyi, L Barsi, D Szabo, and HG Kilian, "Direct observation of abrupt shape transition in ferrogels induced by nonuniform magnetic field," *Journal of Chemical Physics*, vol. 106, pp. 5685–5692, Apr 1997.

[27] Janarthanan T. Venkataraghavan, "Compliant mechanisms," M.S. thesis, Texas A&M University, College Station, Texas, May 2001.

[28] P. Venkateswara Rao, S. Maniprakash, S. M. Srinivasan, and A. R. Srinivasa, "Functional behavior of isotropic magnetorheological gels," *Smart Materials & Structures*, vol. 19, pp. 1–10, Aug 2010.

[29] T.M. Pearce , Gelatinous elastomer and methods of making and using the same and articles made therefrom US Patent 5994450, Nov 1999.

[30] J.Y. Chen , Thermoplastic elastomer gelatinous compositions and articles, US Patent 5508334, Apr 1996.

[31] RW Ogden, *Non-Linear Elastic Deformations*, vol. 1, 16th ed, Dover Pubns, Mineola, New York, 1997.

[32] RS Rivlin, "Large elastic deformations of isotropic materials. i. fundamental concepts," *Philosophical Transactions of the Royal Society of London. Series A, Mathematical and Physical Sciences*, vol. 240, pp. 459–490, 1948.

[33] KC Valanis and RF Landel, "Strain-energy function of a hyperelastic material in terms of extension ratios," *Journal of Applied Physics*, vol. 38, pp. 2997–3002, 1967.

[34] University of Technology Sydney Electrical Technology Class notes on Magnetostatics EET-Chapter III, Retrieved from www.services.eng.uts.edu.au in, Jan 2009.

[35] University of Technology Sydney Electrical Technology Class notes on Magnetic Circuits EET-Chapter IV, Retrieved from www.services.eng.uts.edu.au in, Jan 2009.

APPENDIX A

TABLES

Table I. Initial Proportions of MAP Made

Sample No	Mineral Oil in gm	**Septon in gm**	**WAIP in gm**	**Ratio**
11	20.00	05.00	00.00	80:20:00
12	11.65	05.00	00.00	70:30:00
13	40.00	05.00	05.00	80:10:10
14	35.00	02.50	12.50	70:05:25
15	35.00	05.00	10.00	70:10:20
16	35.00	07.50	07.50	70:15:15
17	30.00	02.50	17.50	60:05:35
18	30.00	05.00	15.00	60:10:30
19	30.00	07.50	12.50	60:15:25
20	30.00	10.00	10.00	60:20:20
21	30.00	12.50	07.50	60:25:15
22	25.00	05.00	20.00	50:10:40
23	20.00	05.00	25.00	40:10:50

Table II. MAP Sample Proportions Having WAIP

Sample No	Mineral Oil in gm	**Septon in gm**	**WAIP in gm**	**Ratio**
24	20.00	05.00	00.00	80:20:00
25	18.00	04.50	02.50	72:18:10
26	16.00	04.00	05.00	64:16:20
27	21.00	05.25	11.25	56:14:30
28	18.00	04.50	15.00	48:12:40
29	15.00	03.75	18.75	40:10:50

Table III. MAP Sample Proportions Having CIP

Sample No	Mineral Oil in gm	**Septon in gm**	**CIP in gm**	**Ratio**
24	20.00	05.00	00.00	80:20:00
26	16.00	04.00	05.00	64:16:20
29	15.00	03.75	18.75	40:10:50
30	19.00	04.75	01.25	40:10:50
31	20.00	05.00	13.46	40:10:50

Table IV. Tests Conducted

Uniaxial Compression		0T			0.19T			0.47T		
		R1	R2	R3	R1	R2	R3	R1	R2	R3
20% CIP (S26) For Repeatability	B8	✓	✓	✓	-	-	-	-	-	-
	B10	✓	✓	✓	-	-	-	-	-	-
	B12	✓	✓	✓	-	-	-	-	-	-
20% CIP (S26) For Geometry	B8 Disc	✓	x	x	-	-	-	-	-	-
	B10 Disc	✓	x	x	-	-	-	-	-	-
	B12 Disc	✓	x	x	-	-	-	-	-	-
Plane Strain Compression		0T			0.19T			0.47T		
		R1	R2	R3	R1	R2	R3	R1	R2	R3
0% CIP (S24)	B1	✓	✓	✓	✓	✓	✓	✓	✓	✓
	B2	✓	✓	✓	✓	✓	✓	✓	✓	✓
	B3	✓	✓	✓	✓	✓	✓	✓	✓	✓
5% CIP (S30)	B1	✓	✓	✓	✓	✓	✓	✓	✓	✓
	B2	✓	✓	✓	✓	✓	✓	✓	✓	✓
	B3	✓	✓	✓	✓	✓	✓	✓	✓	✓
20% CIP (S26)	B8	✓	✓	✓	✓	✓	✓	✓	✓	✓
	B10	✓	✓	✓	✓	✓	✓	✓	✓	✓
	B12	✓	✓	✓	✓	✓	✓	✓	✓	✓
35% CIP (S31)	B1	✓	✓	✓	✓	✓	✓	✓	✓	✓
	B2	✓	✓	✓	✓	✓	✓	✓	✓	✓
	B3	✓	✓	✓	✓	✓	✓	✓	✓	✓
50% CIP (S29)	B1	✓	✓	✓	✓	✓	✓	✓	✓	✓
	B2	✓	✓	✓	✓	✓	✓	✓	✓	✓
	B3	✓	✓	✓	✓	✓	✓	✓	✓	✓
20% WAIP (S26)	B2	✓	✓	✓	✓	✓	✓	x	x	x
	B3	✓	✓	✓	✓	✓	✓	x	x	x
	B4	✓	✓	✓	✓	✓	✓	x	x	x
50% WAIP (S29)	BA	✓	✓	✓	✓	✓	✓	x	x	x
	BB	✓	✓	✓	✓	✓	✓	x	x	x
	BC	✓	✓	✓	✓	✓	✓	x	x	x

Table V. Values of Valanis Landel Model Parameter Alpha

Sample	α **at 0T**	α **at 0.19T**	α **at 0.47T**
00% CIP	4.835234	5.617117	5.174168
05% CIP	5.244581	5.384322	4.424387
20% CIP	5.010552	5.2932	4.13614
35% CIP	4.854805	5.362448	4.693584
50% CIP	4.990972	5.162444	3.993668

APPENDIX B

FIGURES OF CHAPTER II

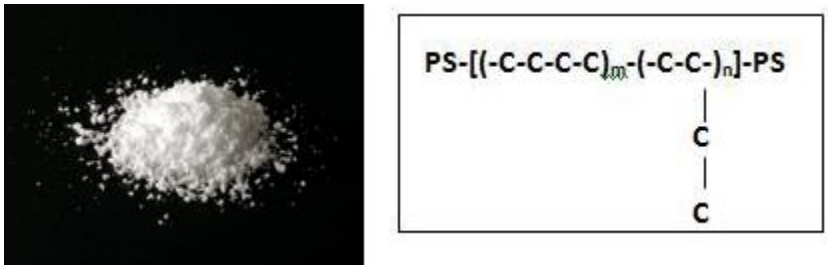

Fig. 3. Septon 8006

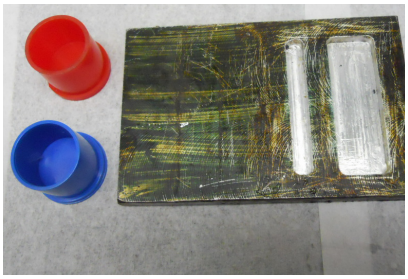

Fig. 4. Molds Used

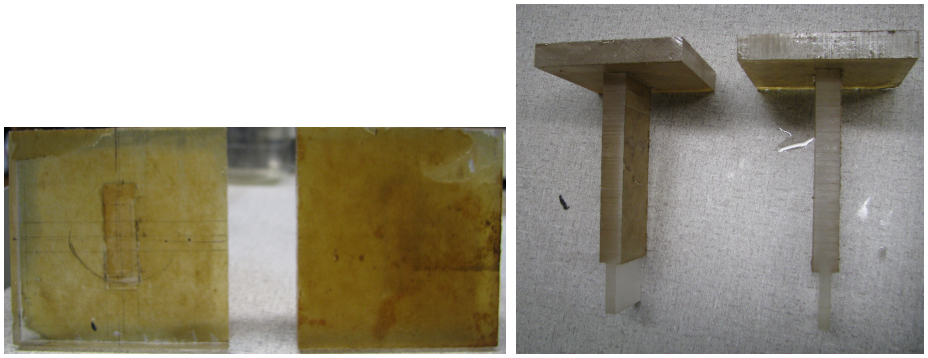

Fig. 5. Uniaxial Compression Fixture a. Front View b. Top View

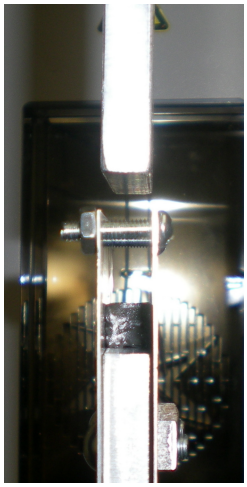

Fig. 6. Plane Strain Compression Fixture With Top and Bottom Platen Attached to Grips of Instron

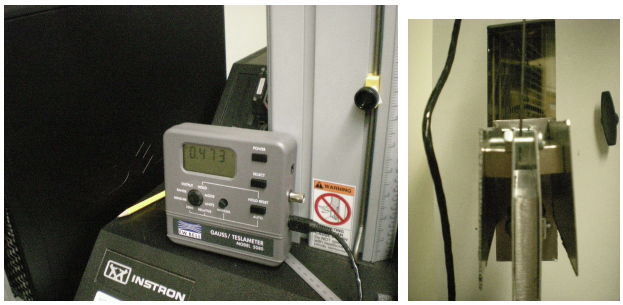

Fig. 7. Magnetic Field Intensity Measurements a.Gaussmeter Measurement of Magnetic Flux Field Intensity of Neodymium Magnets b. Magnetic Field Intensity Measurement of Neodymium Magnets

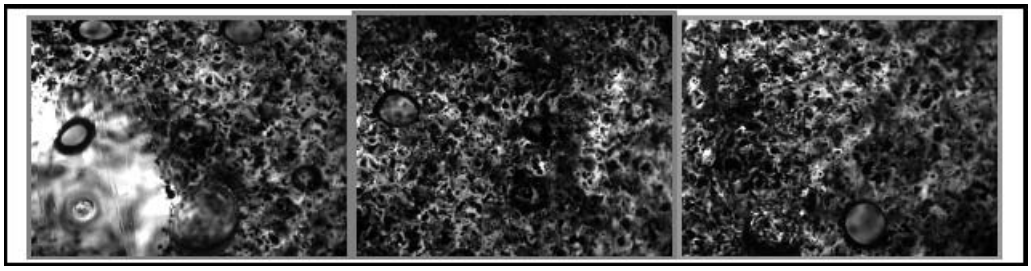

(a) a

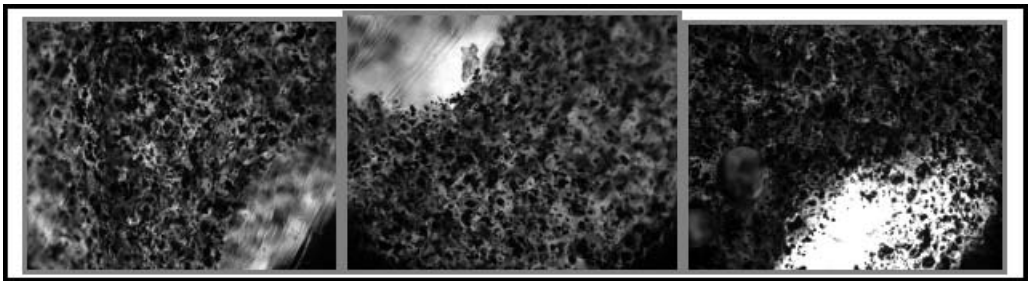

(b) b

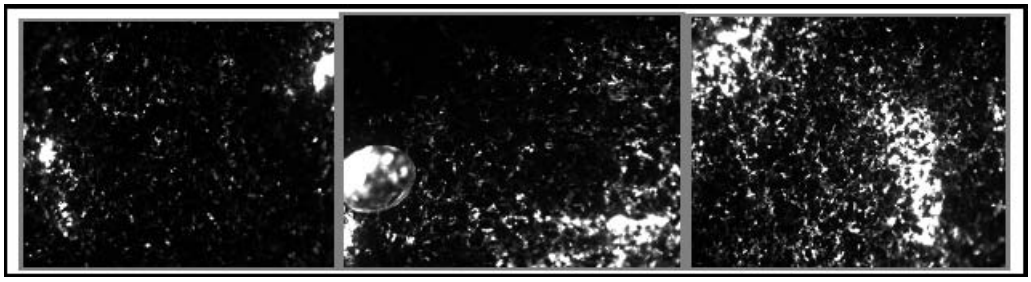

(c) c

Fig. 8. Microscope Images of Samples at 2.5x Optical Zoom a. 10% WAIP Batch A b. 10% WAIP Batch B c. 40% WAIP Batch A Showing Bubbles and Unmelted or Unmixed Polymer Patches

Fig. 9. Uniaxial Compression Setup Shows Instron 5567, With Uniaxial Compression Fixtures Attached to the Grips

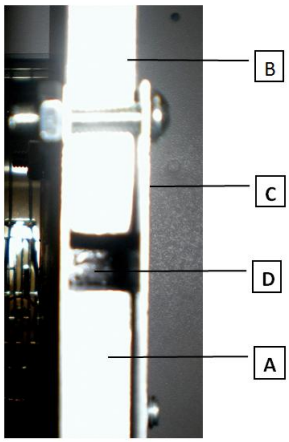

Fig. 10. Plane Strain Compression Closeup

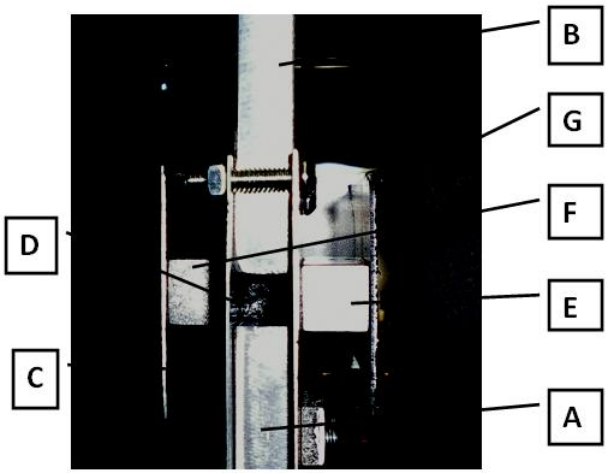

Fig. 11. Plane Strain Compression With Magnetic Field Closeup

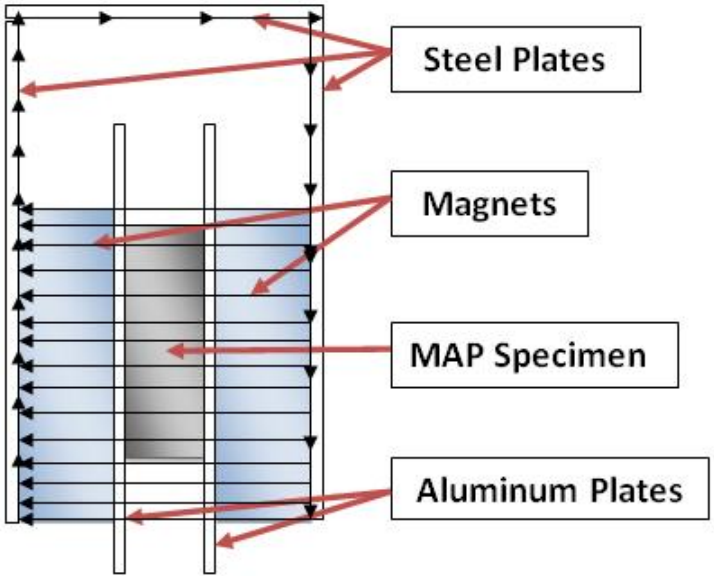

Fig. 12. Magnetic Circuit Analogy for Current Work

APPENDIX C

FIGURES OF CHAPTER III

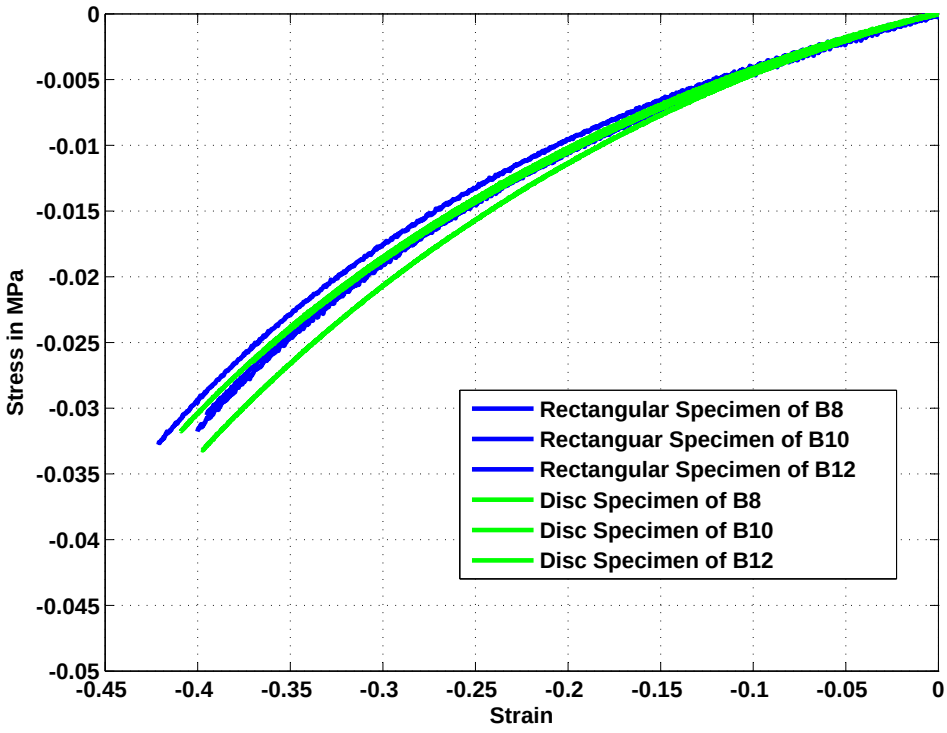

Fig. 13. Influence of Geometry on Stress Response of the Samples

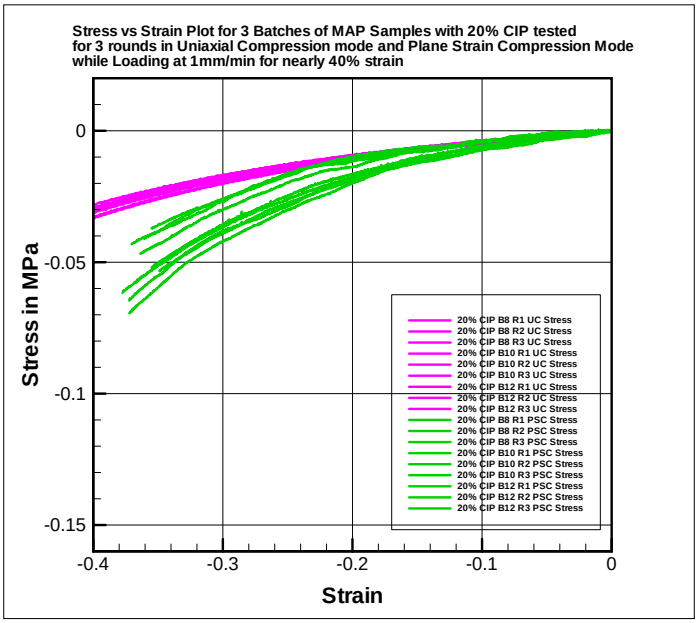

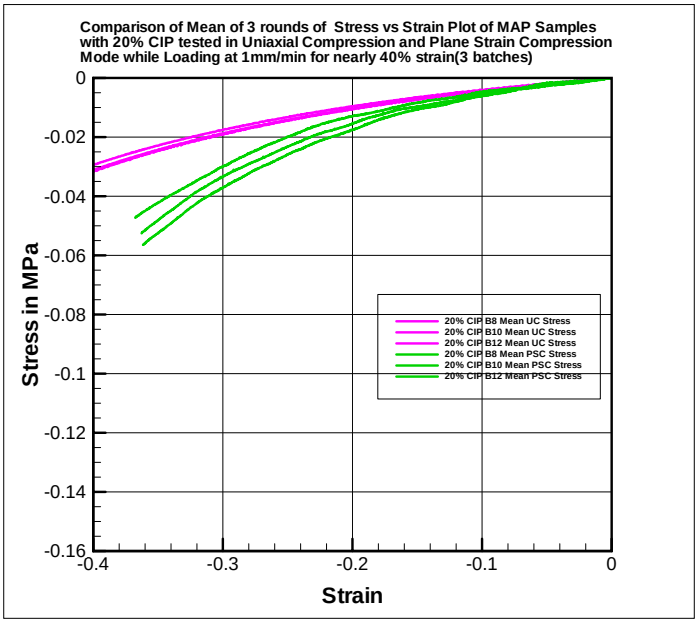

Fig. 14. Comparison of Stress Strain Plot of MAP Samples under Uniaxial and Plane Strain Compression a. Plot for Tests done on All Batches and 3 Rounds b. Mean of 3 Rounds of Data for Different Batches under Uniaxial Compression and Plane Strain Compression

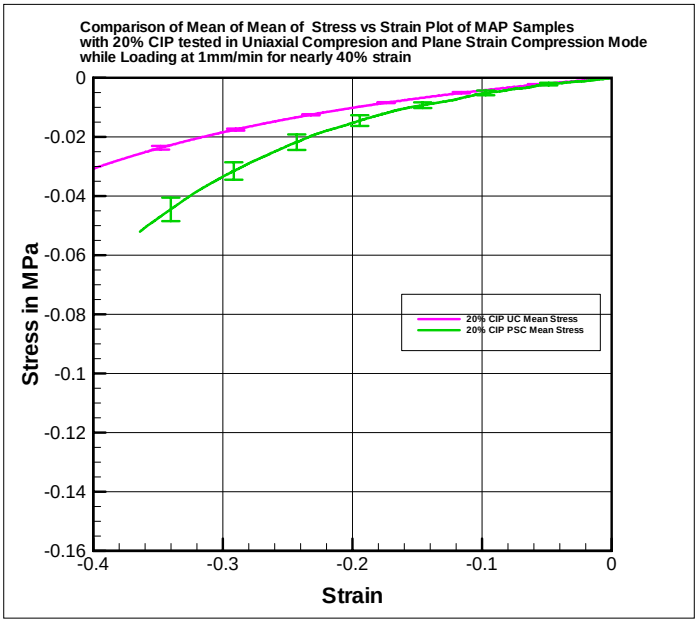

Fig. 15. Averaged Data Response in Uniaxial Compression Mode and Plane Strain Compression Mode Tests

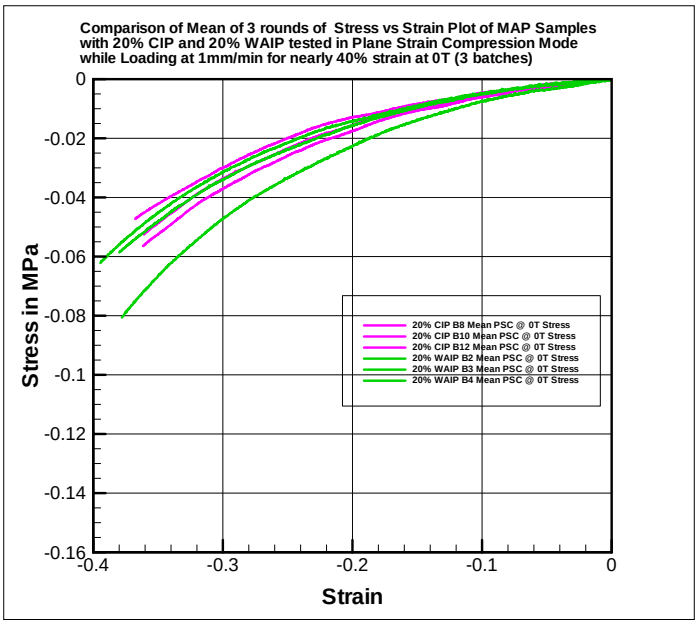

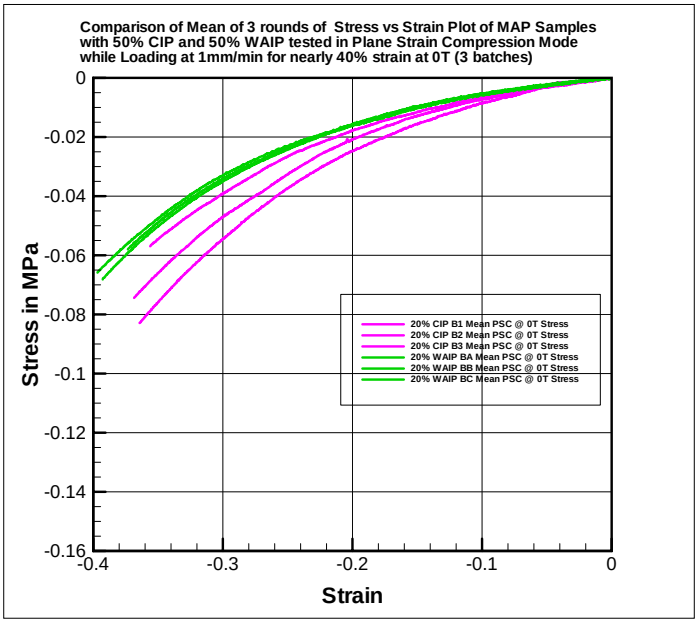

Fig. 16. Response under Plane Strain Compression for Samples with 20% and 50% CIP and WAIP at 0T

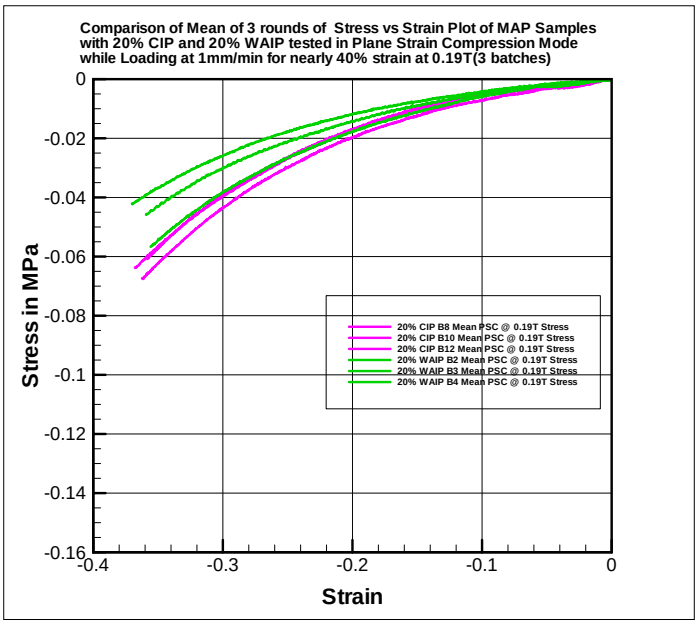

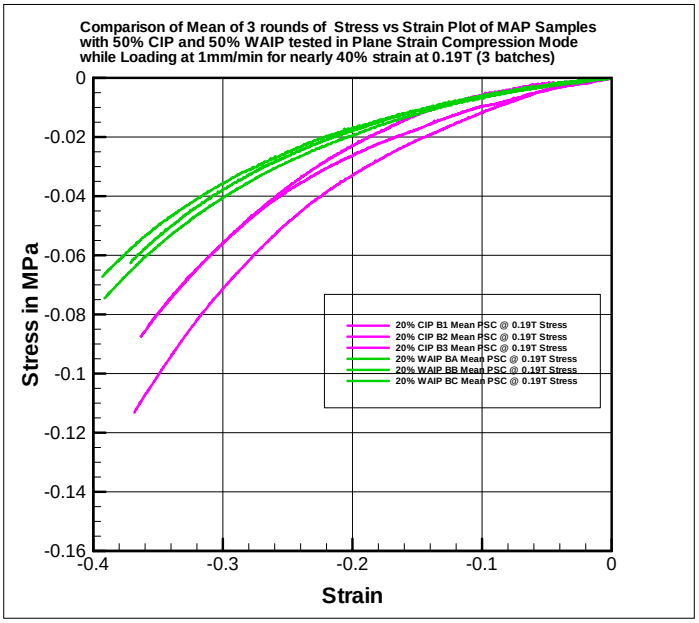

Fig. 17. Response under Plane Strain Compression for Samples with 20% and 50% CIP and WAIP at 0.19T

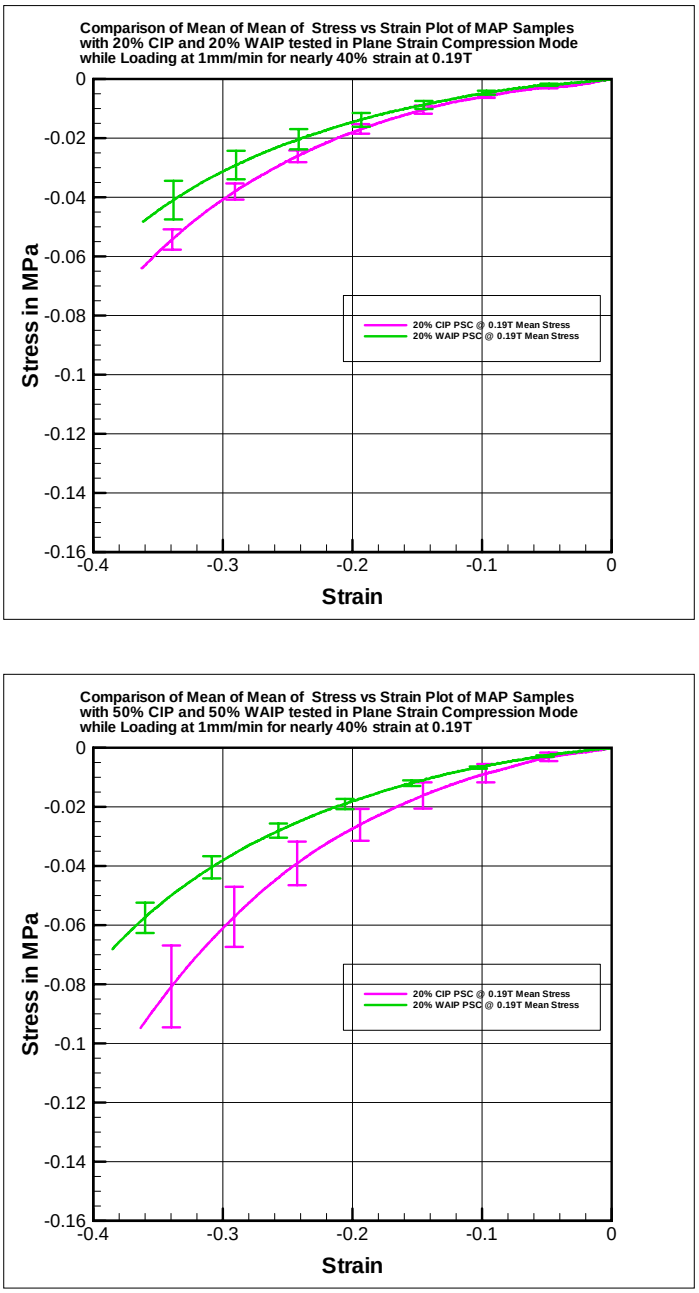

Fig. 18. Averaged Data of Samples with CIP and WAIP at 0.19T

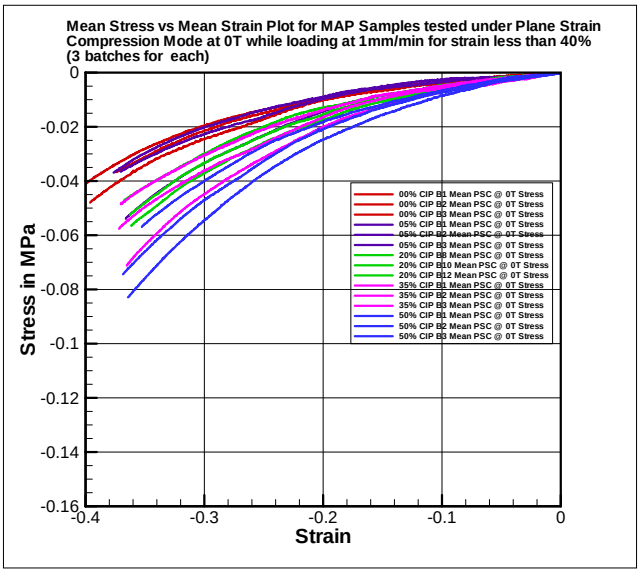

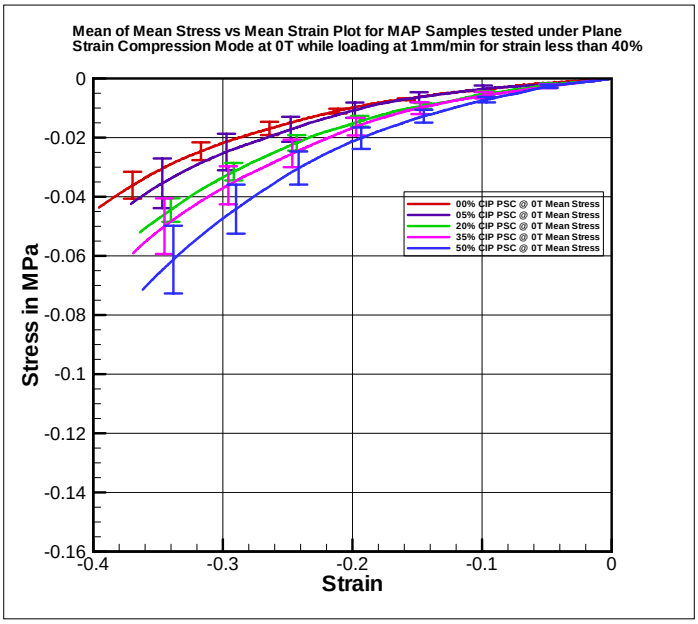

Fig. 19. Response in Plane Strain Compression of Different Concentration MAP Samples at 0T a. Mean of 3 Rounds for MAP Sample Batches at 0T b. Response of Averaged Data of MAP Samples of Different Concentrations at 0T

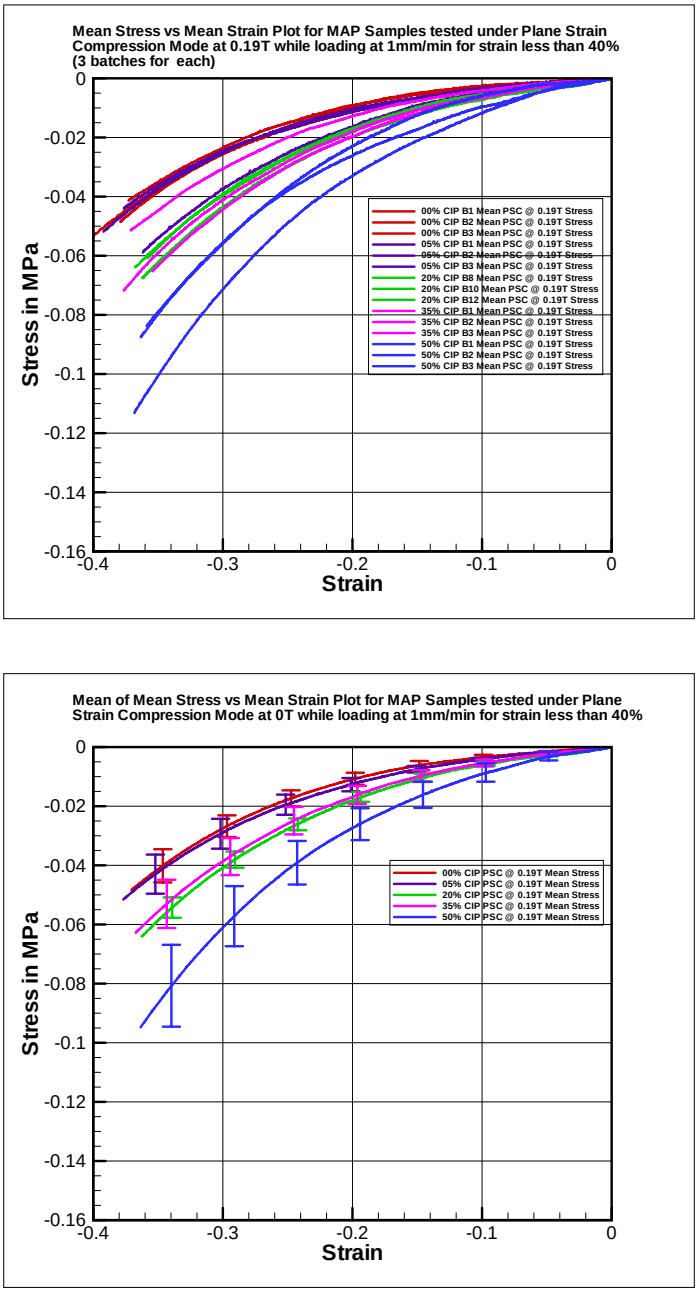

Fig. 20. Response in Plane Strain Compression of Different Concentration MAP Samples at 0.19T a. Mean of 3 Rounds for MAP Sample Batches at 0.19T b. Response of Averaged Data of MAP Samples of Different Concentrations at 0.19T

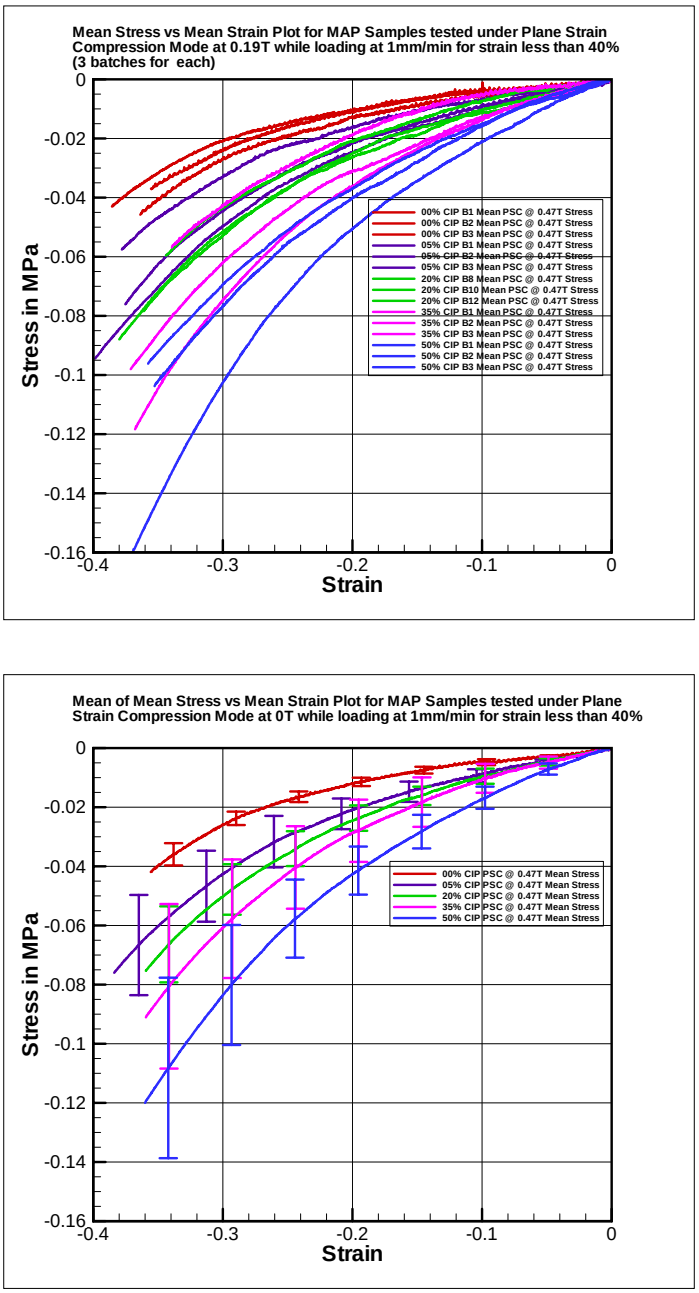

Fig. 21. Response in Plane Strain Compression of Different Concentration MAP Samples at 0.47T a. Mean of 3 Rounds for MAP Sample Batches at 0.47T b. Response of Averaged Data of MAP Samples of Different Concentrations at 0.47T

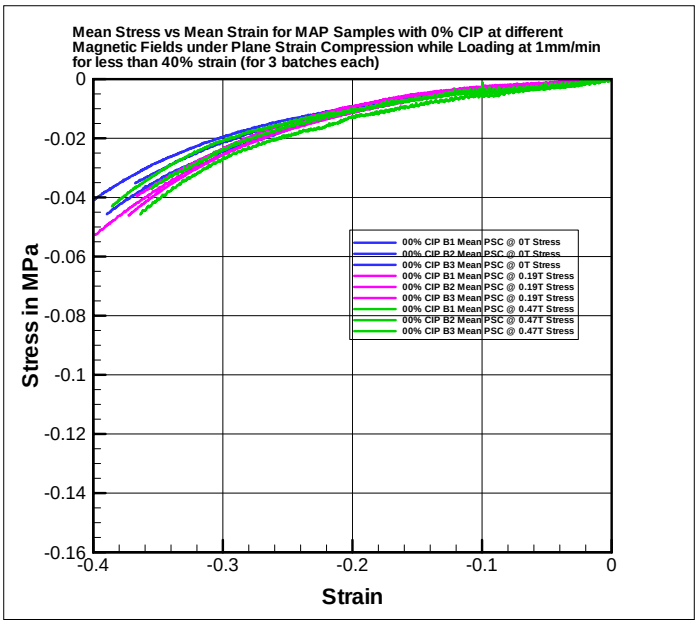

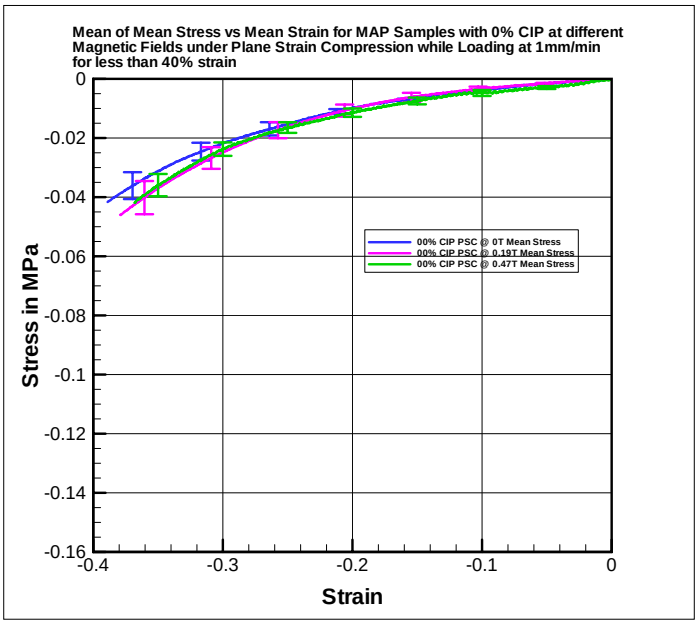

Fig. 22. Response of 0% CIP Samples under Different Magnetic Field a. Mean of 3 Rounds of Each Batch at Different Magnetic Fields b. Response of Averaged Data for 0% CIP Samples at Different Magnetic Fields

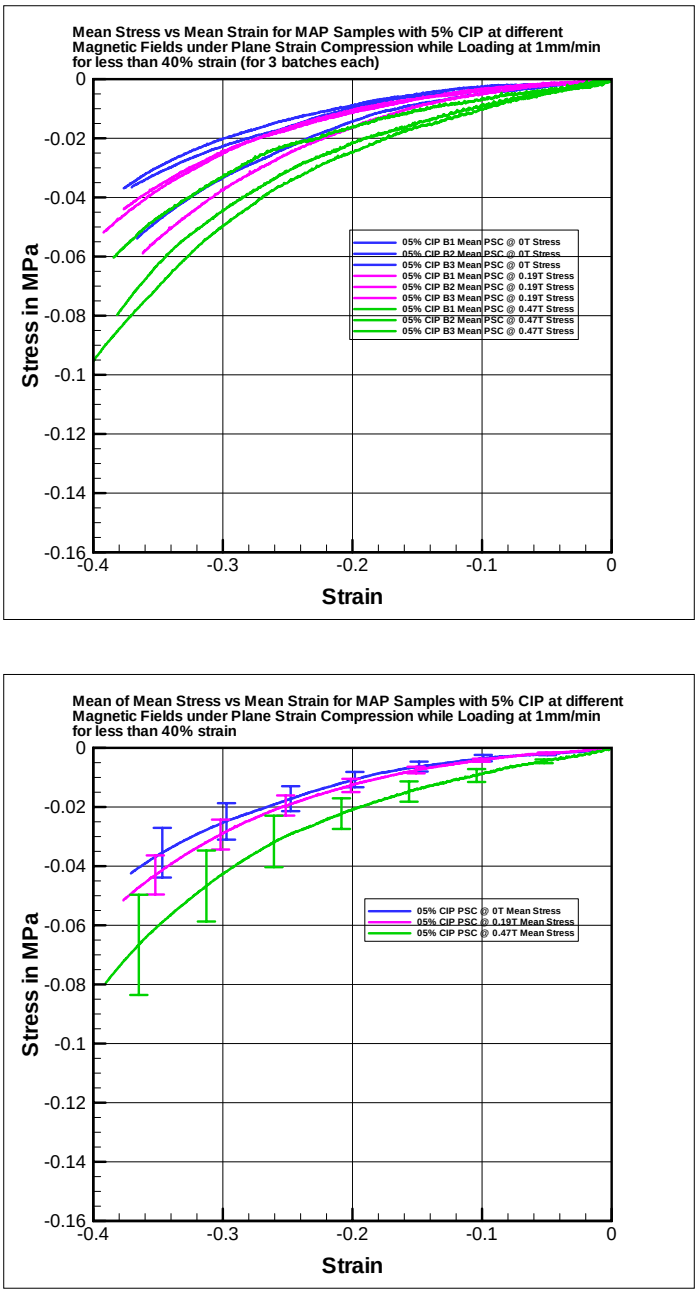

Fig. 23. Response of 5% CIP Samples under Different Magnetic Field a. Mean of 3 Rounds of Each Batch at Different Magnetic Fields b. Response of Averaged Data for 5% CIP Samples at Different Magnetic Fields

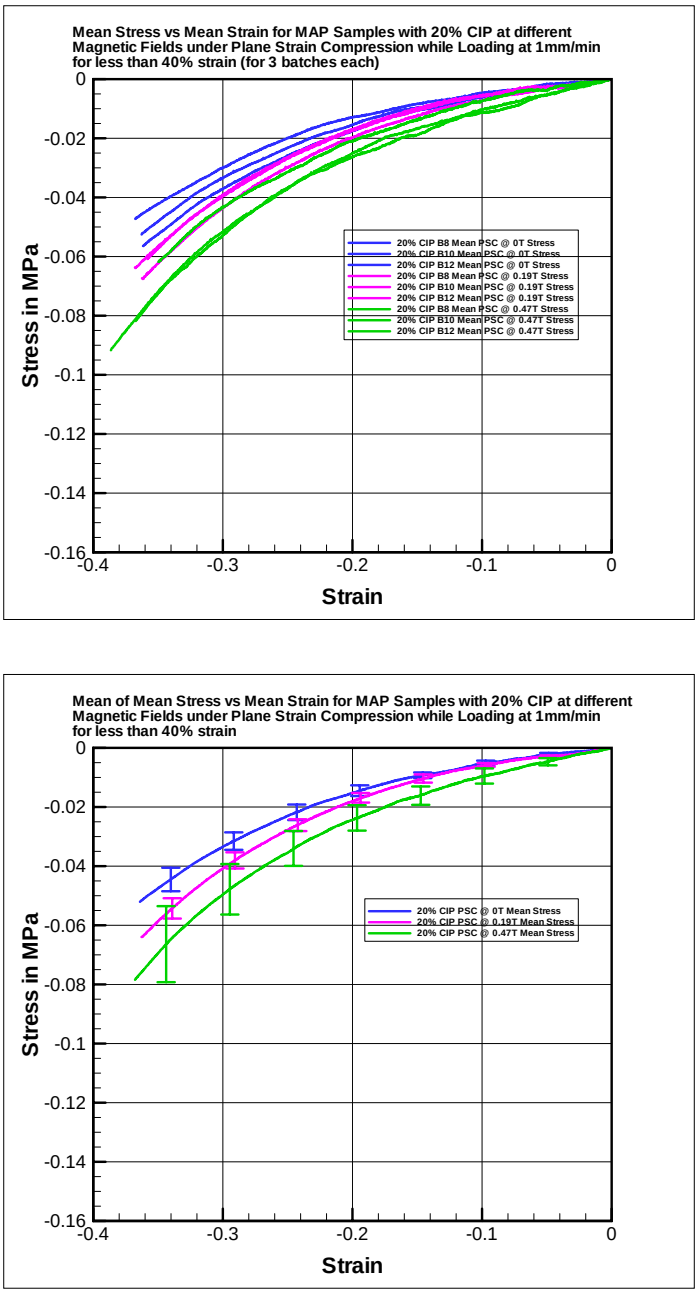

Fig. 24. Response of 20% CIP Samples under Different Magnetic Field a. Mean of 3 Rounds of Each Batch at Different Magnetic Fields b. Response of Averaged Data for 20% CIP Samples at Different Magnetic Fields

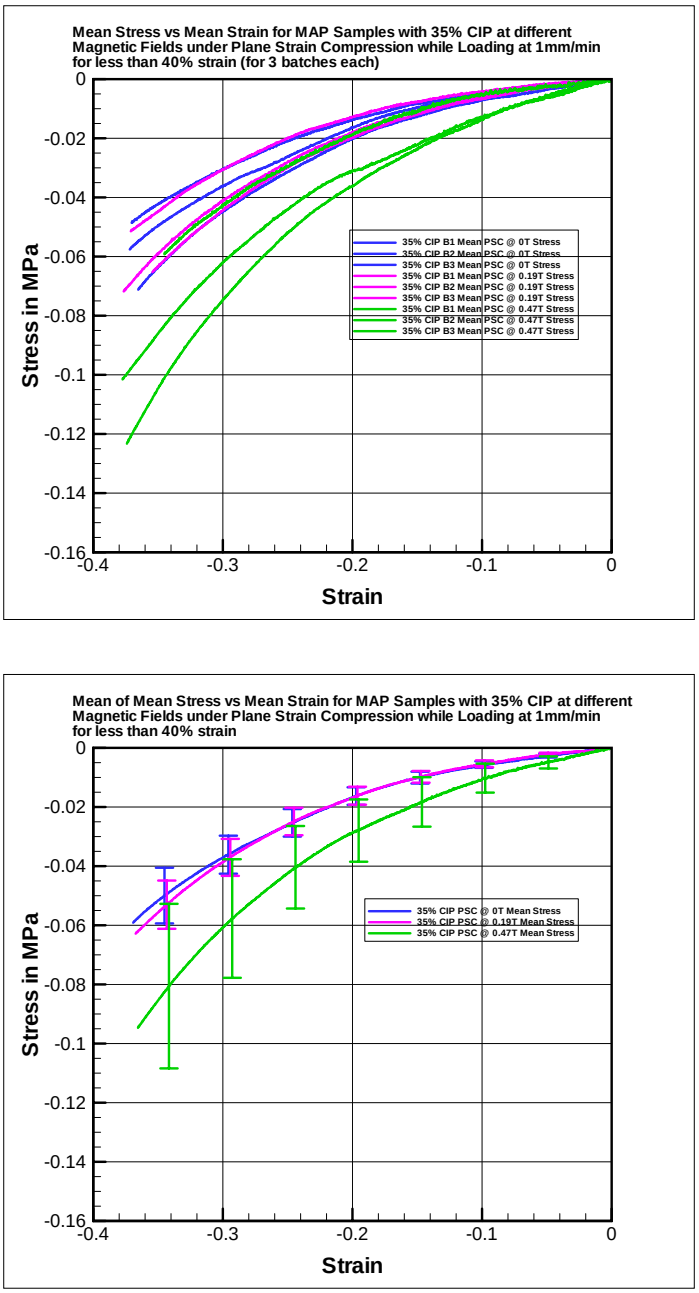

Fig. 25. Response of 35% CIP Samples under Different Magnetic Field a. Mean of 3 Rounds of Each Batch at Different Magnetic Fields b. Response of Averaged Data for 35% CIP Samples at Different Magnetic Fields

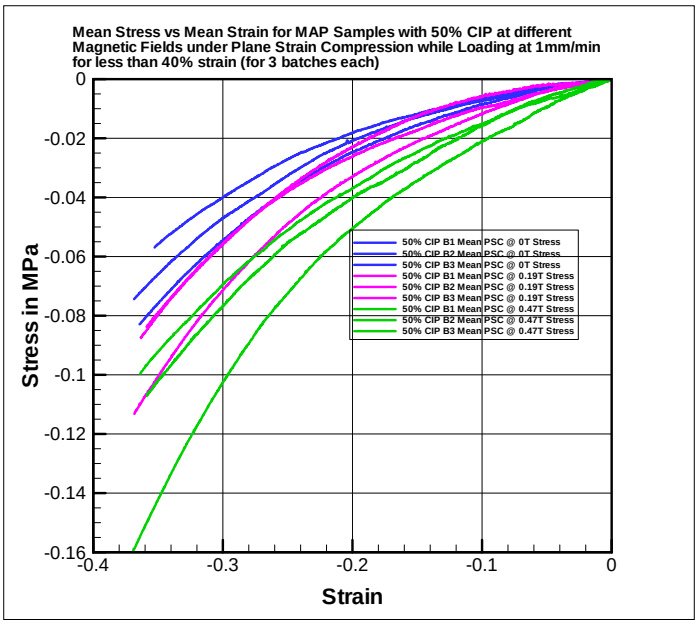

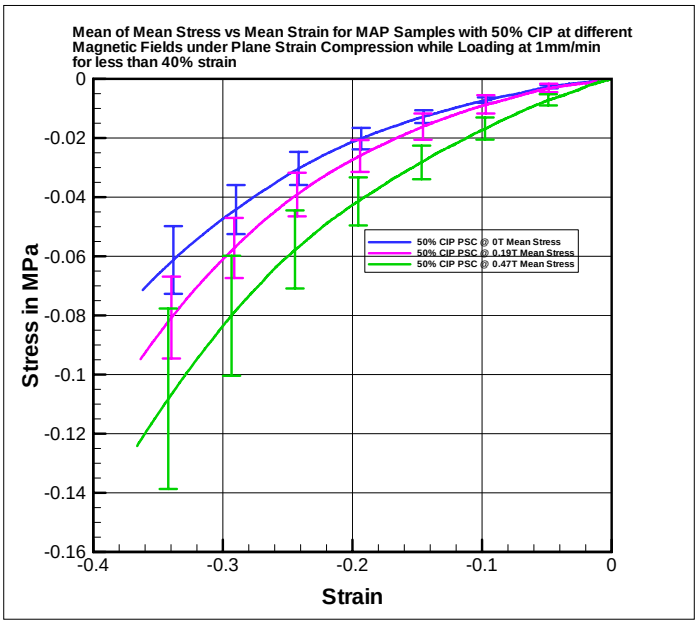

Fig. 26. Response of 50% CIP Samples under Different Magnetic Field a. Mean of 3 Rounds of Each Batch at Different Magnetic Fields b. Response of Averaged Data for 50% CIP Samples at Different Magnetic Fields

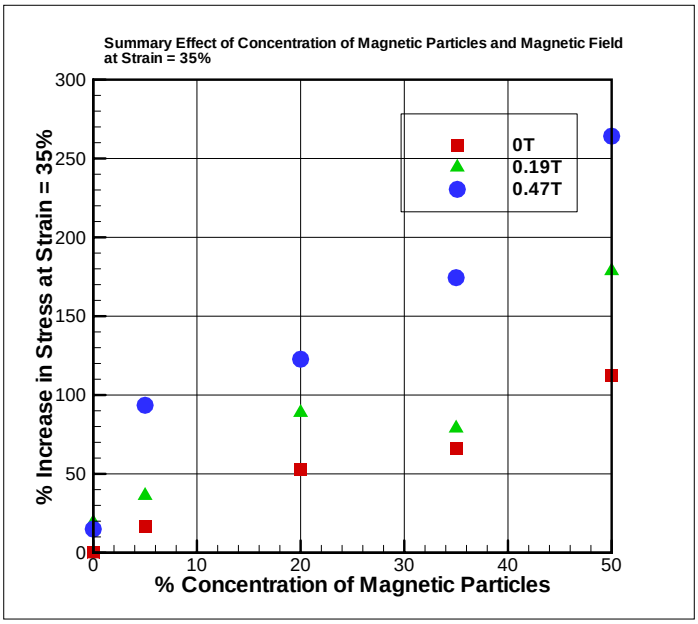

Fig. 27. Summary of Effect of Concentration and Magnetic Field on Stress Response of MAP Samples

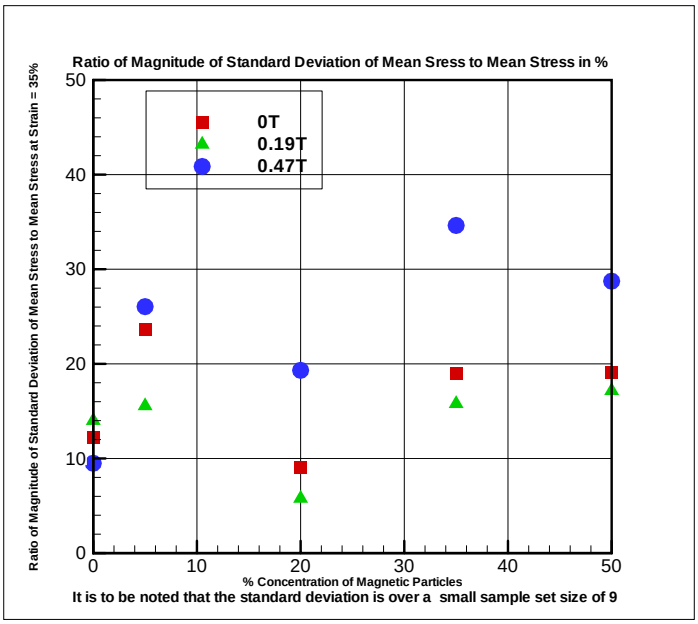

Fig. 28. Ratio of Standard Deviation of Averaged Data to Averaged Data at 35% Strain

APPENDIX D

FIGURES OF CHAPTER IV

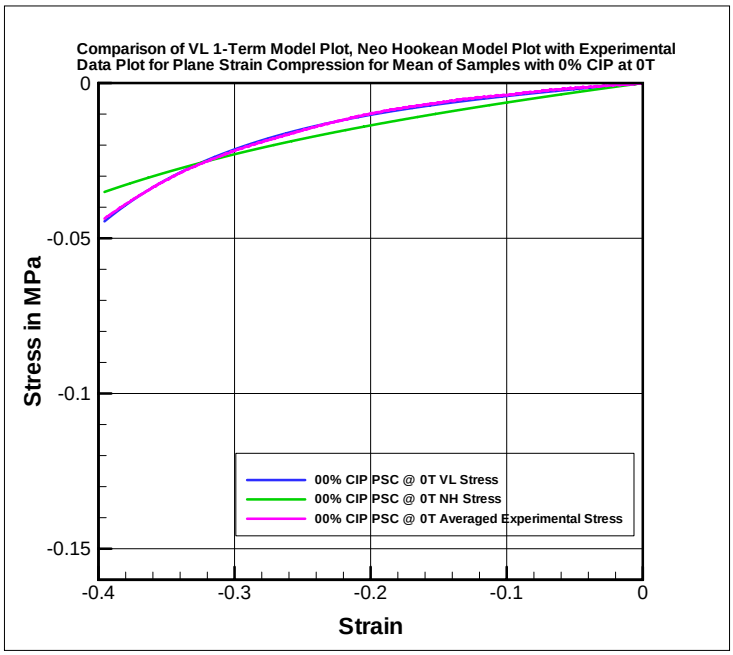

Fig. 29. 0% CIP 0T Model Fitting. $\mu_{VL} = 0.00336$ MPa, and $\mu_{NH} = 0.011070$ MPa

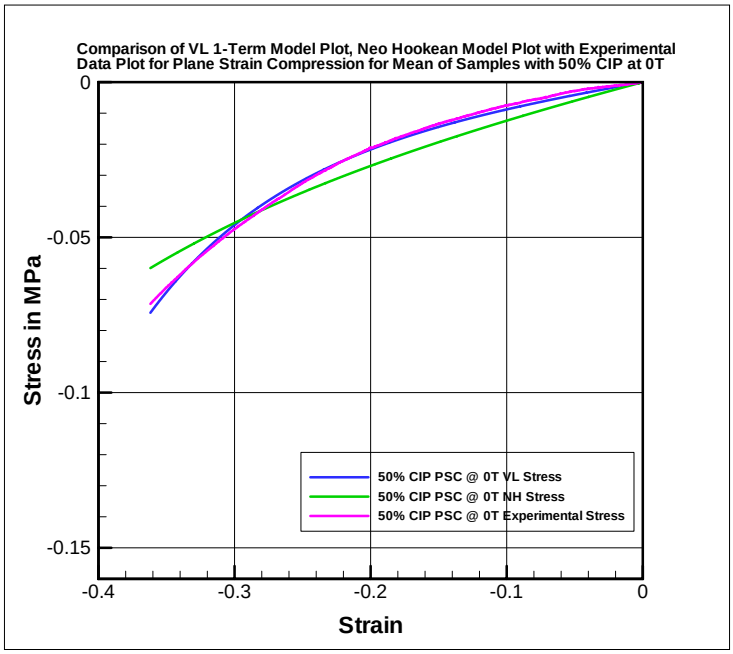

Fig. 30. 50% CIP 0T Model Fitting $\mu_{VL} = 0.007985$ MPa, and $\mu_{NH} = 0.022421$ MPa

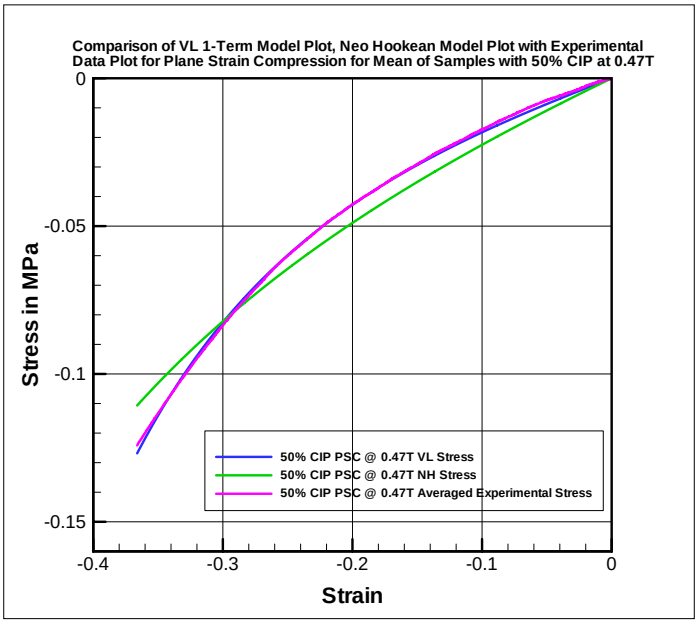

Fig. 31. 50% CIP 0.47T Model Fitting $\mu_{VL} = 0.021091$ MPa, and $\mu_{NH} = 0.045659$ MPa

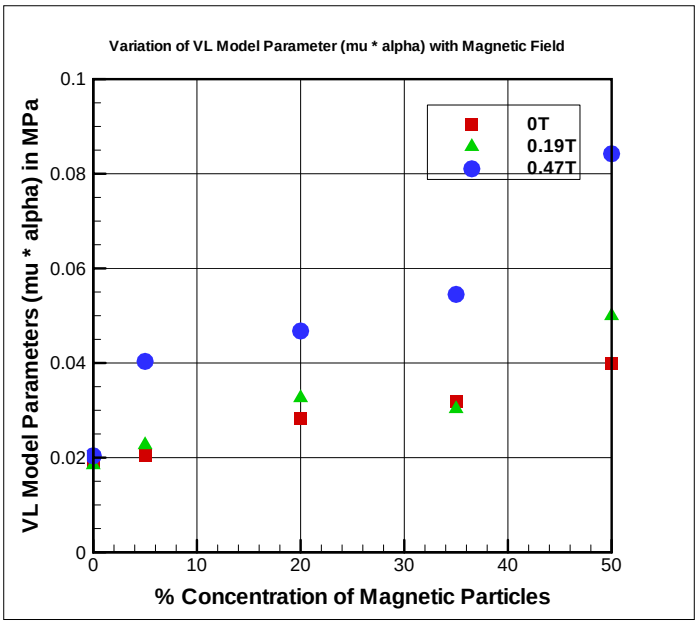

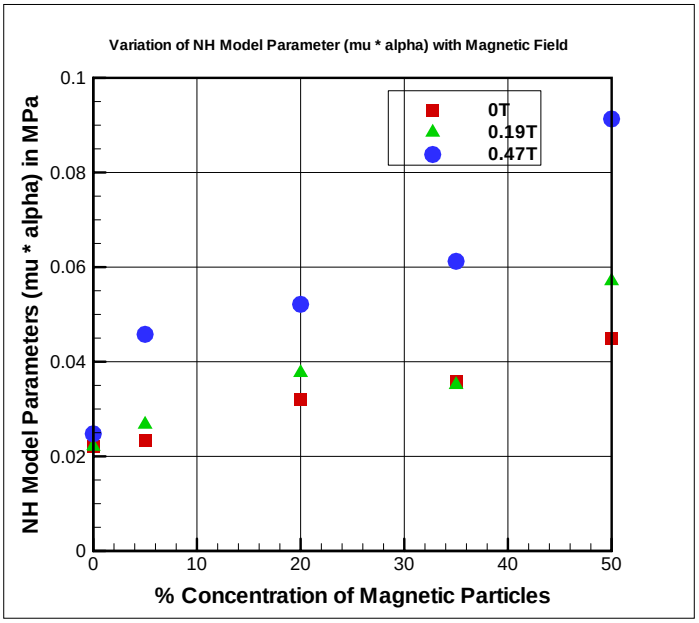

Fig. 32. Variation of Shear Modulus of MAP Samples with Magnetic Field a. Valanis Landel Model b. Neo-Hookean Model

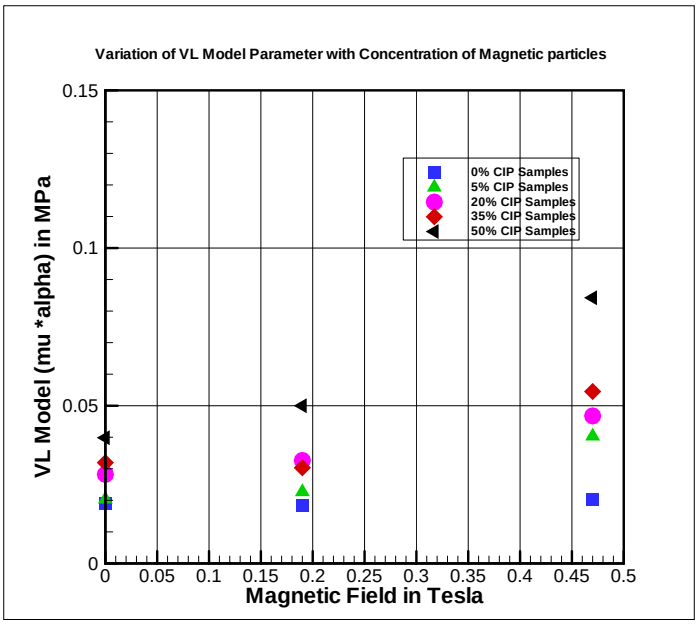

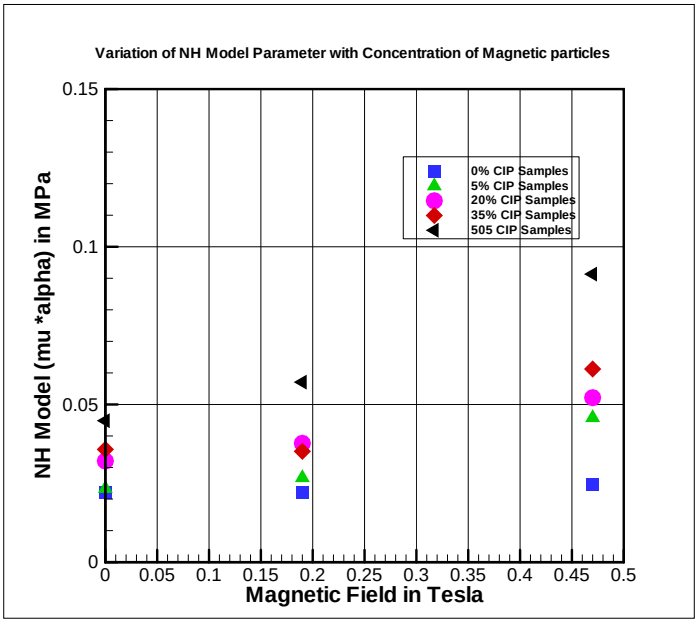

Fig. 33. Variation of Shear Modulus of MAP Samples with Concentration a. Valanis Landel Model b. Neo-Hookean Model

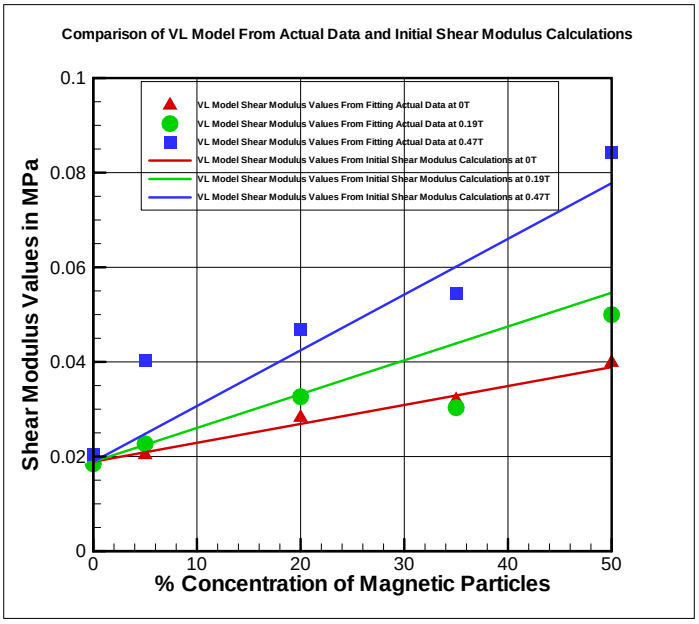

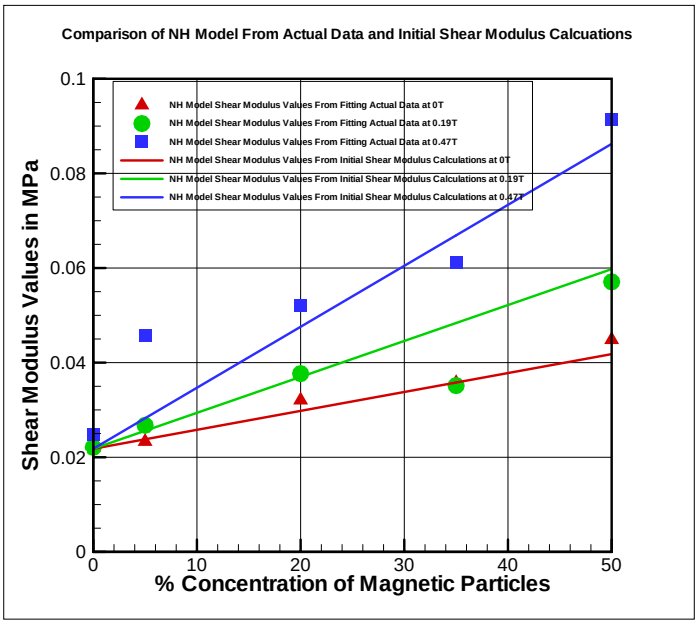

Fig. 34. Comparison of Shear Modulus of VL Model and NH Model Calculated from the Shear Modulus Equation and Experimental Data

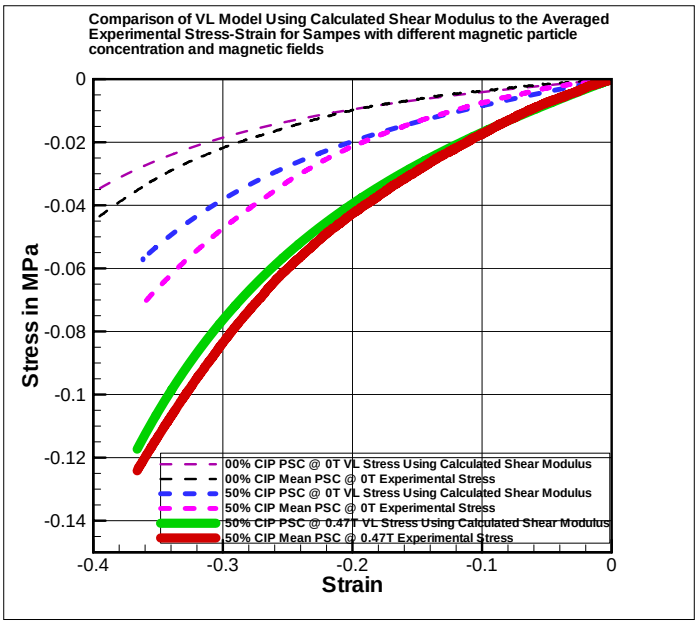

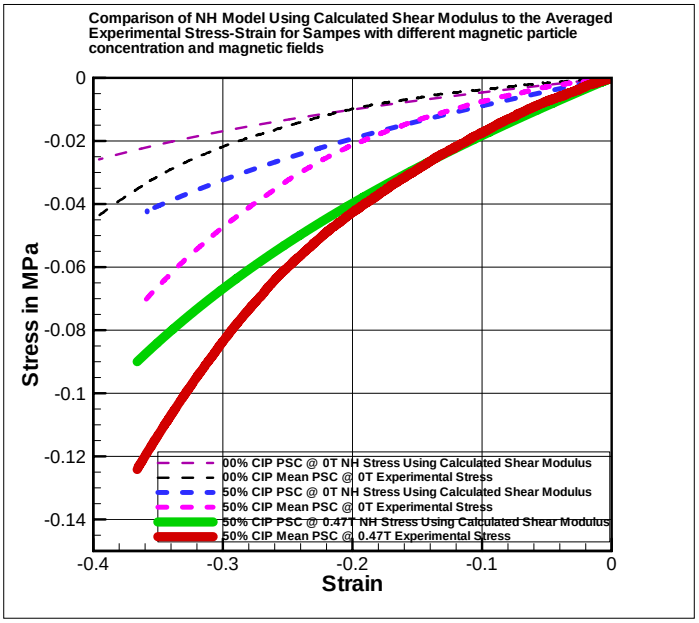

Fig. 35. Comparison of VL Model and NH Model with Experimental Data Using Calculated Shear Modulus Values

APPENDIX E

MAGNETS AND MAGNETIC CIRCUITS

The current work deals with studying magnetoactive polymers which mainly involves studying their properties in presence of magnetic field. It is mandatory to be acquainted with terminologies of magnetic field, quantify their effect. In order to understand the experimental setup that is used and the way in which we generally (nominally) uniform magnetic fields, it is imperative to understand magnetic circuits.

A magnet is a material or object that produces a magnetic field. This magnetic field is invisible and attracts or repels other materials. Magnetic fields can be produced by permanent magnets or electromagnets.

Materials that can be magnetized, which are also the ones that are strongly attracted to a magnet, are called ferromagnetic (or ferrimagnetic). These include iron, nickel, cobalt, some alloys of rare earth metals, and some naturally occurring minerals such as lodestone. Ferromagnetic materials can be divided into magnetically "'soft"' materials like annealed iron which can be magnetized but don't tend to stay magnetized, and magnetically "'hard"' materials, which do.

Permanent magnets are hard materials that manufactured by such a process that their internal structure is aligned making them ferromagnetic by nature. Their structure is fixed such that it is difficult to demagnetize them. There are several types of permanent magnets available in the market. Most common types are Alnico (AlNiCo), ceramic(Strontium Ferrite), smarium Cobalt(SmCo) and Neodymium(NdFeB). There are several shapes available and the common ones of them are rings, discs, blocks and bars. These different types of magnets have different properties.

An electromagnet is made from a coil of wire which acts as a magnet when an electric current passes through it, but stops being a magnet when the current stops.

Often an electromagnet is wrapped around a core of ferromagnetic material like steel, which enhances the magnetic field produced by the coil.

Magnetic fields could be understood as the force exerted by magnet on other magnetic material. Magnetic field is denoted by B. B and H have the same value for magnetic field in vacuum but different in other medium. B is the flux per unit area normal to the direction of magnetic path and is measured in Tesla ((Newton A second)/(Coulomb A meter)) in SI units and gauss in CGS.(1 Tesla = 10000 gauss). H is measured in ampere-turn per meter in SI units and oersteds in CGS.

As per elementary atomic model, each atom has a positively charges nucleus and negatively charged electron orbiting the nucleus. The orbiting electrons are responsible for microscopic magnetic dipoles. In addition to orbiting, both electrons and nucleus spin about their own axis. The magnetic dipole of spinning of nucleus is negligible to spinning and orbiting of electrons.

Magnetic moment of a magnet is a measure of its tendency to align with a magnetic field. The direction of the magnetic moment points from the south to north pole of a magnet.

In absence of external magnetic field, magnetic dipoles of all materials except permanent magnets are randomly oriented. The application of an external magnetic field cause both an alignment of magnetic moments of the spinning electrons and an induced magnetic moment due to a charge in orbital motion of electrons. Magnetization, M, is defined as the quantity of magnetic moment per unit volume, V; $M = \frac{N}{V}m$. Here, N is the number of magnetic moments in the sample. The quantity $\frac{N}{V}$ is usually written as n, the number density of magnetic moments. The M-field is measured in amperes per meter (A/m) in SI units. [34]

In a magnetized material, the magnetic flux density B has two components contributed respectively by the external magnetic field and the magnetization:

In SI Units, $B = \mu_0(H + M)$

When the magnetic properties of the medium are linear and isotropic, the magnetization is directly proportional to the magnetic field strength:

$M = \chi_m H$ where χ_m is volume magnetic susceptibility.

Therefore, $B = \mu_0(1 + \chi_m)H$ and $B = \mu_0\mu_r H$ and $B = \mu H$

where, $\mu_r = (1 + \chi_m)$ is another dimensionless quantity called as relative permeability and $\mu = \mu_0\mu_r$ is called as the absolute permeability.

Based on relative magnetic field, a material can be classified as either Diamagnetic, Paramagnetic, and Ferromagnetic.

- Diamagnetic, $\mu_r \approx 1$ and $\mu_r < 1$
- Paramagnetic, $\mu_r \approx 1$ and $\mu_r > 1$
- Ferromagnetic, $\mu_r \gg 1$

Diamagnetic material have their magnetic moments cancel due to the symmetrical arrangement of its electrons. On application of magnetic field, a force is is applied on the orbiting electrons, thus causing a net magnetic moment. Diamagnetism arises mainly from the orbital motion of the electrons within an atom and is present in all materials. In most materials it is too weak to be of any practical importance. Examples of diamagnetic materials are bismuth, copper, lead, mercury, germanium, silver, gold, diamond. The diamagnetic effect is masked in paramagnetic and ferromagnetic materials. Diamagnetic materials exhibit no permanent magnetism, and the induced magnetic moment disappears when the applied field is withdrawn. [34]

Paramagnetic materials are materials which by atoms with electrons not symmetrically arranged. Thus have a net magnetic moment even in absence of magnetic field. On application of external magnetic field, in addition to inherent magnetic moment, these materials develop a magnetic moment like diamagnetic materials. Thus

they have a positive susceptibility. Paramagnetism arises mainly from the magnetic dipole moments of the spinning electrons. The alignment forces, acting upon molecular dipoles by the applied field, are counteracted by the deranging effects of thermal agitation. Unlike diamagnetism, which is essentially independent of temperature, the paramagnetic effect is temperature dependent, being stronger at lower temperatures where there is less thermal collision. Examples of paramagnetic materials include, aluminum, magnesium, titanium, and tungsten. [34]

Ferromagnetic materials are materials whose atoms are arranged with their magnetic moments in parallel so that they supplement, rather than cancel, one another unlike other paramagnetic or diamagnetic materials. They are iron, nickel, cobalt, dysprosium, and gadolinium; A number of alloys of these five elements, which include nonferromagnetic elements in their composition, also possess the property of ferromagnetism. Ferromagnetic materials are divided into many microscopic magnetic domains. These domains generally having 10^{15} to 10^{16} atoms, contain aligned magnetic dipoles due to spinning of electrons even in absence of magnetic field. In an unmagnetized state the magnetic moments of the adjacent domains in a ferromagnetic material have different directions. On application of external magnetic field, these magnetic domains get oriented in the same direction thus resulting in a very large magnetic moment. [34]

For weak applied fields, domain wall movements are reversible. But when an applied field becomes stronger, domain wall movements are no longer reversible, and domain rotation toward the direction of the applied field will also occur. This phenomenon of magnetization lagging behind the field producing it is called magnetic hysteresis. As the applied field becomes even much stronger, domain wall motion and domain rotation will cause essentially a total alignment of the microscopic magnetic moments with the applied field, at which point the magnetic material is said to

have reached saturation. The curve $OP_1P_2P_3$ on the B-H plane is called the normal magnetization curve as shown in Fig 36. [34]

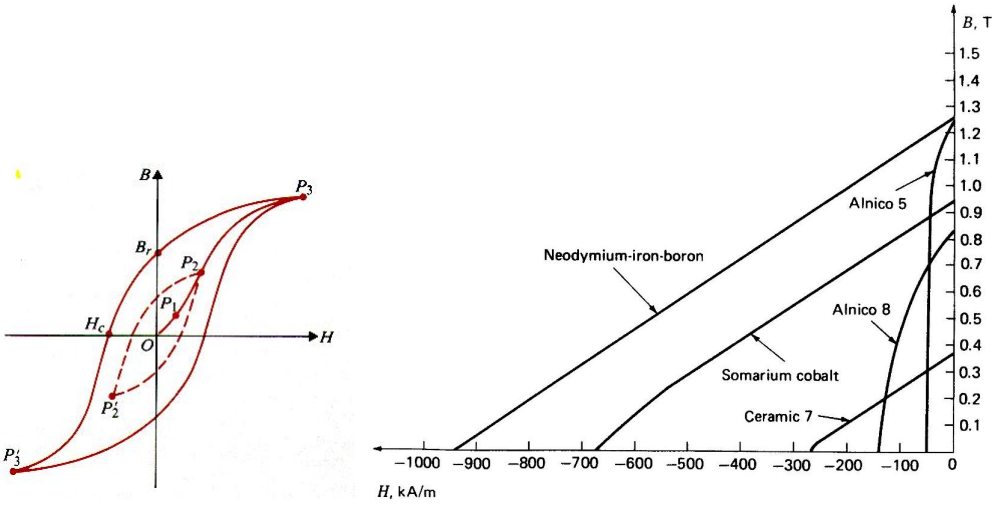

(a) a (b) b

Fig. 36. a. Hysteresis loops in the B-H plane for Permanent Magnets b. Demagnetization curves of Permanent Magnets [34]

If the applied magnetic field is reduced to zero from any value, the magnetic flux density does not go to zero but assumes the value at B_r. This value is called the residual or remanent flux density (in Wb/m^2 or T) and is dependent on the maximum applied field strength. The existence of a remanent flux density in a ferromagnetic material makes permanent magnets possible. To make the magnetic flux density of a specimen zero, it is necessary to apply a magnetic field strength H_c in the opposite direction. This required H_c is called coercive force or coercive field strength (in A/m). In other words, to demagnetize a saturated magnet, a certain magnetic field must be applied and this threshold depends on coercivity of the respective material. "'Hard"' materials have high coercivity whereas "'soft"' materials have low coercivity. [35]

Simple predictions about physical behavior of magnetic fields, sufficient for our experimental setup, can be done using magnetic circuit analogy. The study of mag-

netic circuits is also useful in identifying means for channeling the magnetic flux through the sample. For this analysis, the circuit should be closed containing magnetic flux. Magnetic circuits exploit the correspondence to electric circuits as shown in Fig 37. Magnetomotive Force(MMF) corresponding to EMF used to drive the magnetic flux through magnetic circuits. It is given as $MMF = H_c l_c$ where H_c is the magnetic field strength. Magnetic flux through the cross section of the circuit is given as $\phi_c = B_c A_c$, where ϕ_c is the magnetic flux, B_c is the magnetic flux density, A_c is the cross section area. B_c can be measured using a Gaussmeter and is given by the relation $B_c =_c$. Considering the analogy of electric circuits, for magnetic circuits magnetic flux can be described as $\phi = \frac{MMF}{R_c}$ where R is the magnetic reluctance of the circuit. Magnetic Reluctance can be thought as resistance in electric circuits and is given as $R_c = \frac{l_c}{\mu_c A_c}$. Kirchhoff's voltage laws in electric circuit theory can be used for Magnetic Reluctance as in $\sum R_c \phi_c = \sum MMF$ [35].

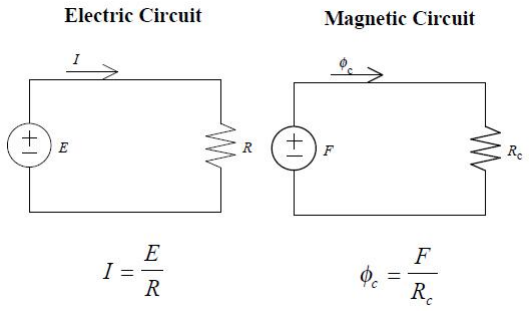

Fig. 37. Magnetic Circuit[35]

Magnetic Circuit for Permanent Magnets with linear demagnetization curve can be treated as described. Considering a piece of permanent magnet of a uniform cross sectional area of A_m and a length l_m, and the demagnetization curve of the magnet is a straight line with a coercive force of H_c and a remanent flux density of B_r as shown in Fig 36. The demagnetization curve can be expressed analytically as

$B_m = \frac{B_r}{H_c}(H_m + H_c)$ or $B_m = \mu_m(H_m + H_c)$ [35].

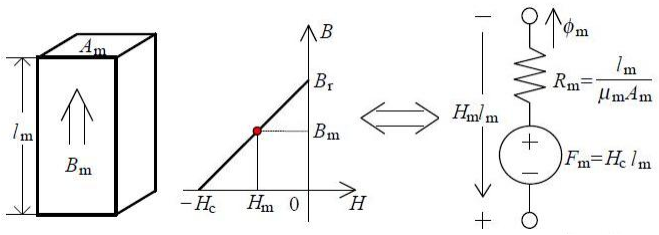

Fig. 38. Magnetic Circuit Model for Permanent Magnet with Linear Demagnetization Curve [35]

The magnetic voltage drop across the magnet can be expressed as $H_m l_m = (\frac{B_m}{\mu_m} - H_c)l_m = R_m\phi_m - F_m$ where $R_m = \frac{l_m}{\mu_m A_m}$ is reluctance and $F_m = H_c l_m$ is the magnetomotive force.It is noted that B_m and H_m are opposite in direction.

However, there are a few limitations in using this analogy which should be noted.

- Electric Circuits represent flow of electrons whereas Magnetic Circuits do not represent any actual flow.
- Leakage in electric circuits is very minimal, which is not the case of magnetic circuits.
- Magnetic Circuits are non-linear, that is reluctance is not constant, as in resistance and varies with magnetic field. At high magnetic fluxes, when the circuit saturates,limiting the magnetic flux and thus reluctance increases rapidly.

APPENDIX F

RAW RESULTS PLOTS

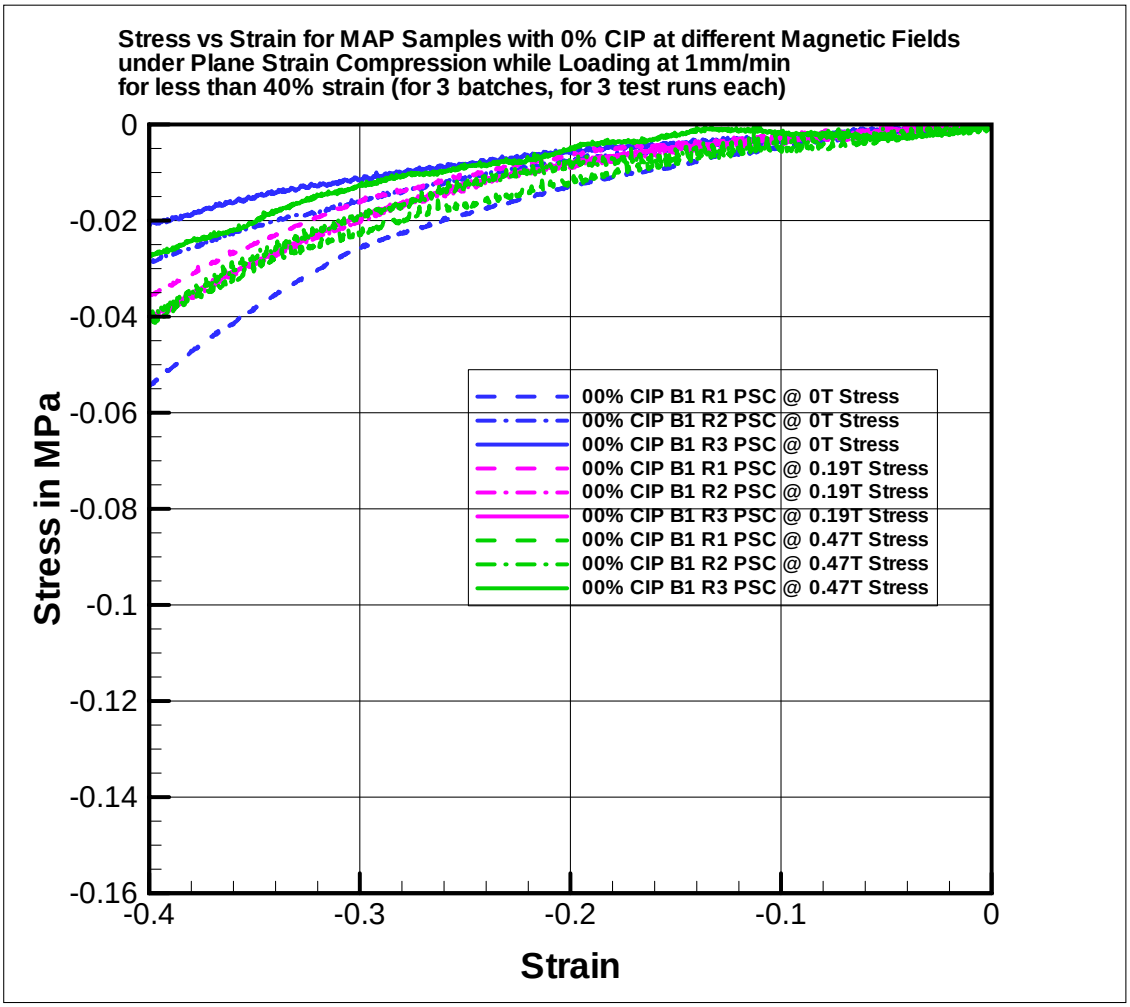

Fig. 39. Stress vs Strain Plot for Sample with 0% CIP and Batch 1

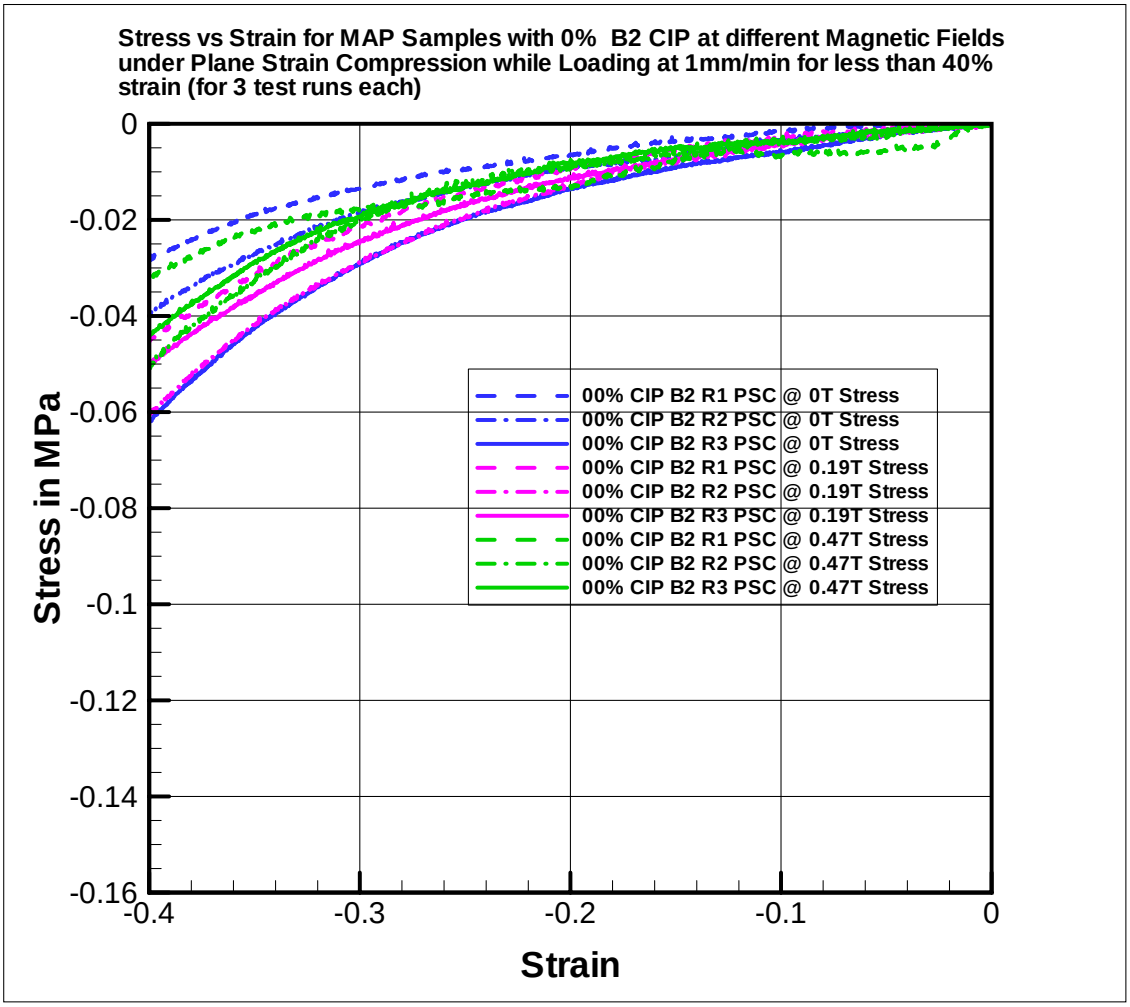

Fig. 40. Stress vs Strain Plot for Sample with 0% CIP and Batch 2

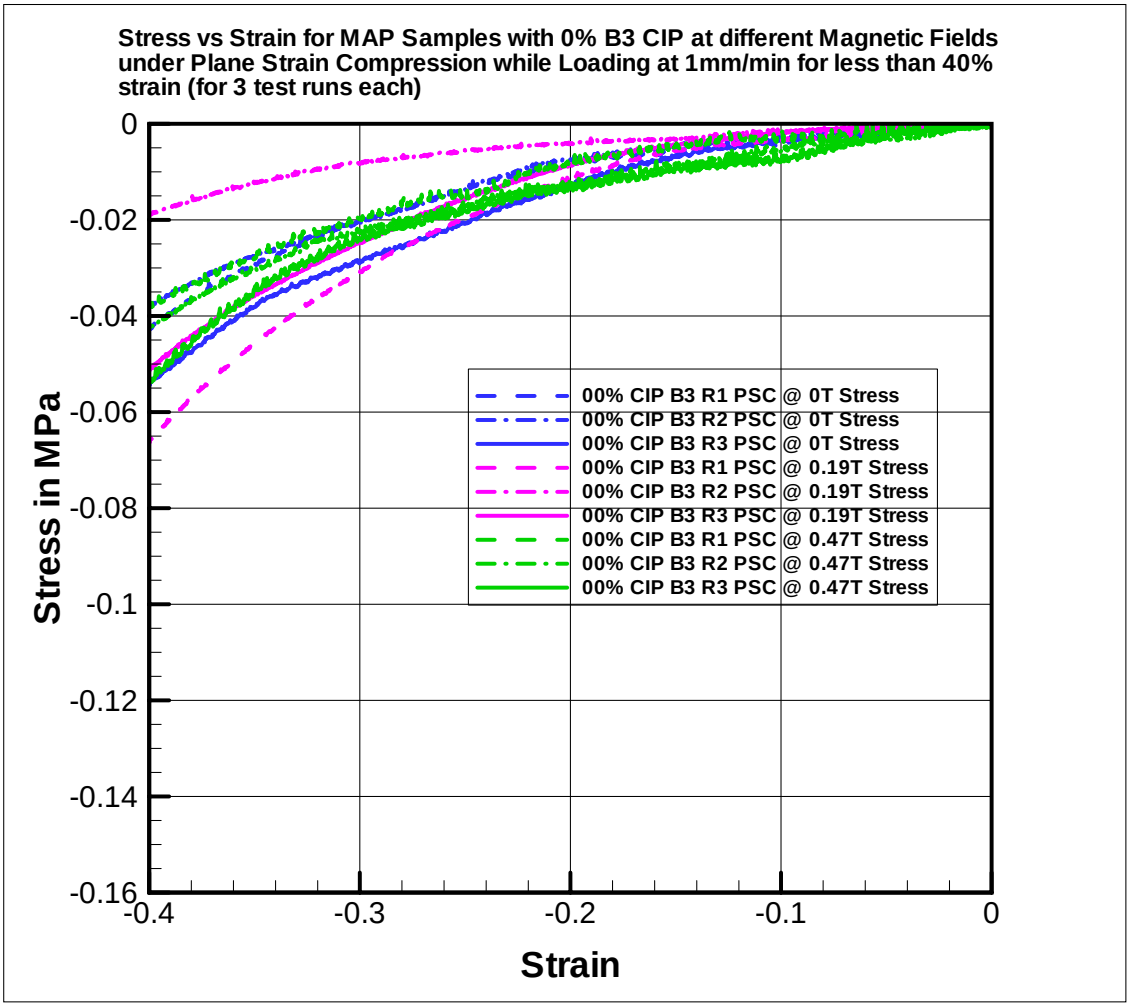

Fig. 41. Stress vs Strain Plot for Sample with 0% CIP and Batch 3

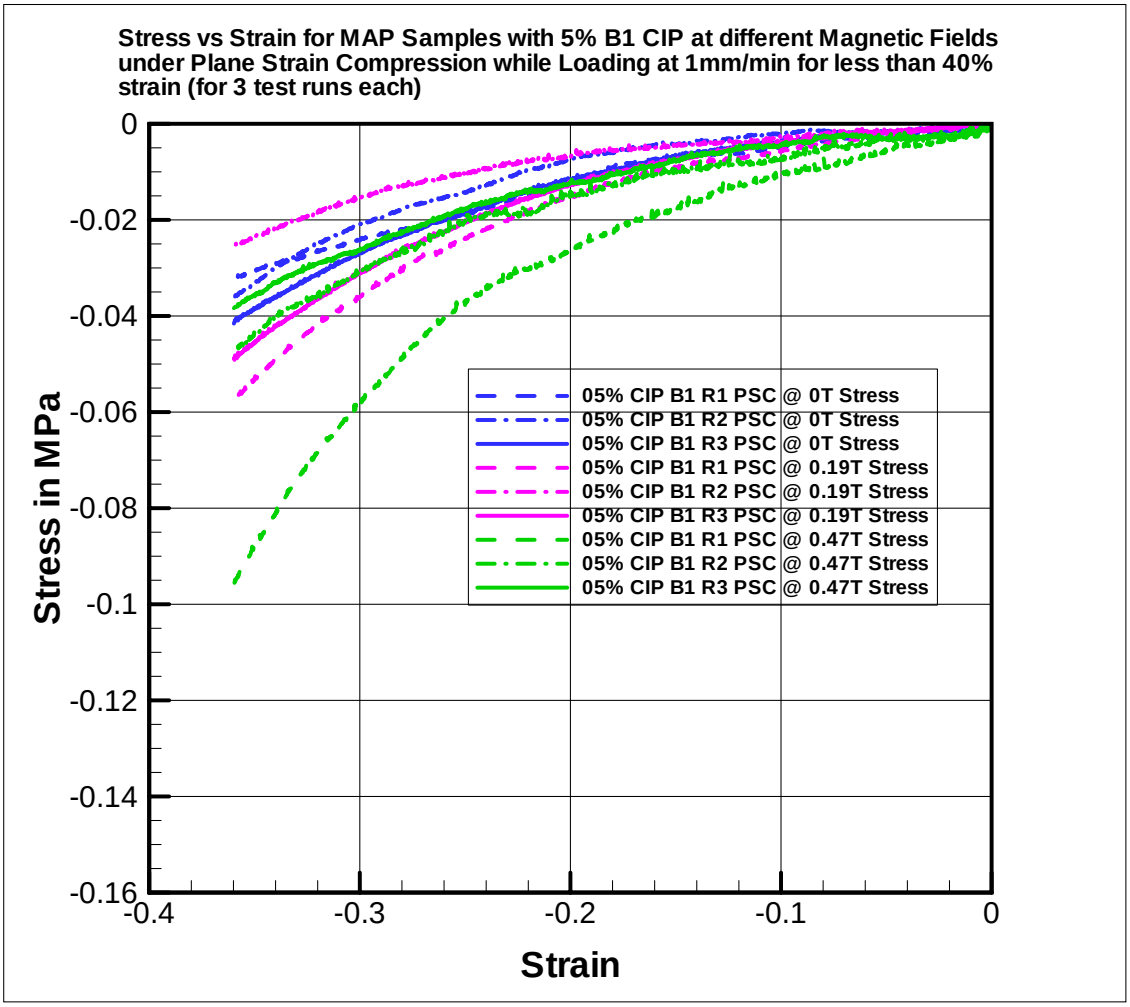

Fig. 42. Stress vs Strain Plot for Sample with 5% CIP and Batch 1

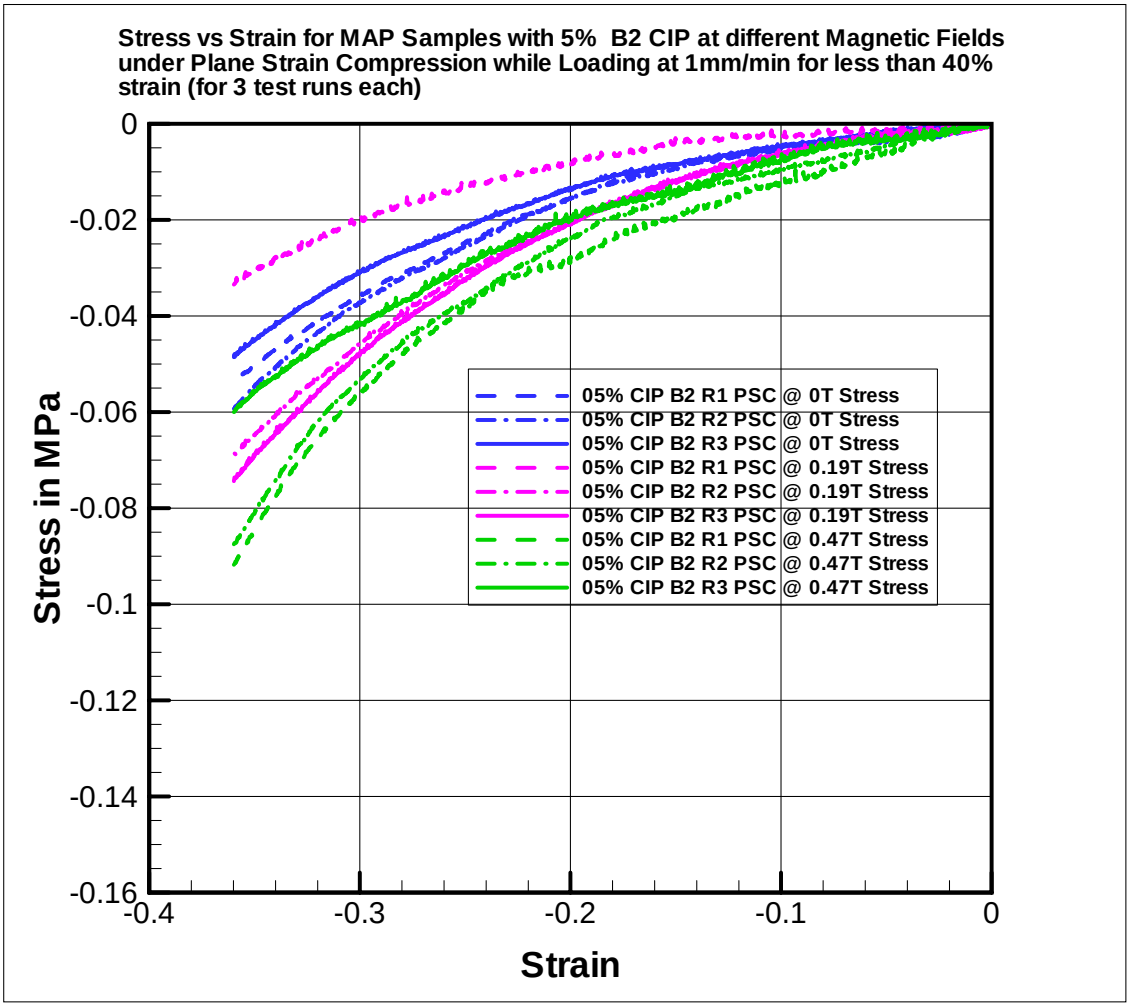

Fig. 43. Stress vs Strain Plot for Sample with 5% CIP and Batch 2

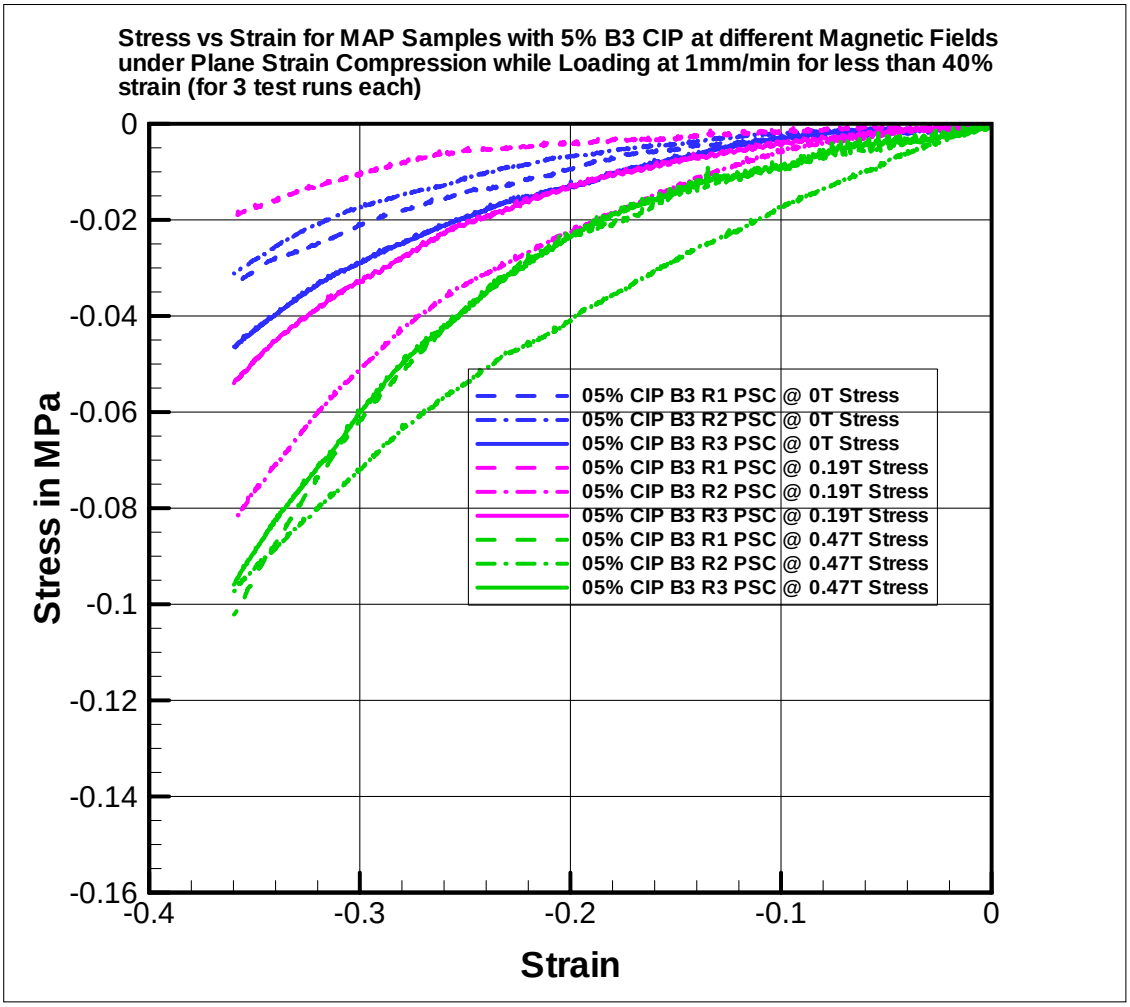

Fig. 44. Stress vs Strain Plot for Sample with 5% CIP and Batch 3

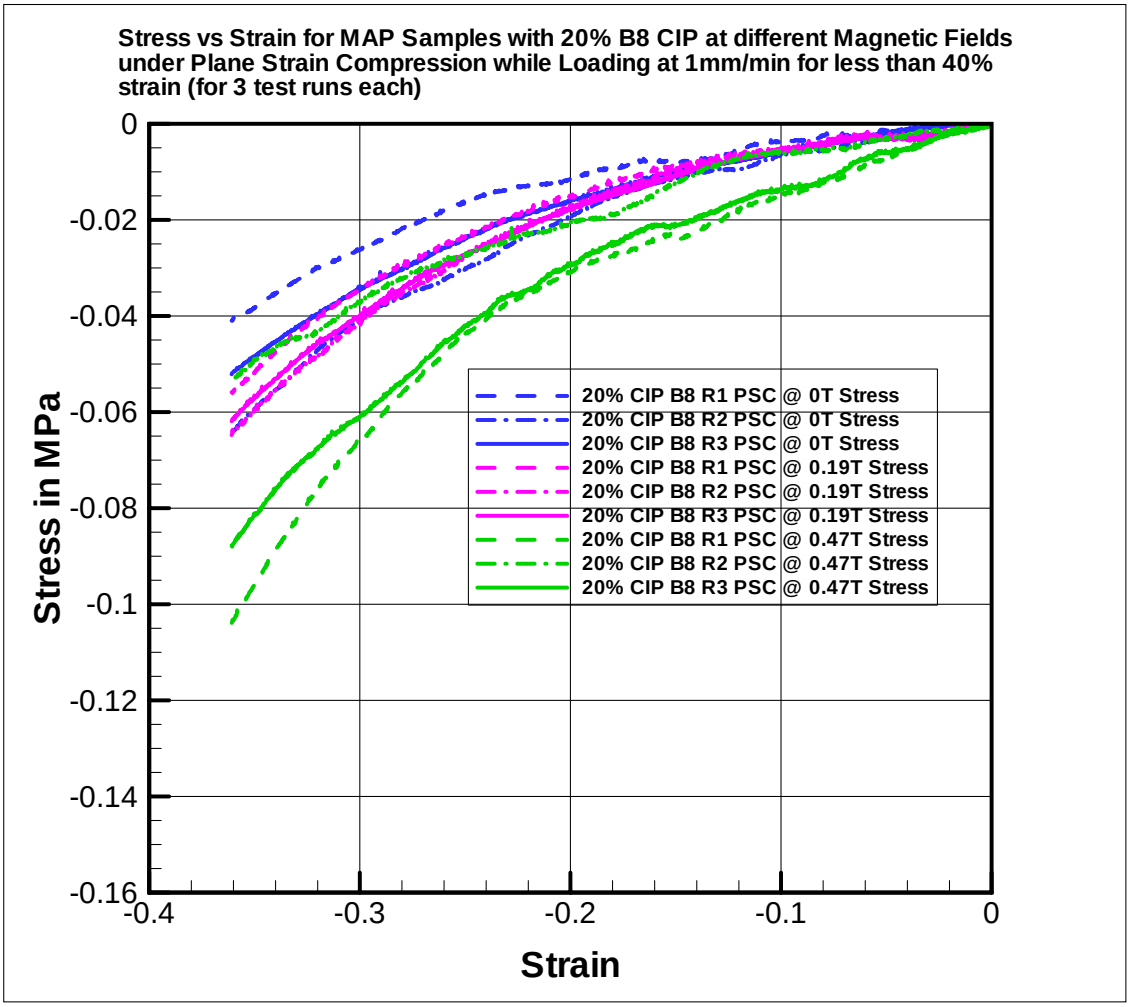

Fig. 45. Stress vs Strain Plot for Sample with 20% CIP and Batch 1

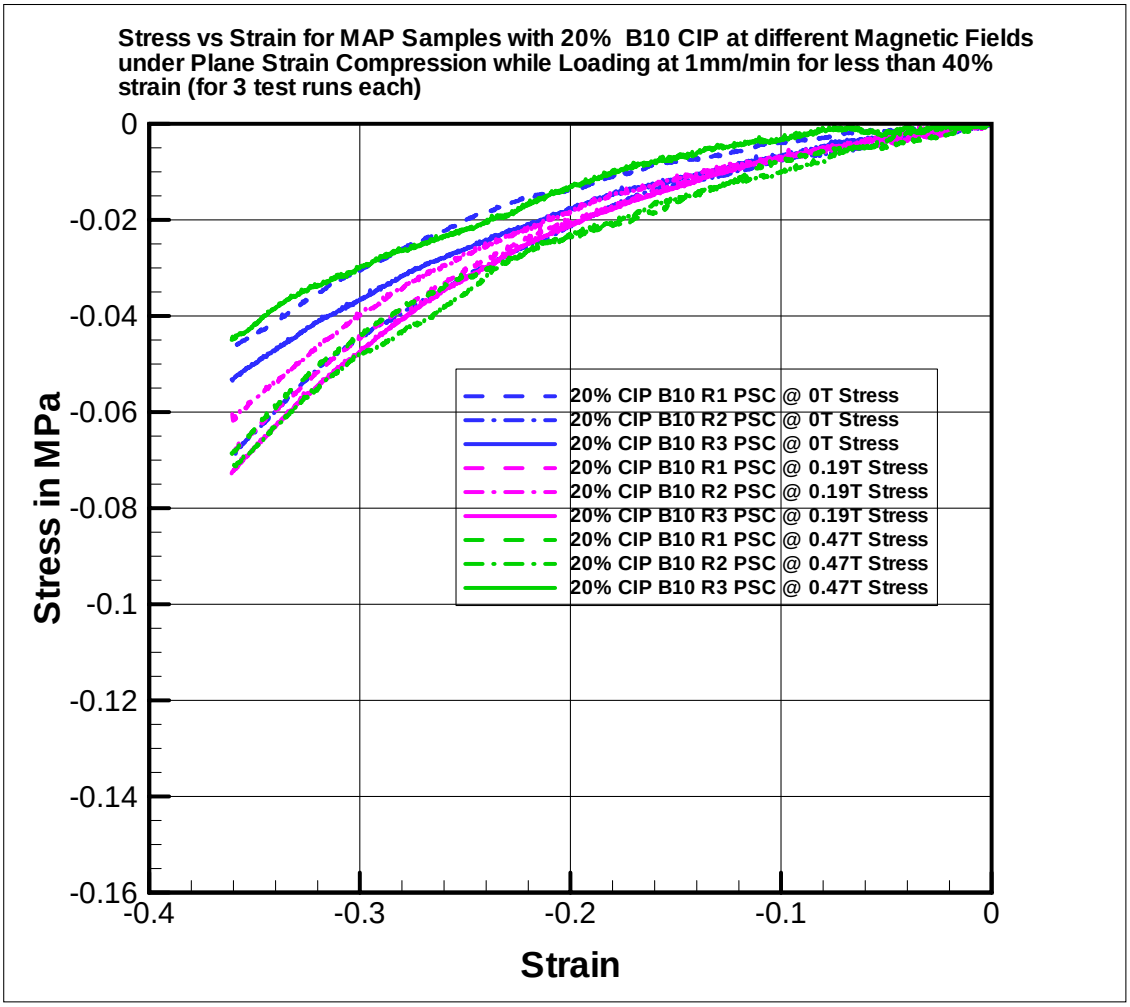

Fig. 46. Stress vs Strain Plot for Sample with 20% CIP and Batch 2

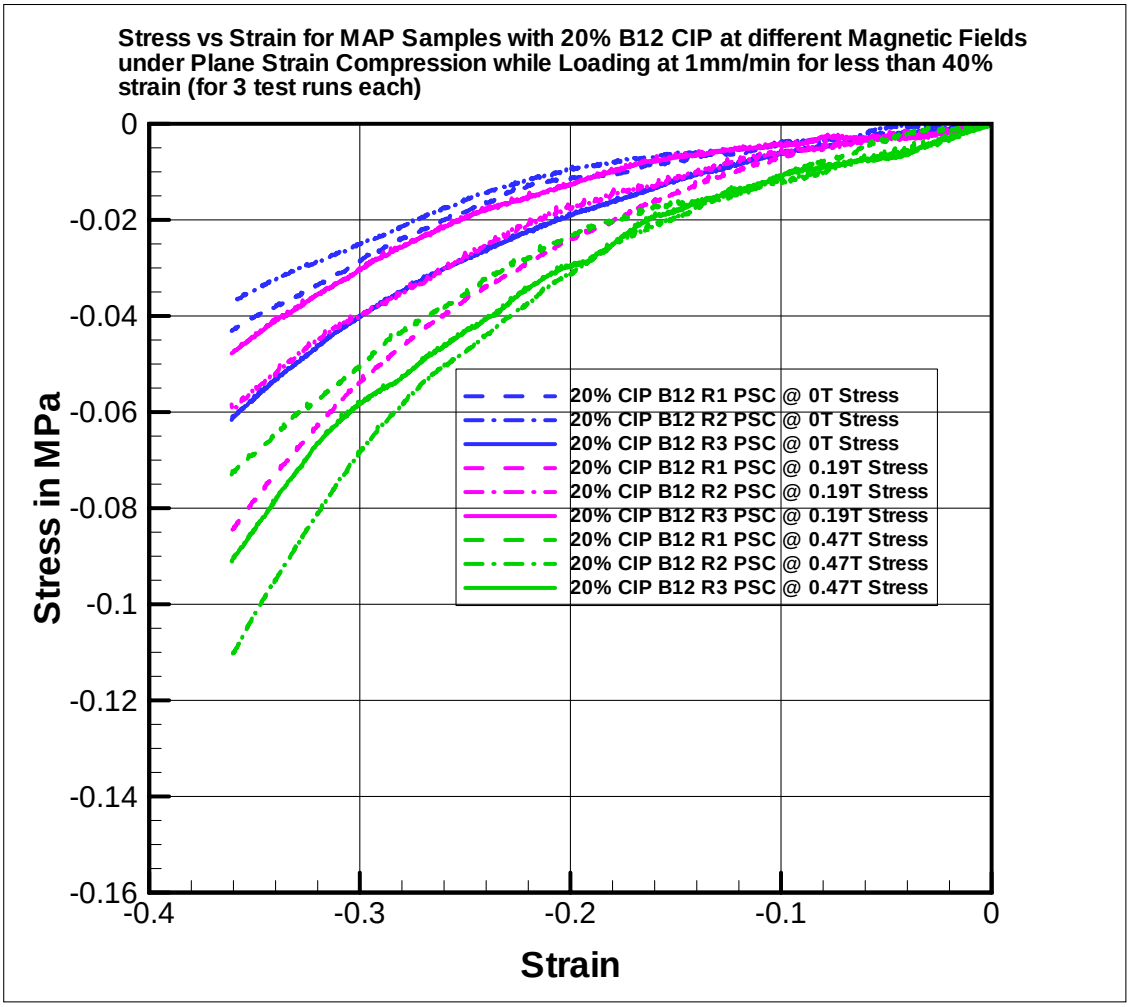

Fig. 47. Stress vs Strain Plot for Sample with 20% CIP and Batch 3

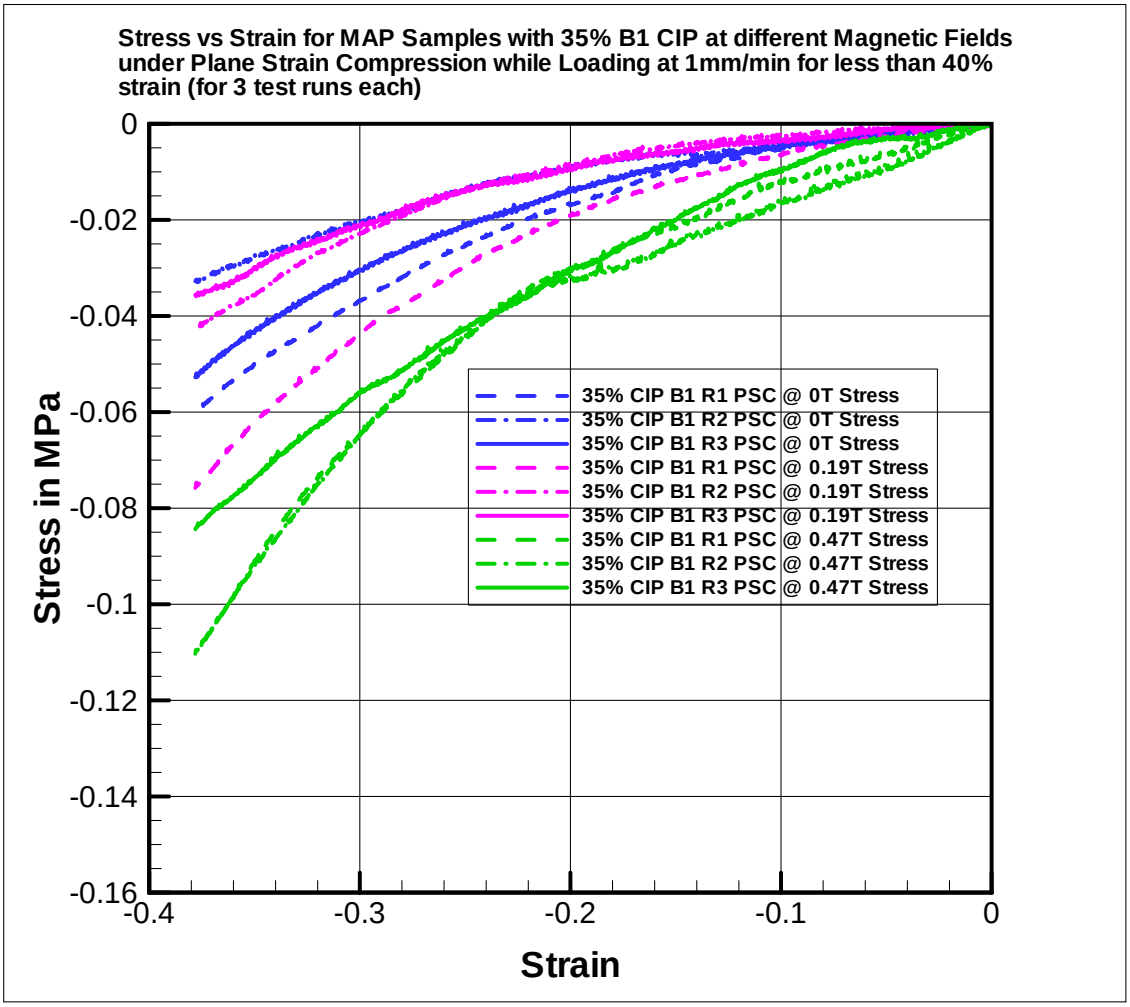

Fig. 48. Stress vs Strain Plot for Sample with 35% CIP and Batch 1

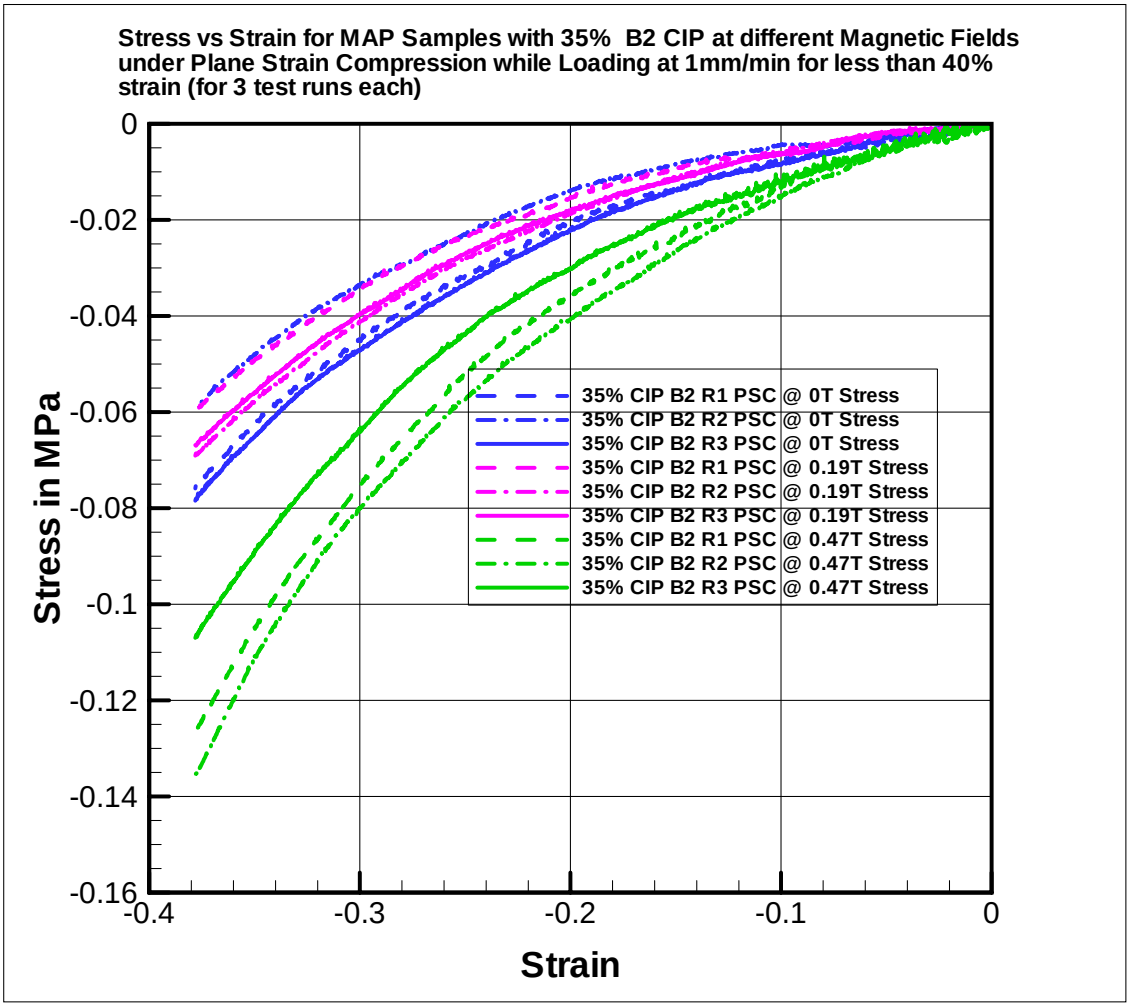

Fig. 49. Stress vs Strain Plot for Sample with 35% CIP and Batch 2

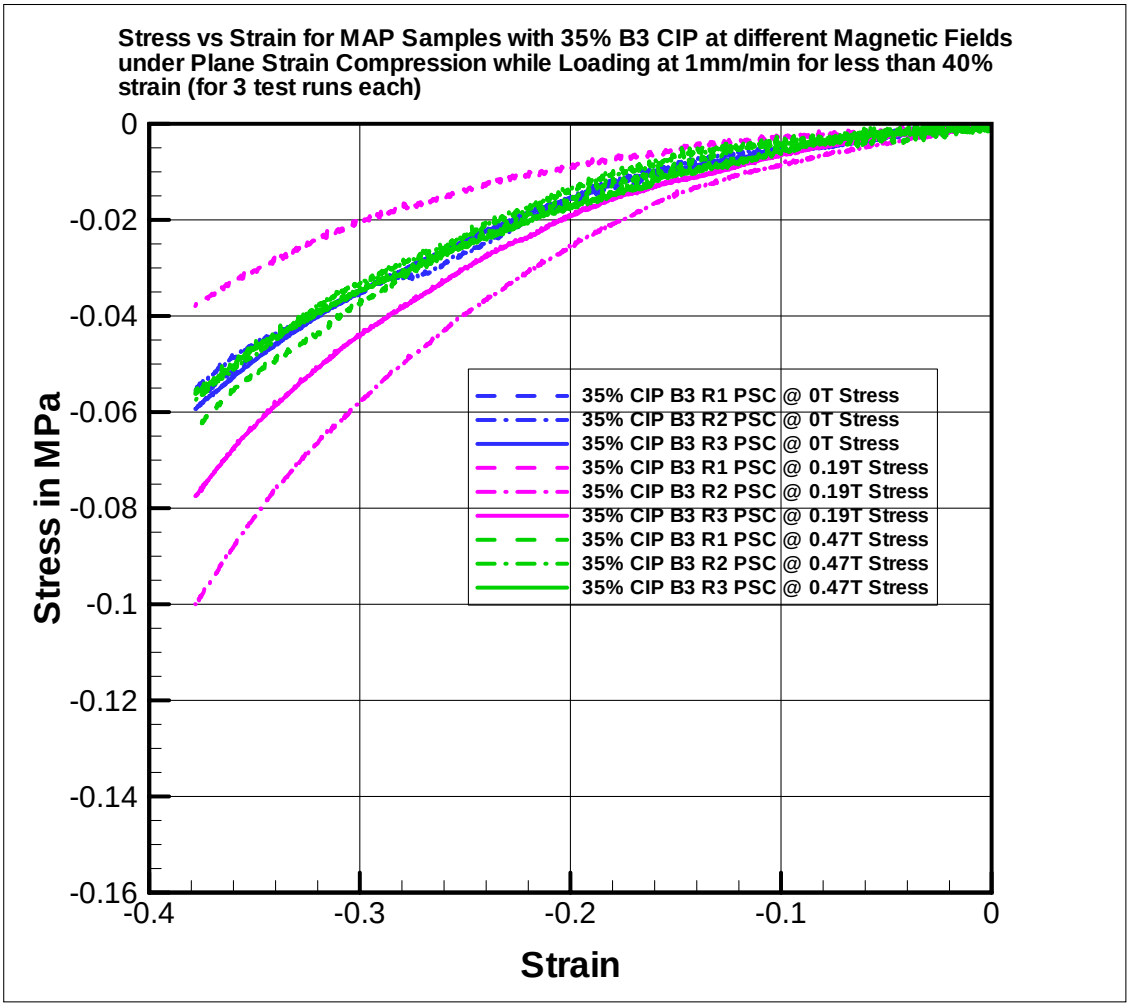

Fig. 50. Stress vs Strain Plot for Sample with 35% CIP and Batch 3

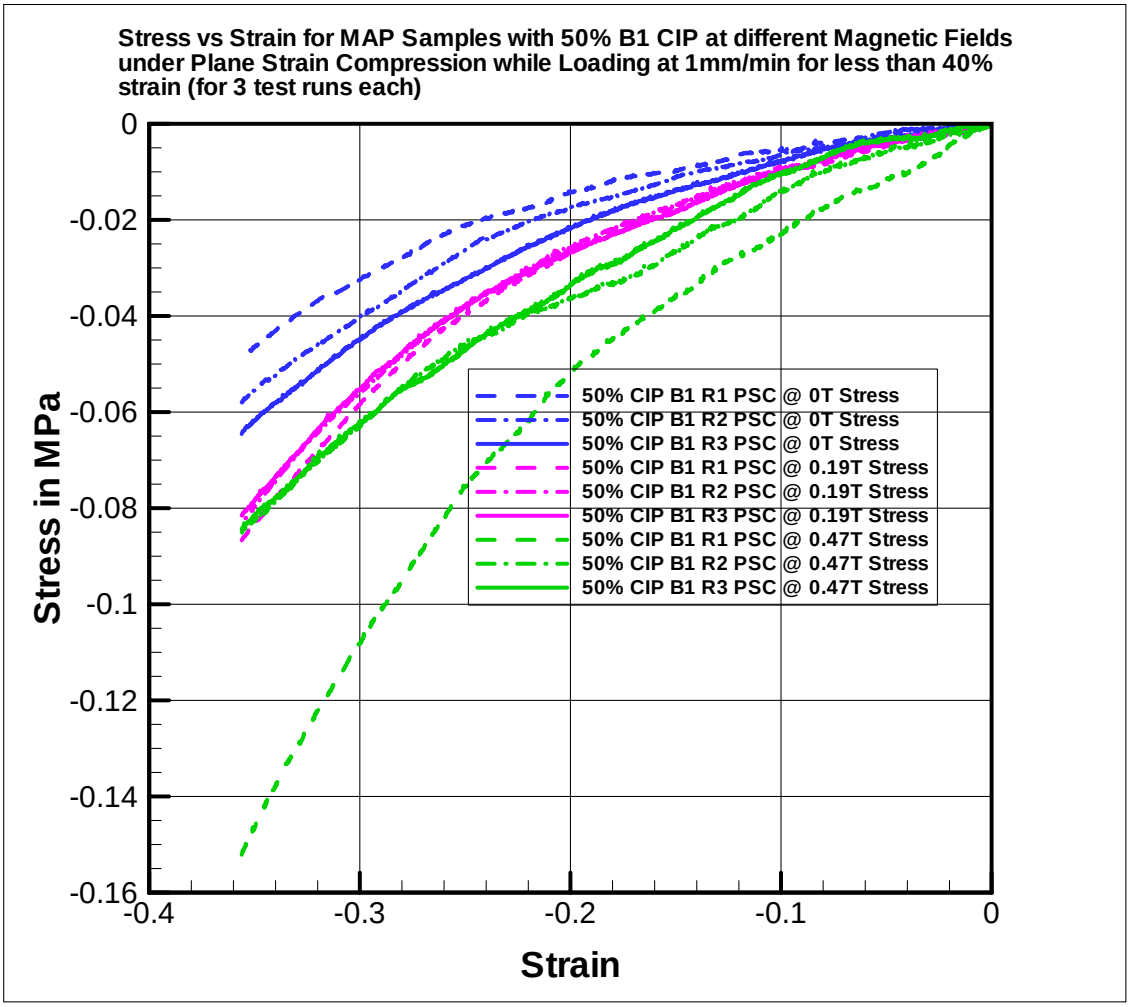

Fig. 51. Stress vs Strain Plot for Sample with 50% CIP and Batch 1

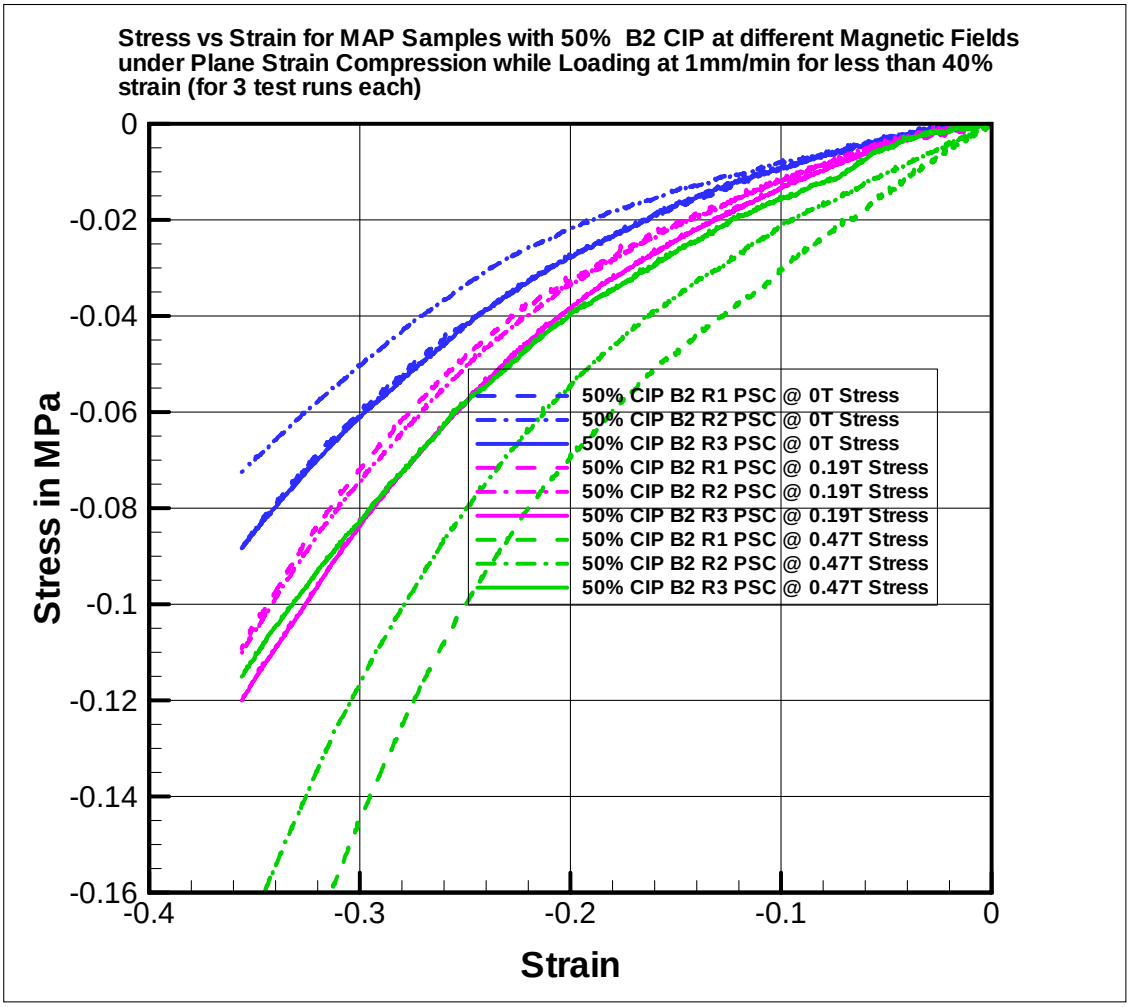

Fig. 52. Stress vs Strain Plot for Sample with 50% CIP and Batch 2

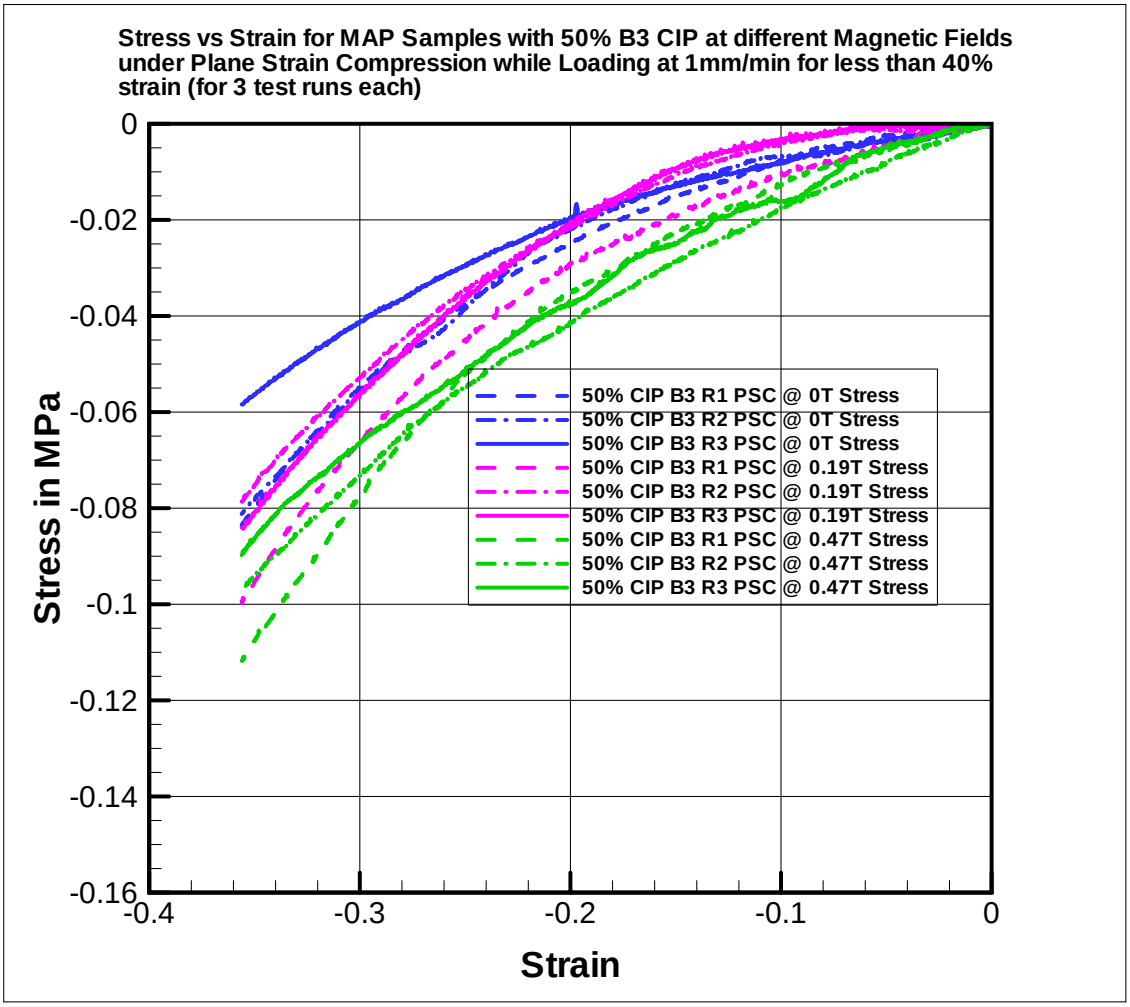

Fig. 53. Stress vs Strain Plot for Sample with 50% CIP and Batch 3

APPENDIX G

MODEL FITTING PLOTS

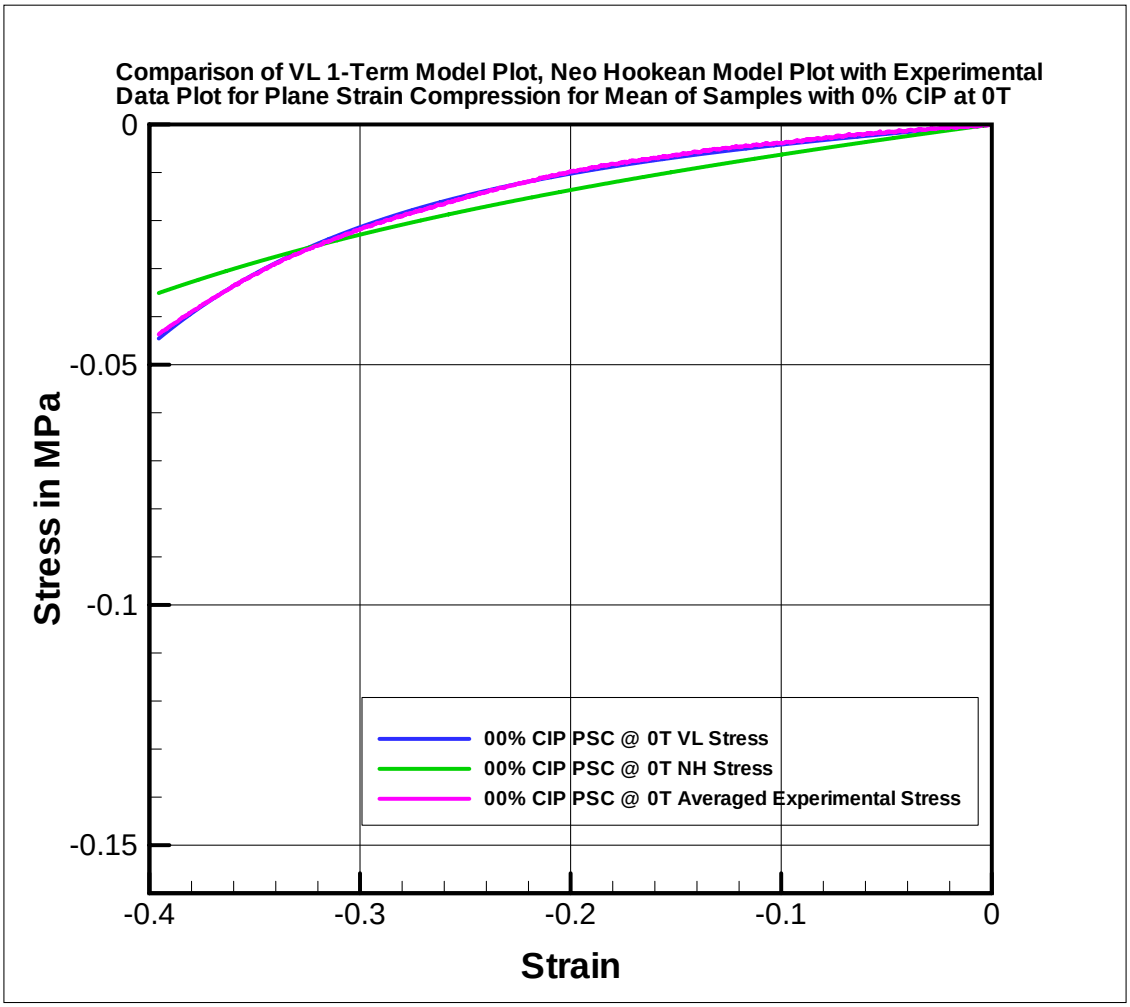

Fig. 54. 0% CIP 0T Model Fitting. $\mu_{VL} = 0.00336 MPa, and \mu_{NH} = 0.011070 MPa$

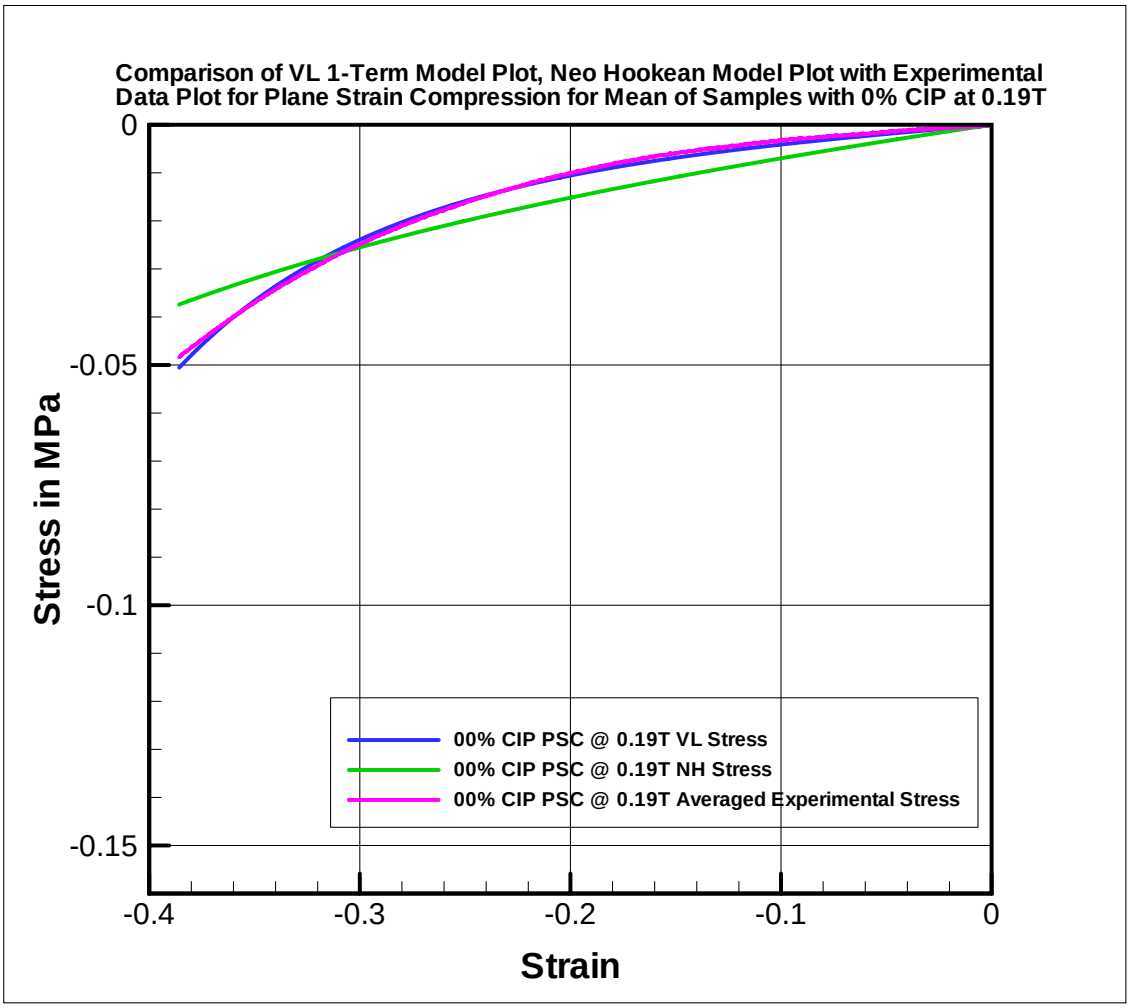

Fig. 55. 0% CIP 0.19T Model Fitting $\mu_{VL} = 0.0032386MPa, and \mu_{NH} = 0.011045MPa$

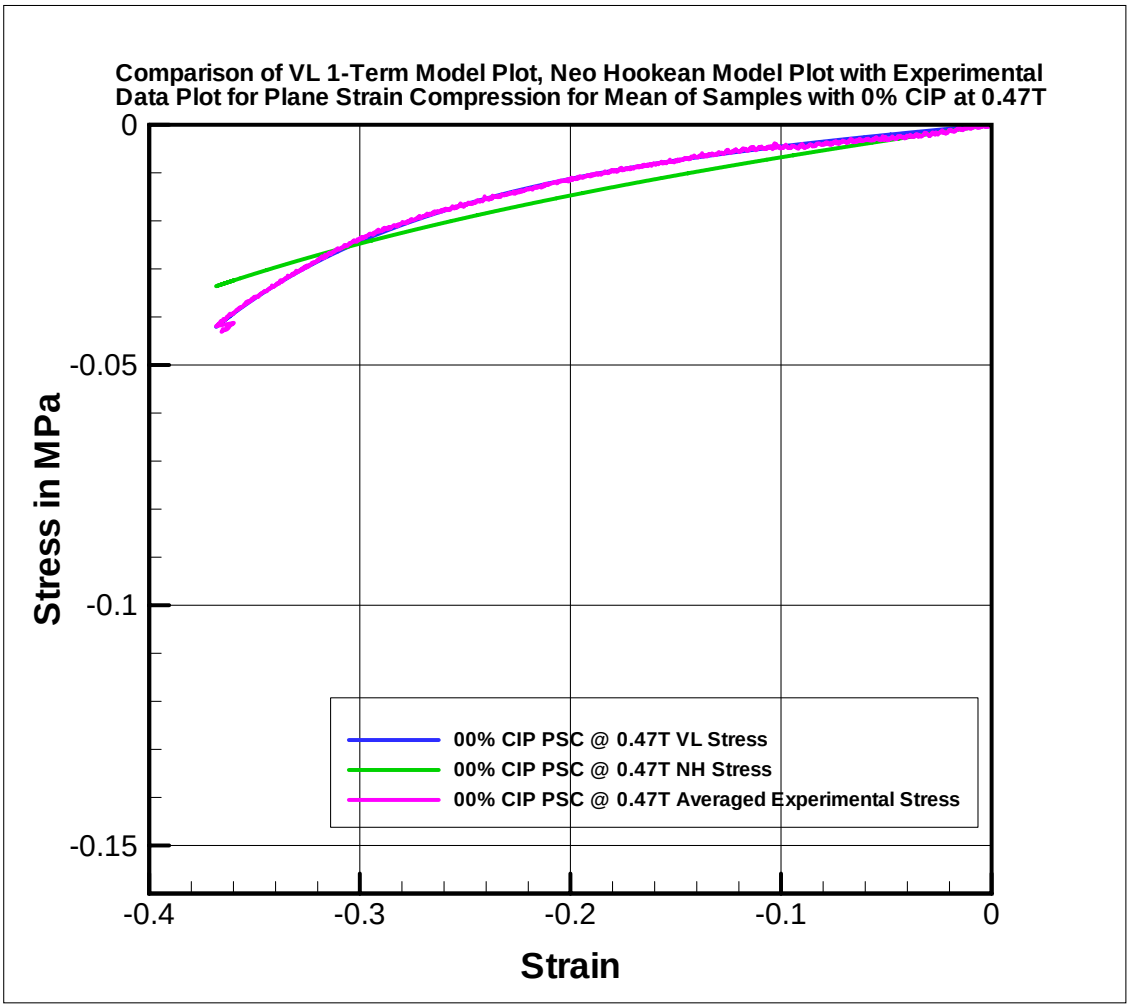

Fig. 56. 0% CIP 0.47T Model Fitting $\mu_{VL} = 0.0039340MPa, and \mu_{NH} = 0.012384MPa$

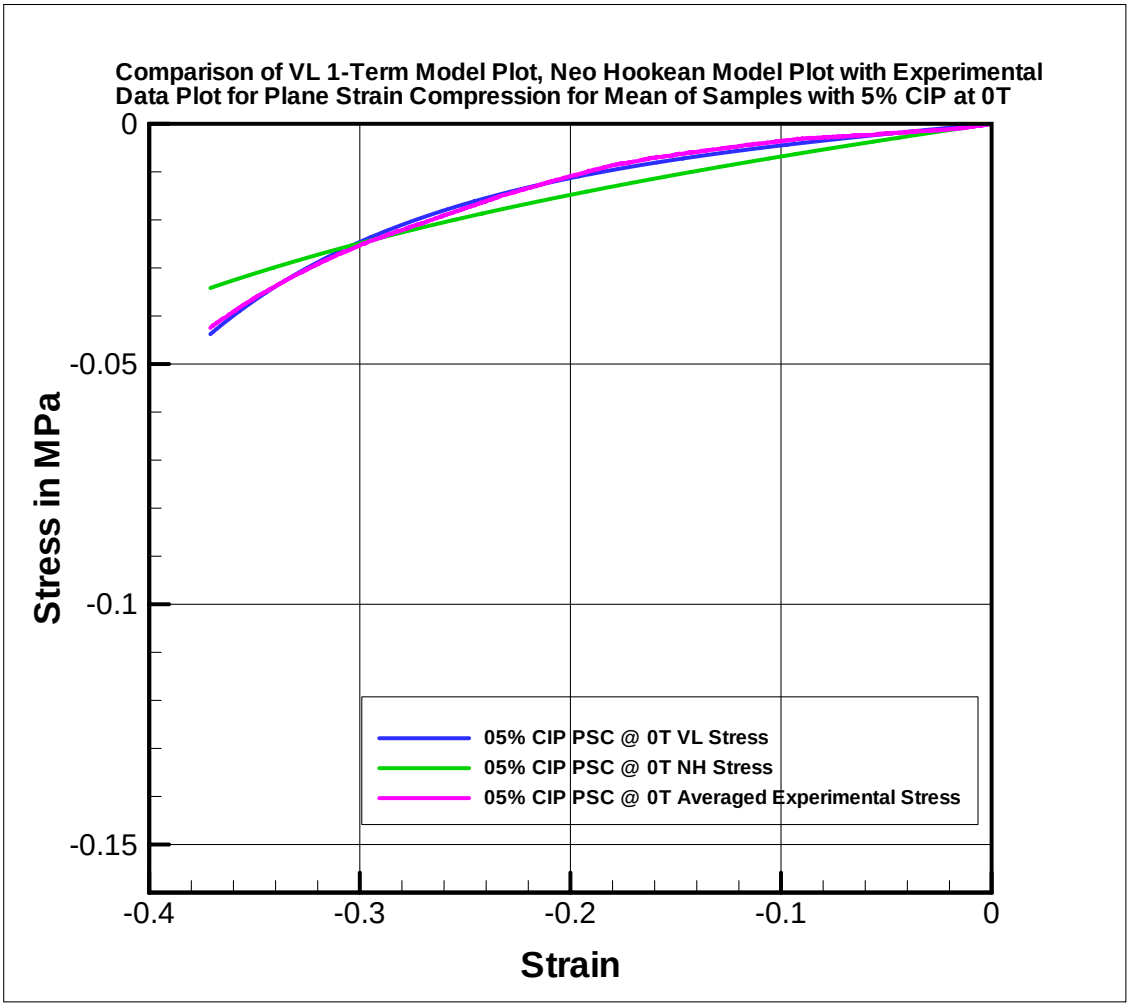

Fig. 57. 5% CIP 0T Model Fitting $\mu_{VL} = 0.003880MPa, and \mu_{NH} = 0.011659MPa$

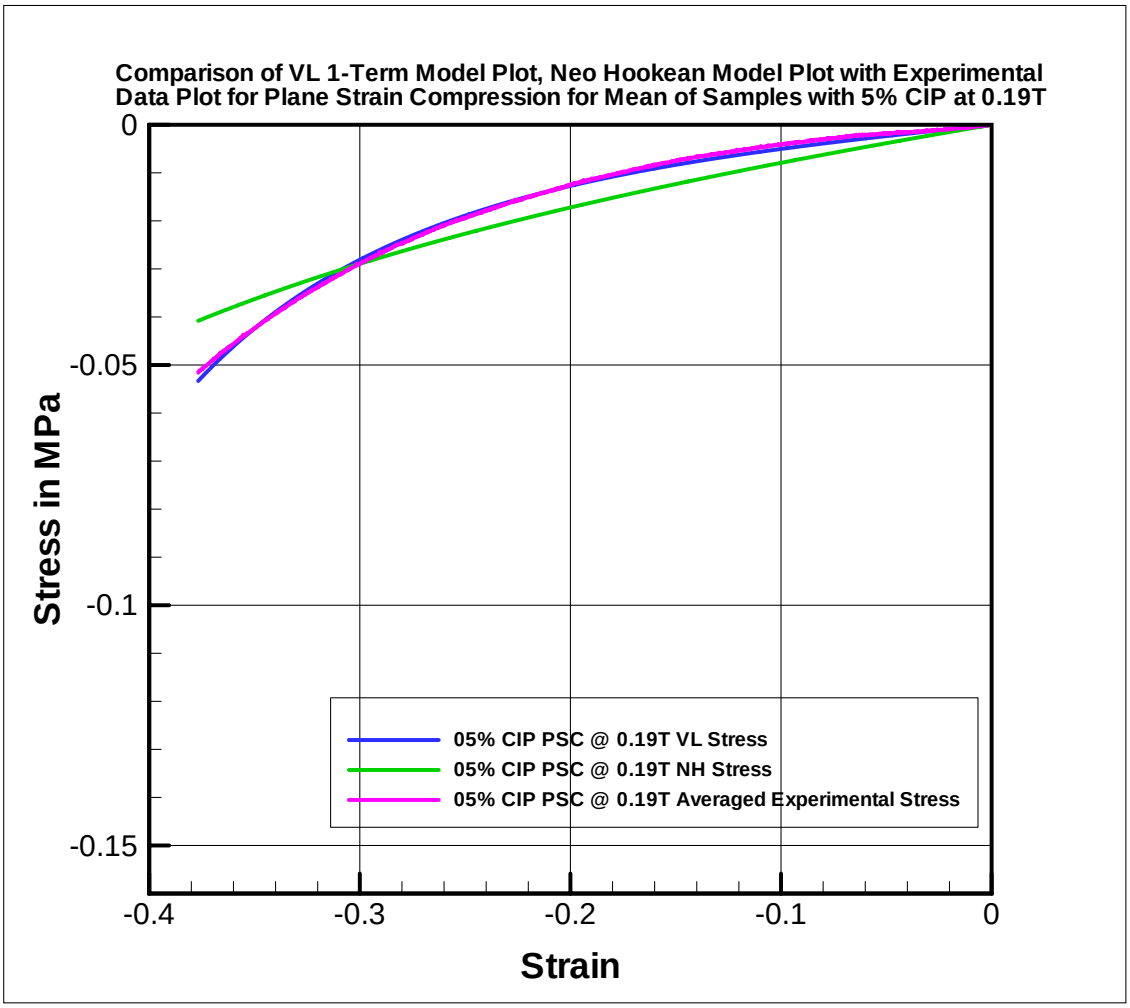

Fig. 58. 5% CIP 0.19T Model Fitting $\mu_{VL} = 0.004207MPa, and \mu_{NH} = 0.013376MPa$

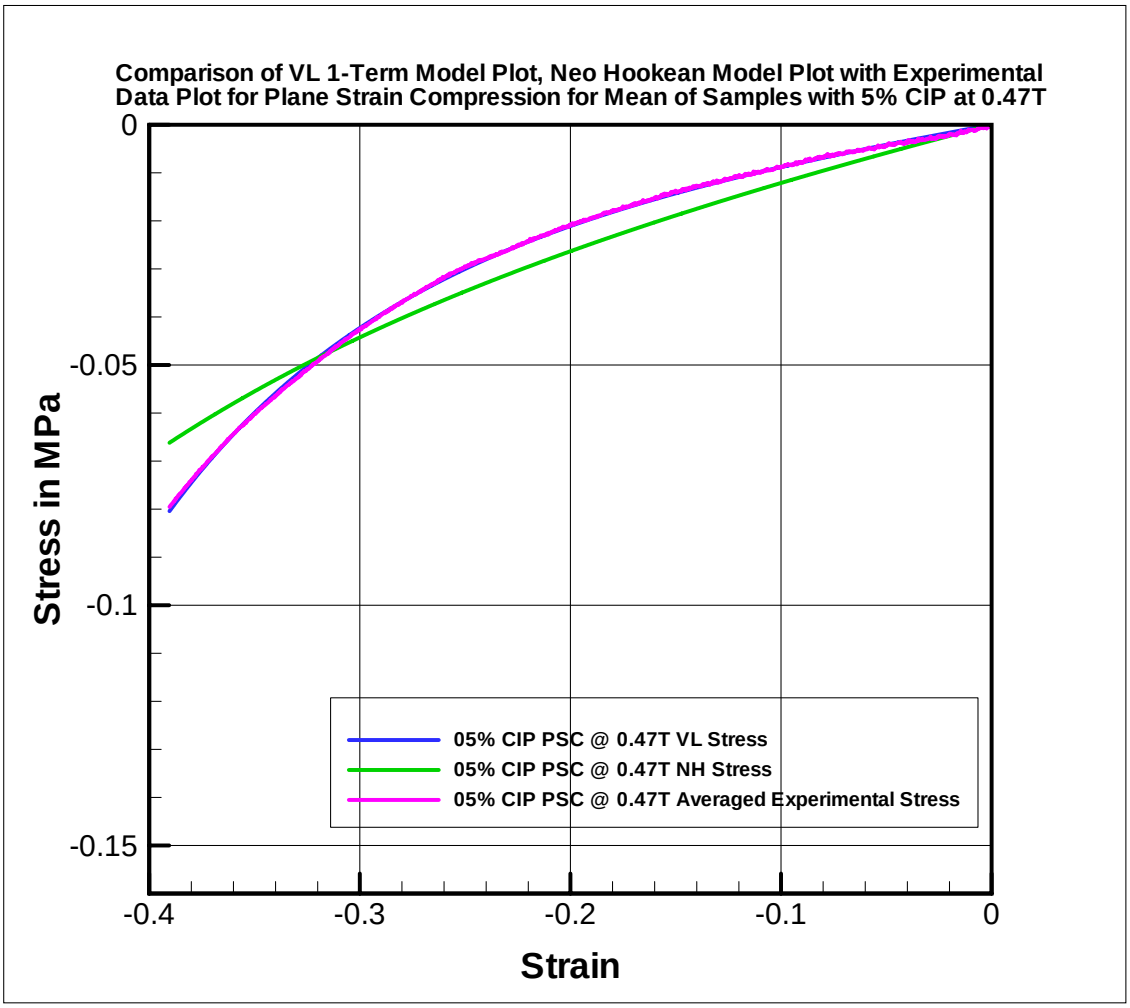

Fig. 59. 5% CIP 0.47T Model Fitting $\mu_{VL} = 0.009117MPa, and \mu_{NH} = 0.02294MPa$

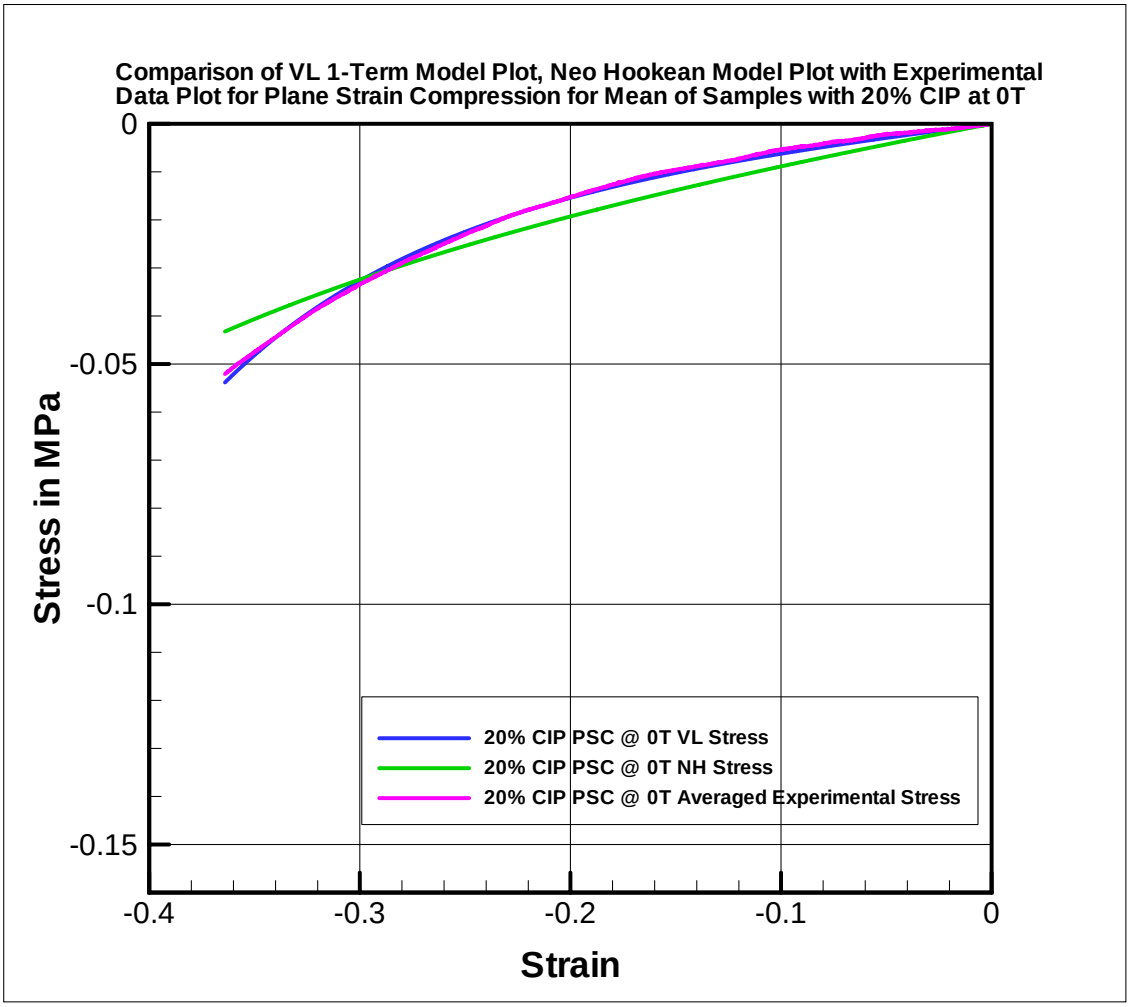

Fig. 60. 20% CIP 0T Model Fitting $\mu_{VL} = 0.005635MPa, and \mu_{NH} = 0.016036MPa$

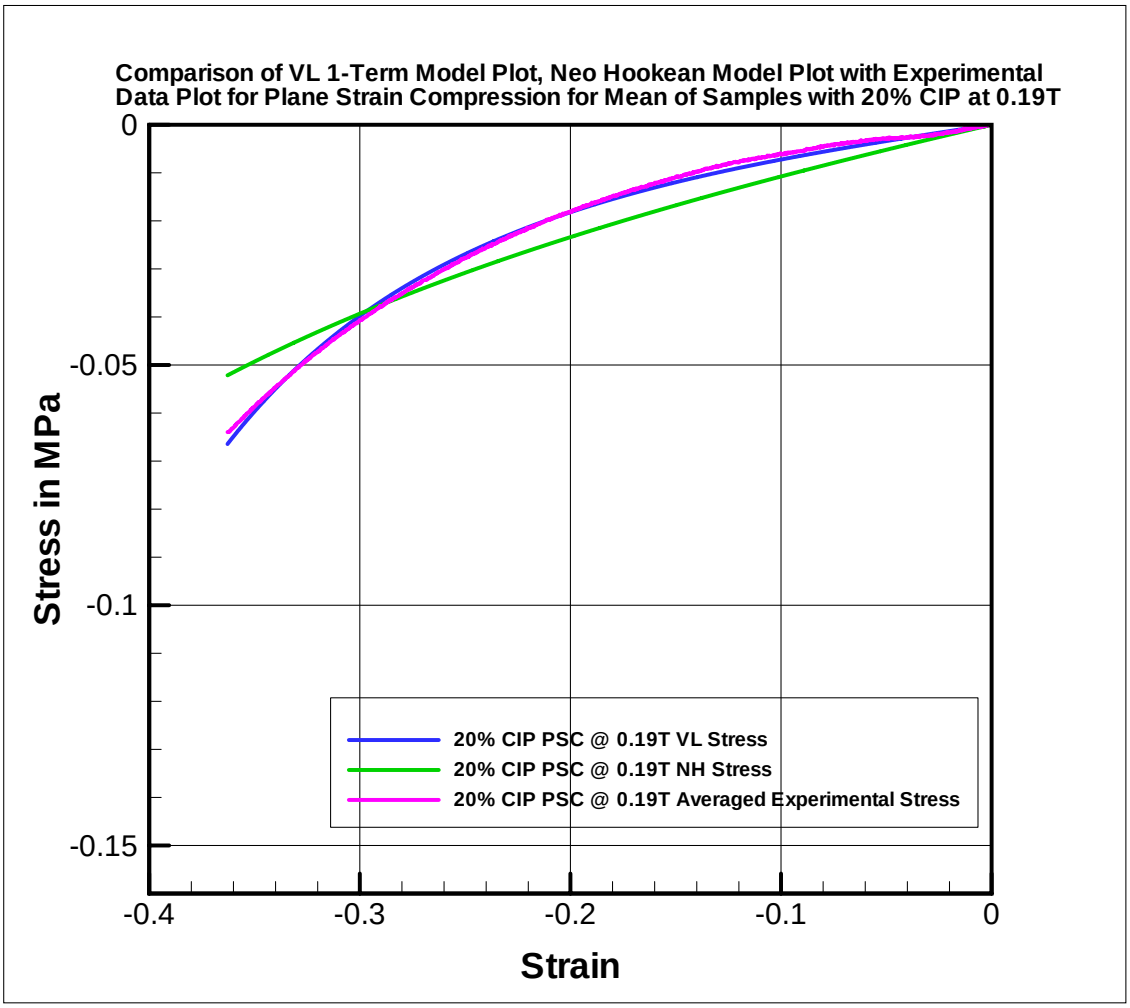

Fig. 61. 20% CIP 0.19T Model Fitting $\mu_{VL} = 0.006167MPa, and \mu_{NH} = 0.018840MPa$

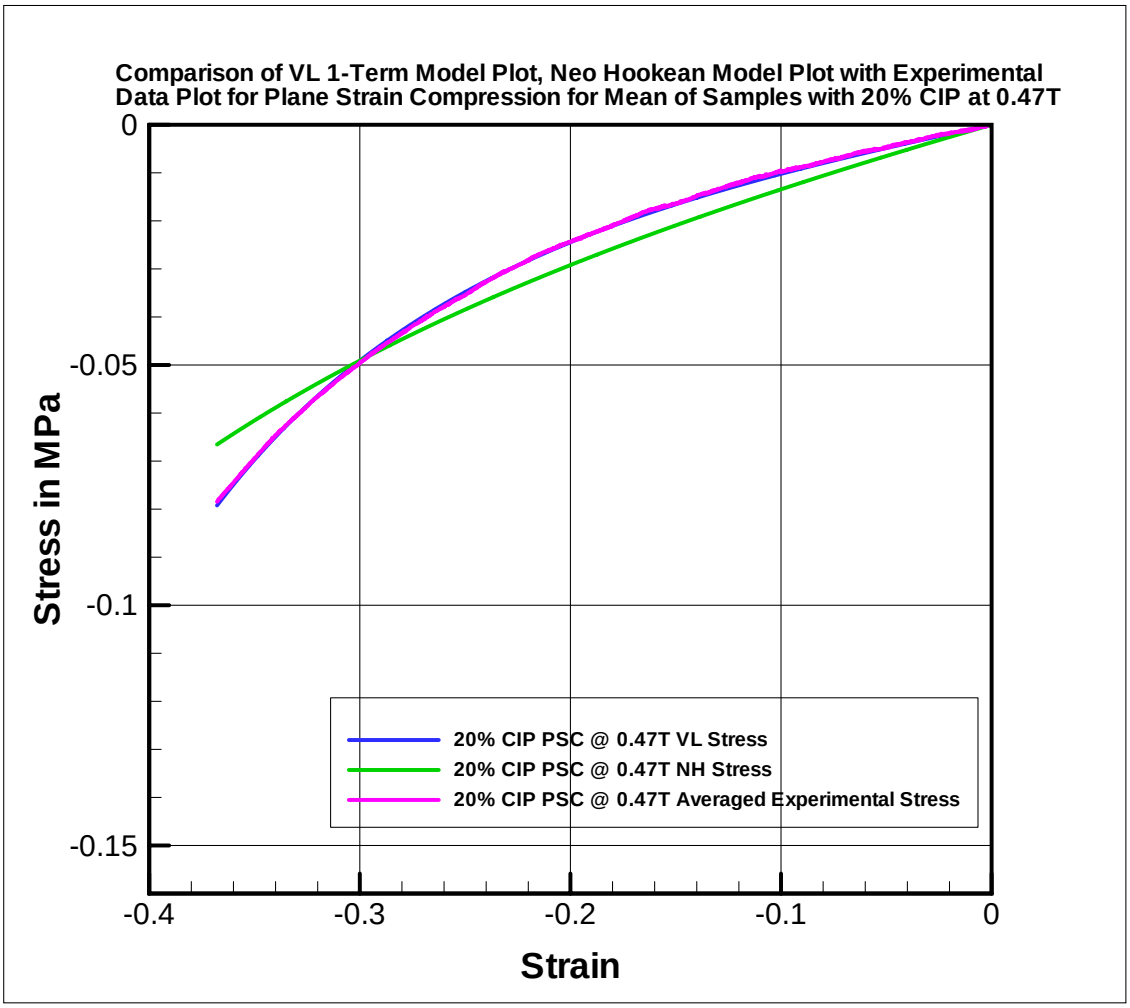

Fig. 62. 20% CIP 0.47T Model Fitting $\mu_{VL} = 0.010543MPa, and \mu_{NH} = 0.026071MPa$

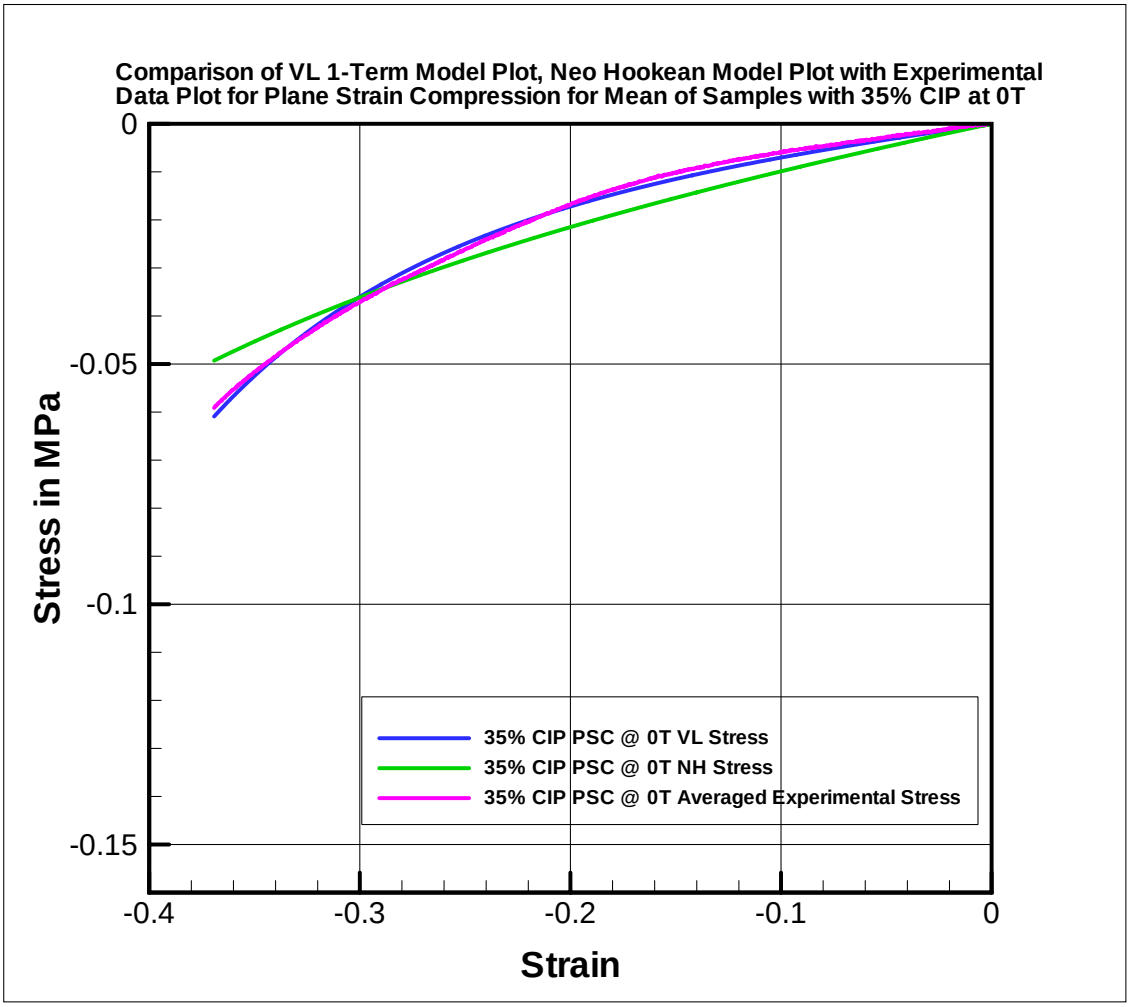

Fig. 63. 35% CIP 0T Model Fitting $\mu_{VL} = 0.006581 MPa, and \mu_{NH} = 0.017869 MPa$

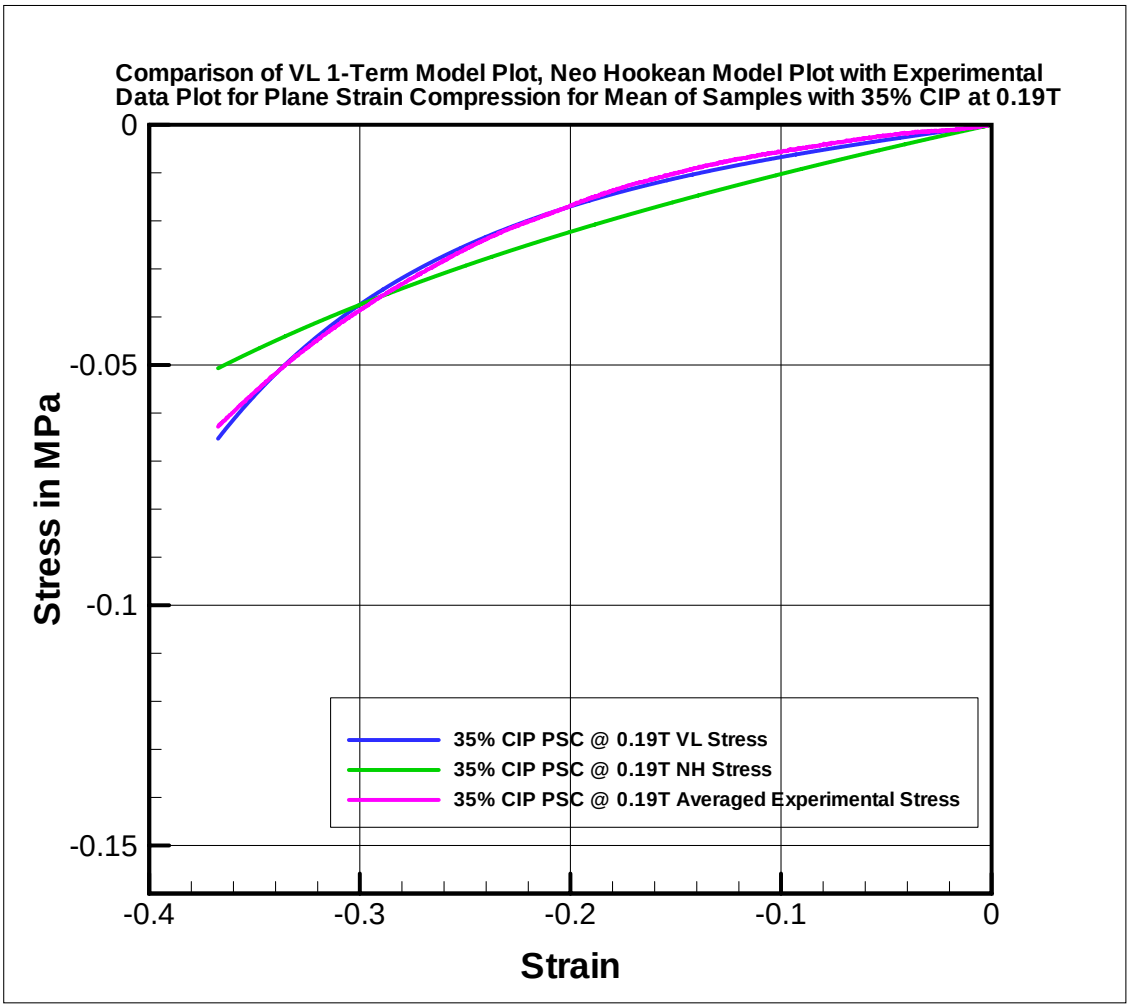

Fig. 64. 35% CIP 0.19T Model Fitting $\mu_{VL} = 0.005652MPa, and \mu_{NH} = 0.017572MPa$

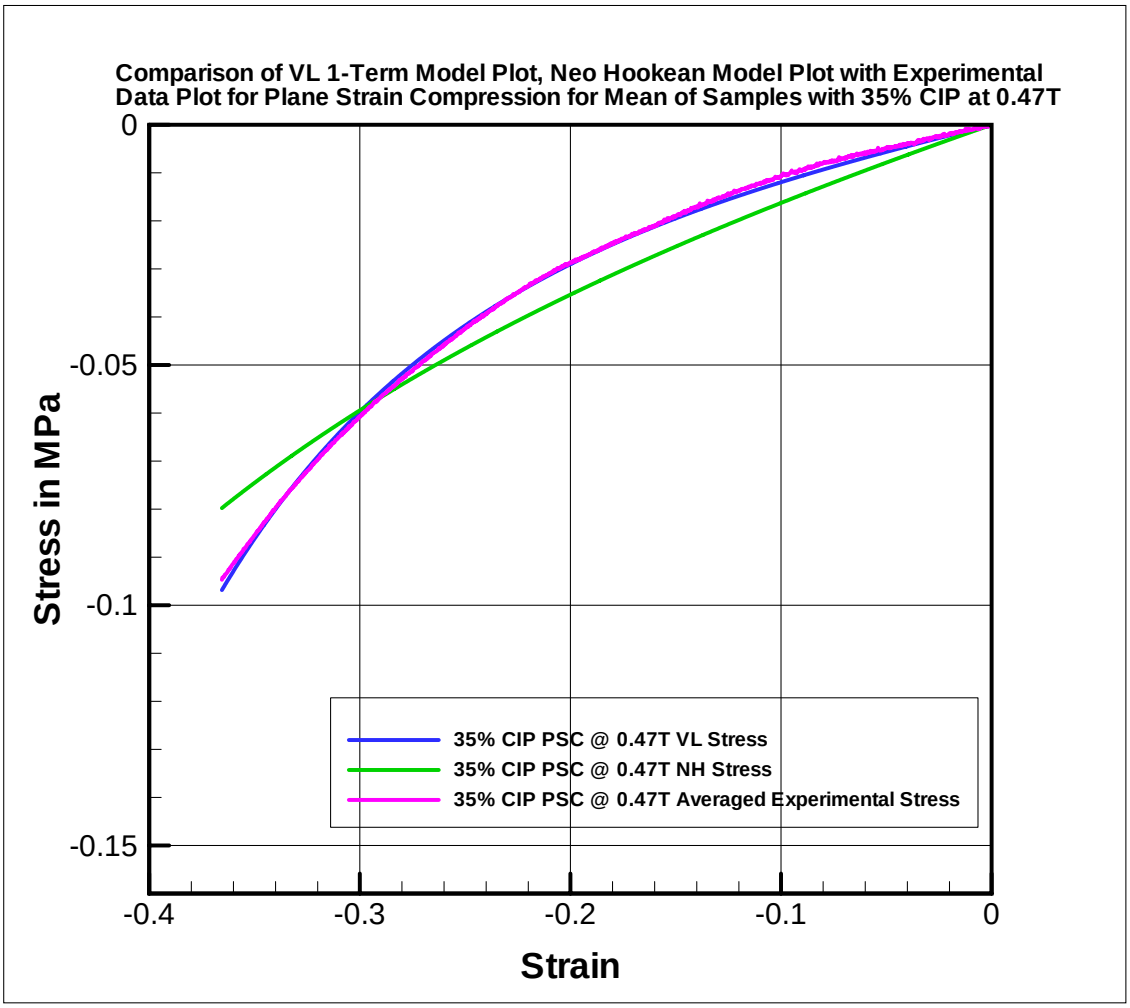

Fig. 65. 35% CIP 0.47T Model Fitting $\mu_{VL} = 0.01172MPa, and \mu_{NH} = 0.030615MPa$

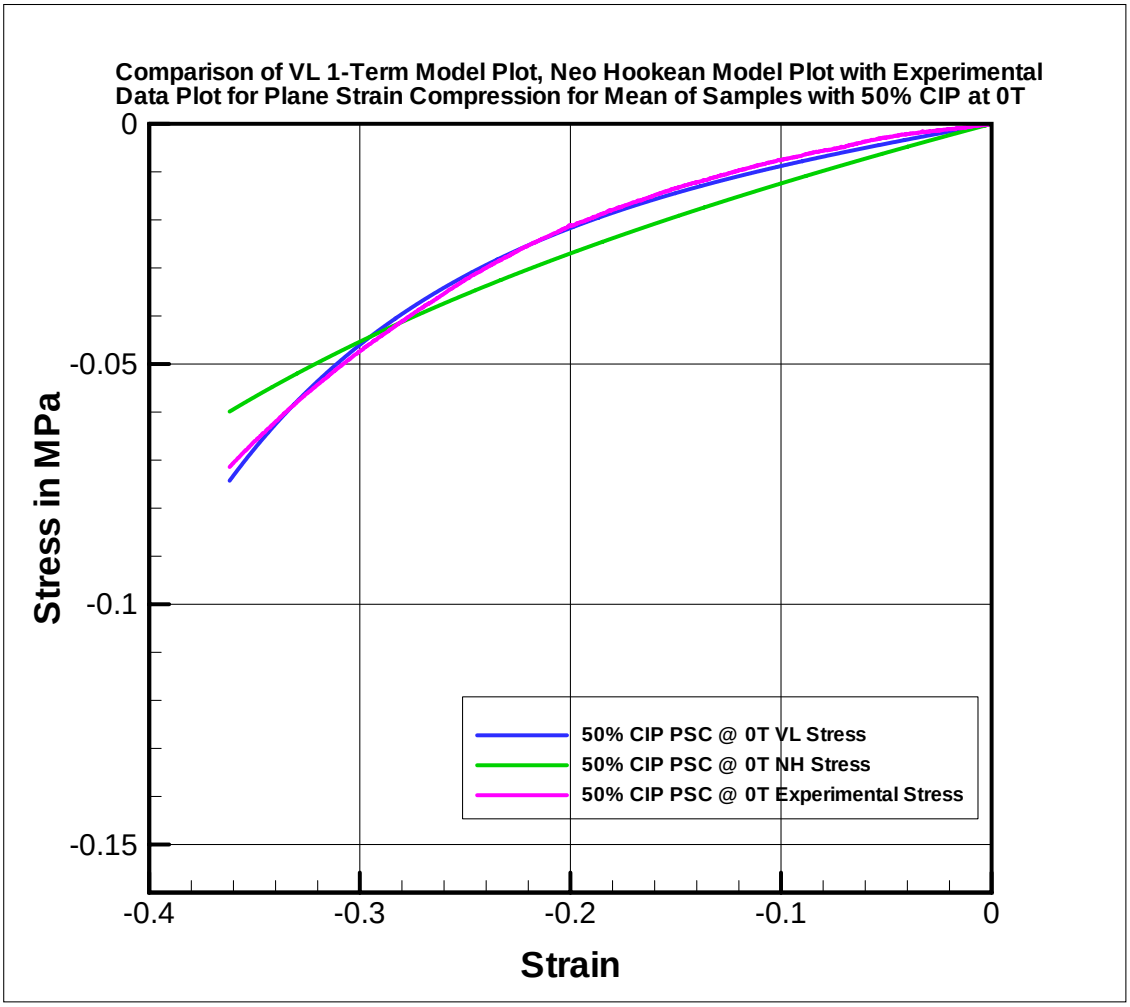

Fig. 66. 50% CIP 0T Model Fitting $\mu_{VL} = 0.007985MPa, and \mu_{NH} = 0.022421MPa$

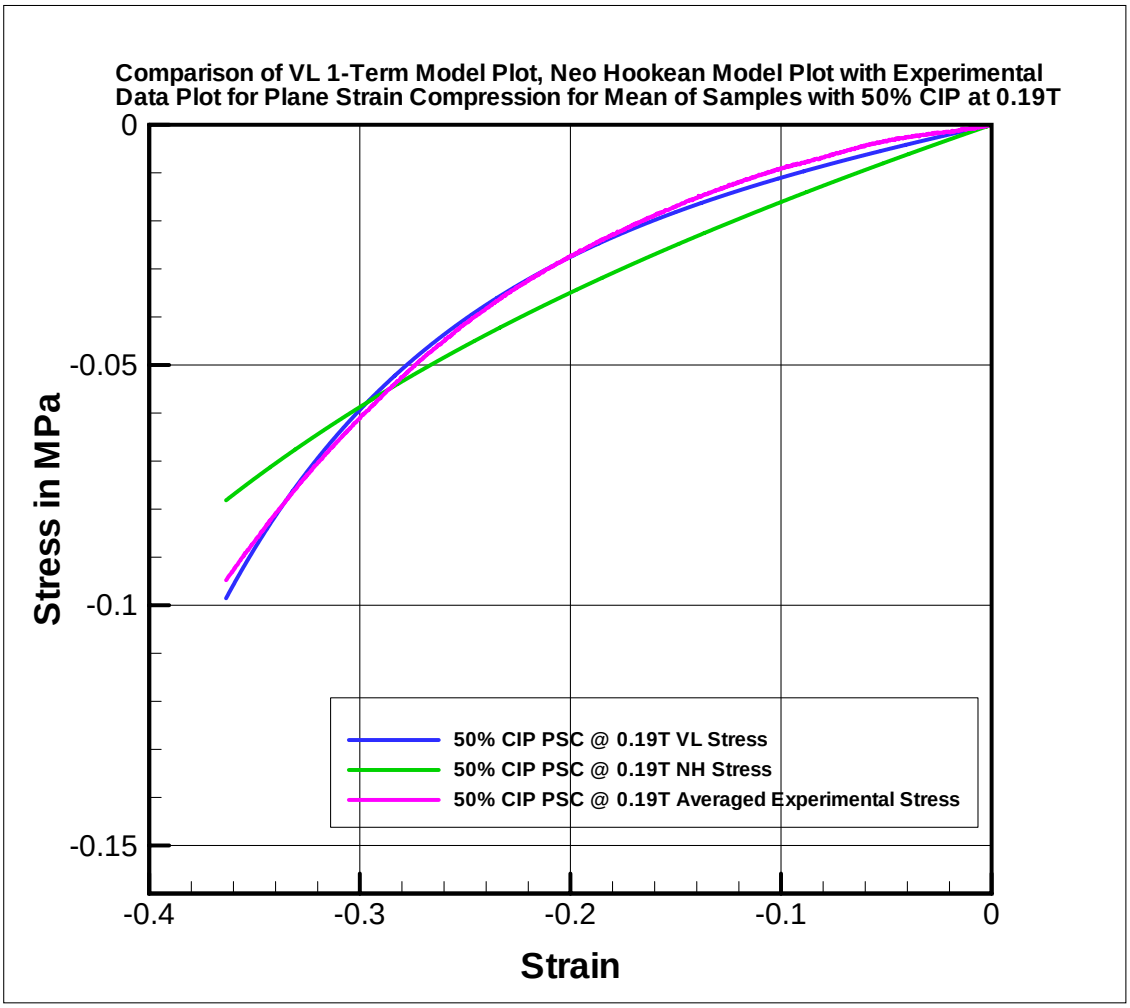

Fig. 67. 50% CIP 0.19T Model Fitting $\mu_{VL} = 0.009658MPa, and \mu_{NH} = 0.028538MPa$

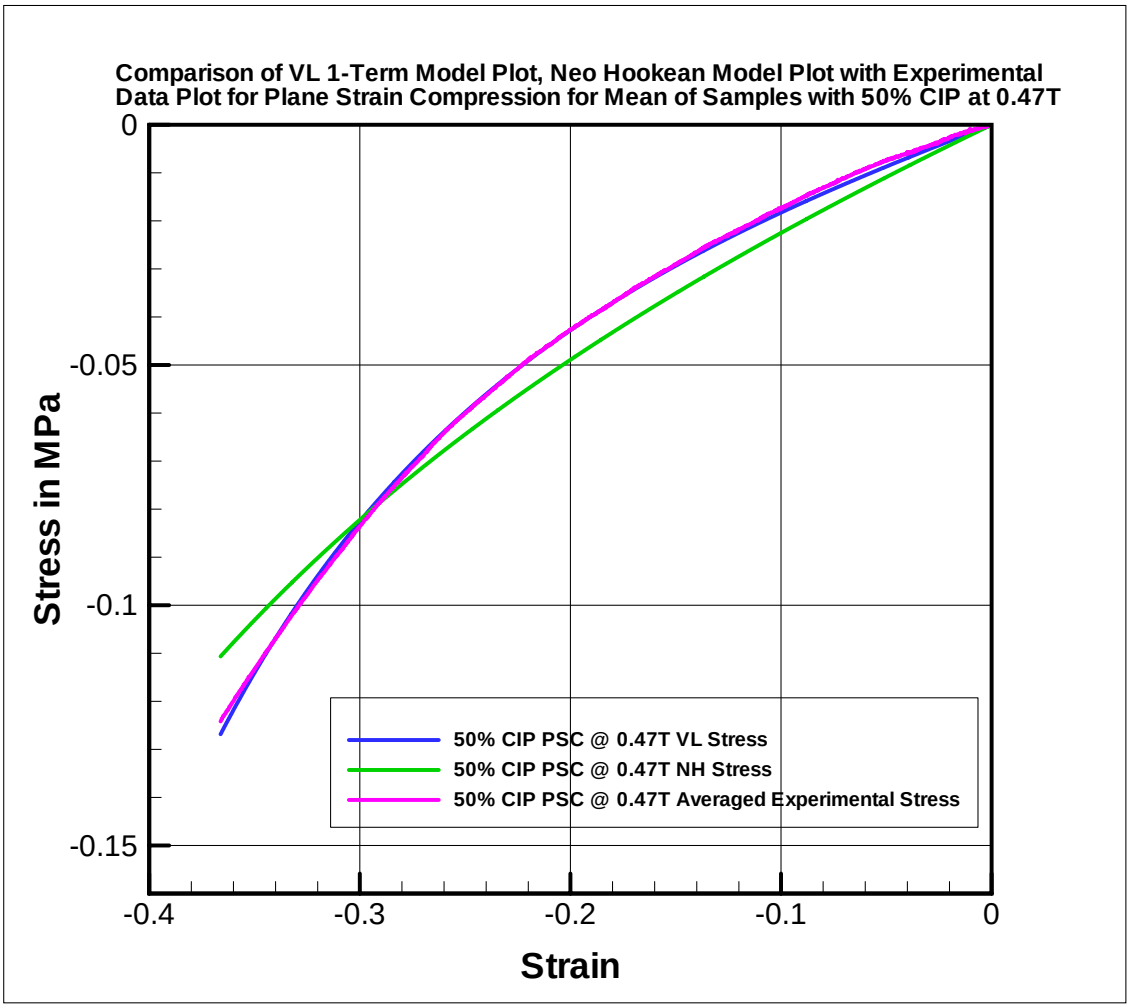

Fig. 68. 50% CIP 0.47T Model Fitting $\mu_{VL} = 0.021091 MPa, and \mu_{NH} = 0.045659 MPa$

APPENDIX H

VL MODEL PLOTS WITH POWER LAW CO-EFFICIENT AS 4 AND MEASURED SHEAR MODULUS

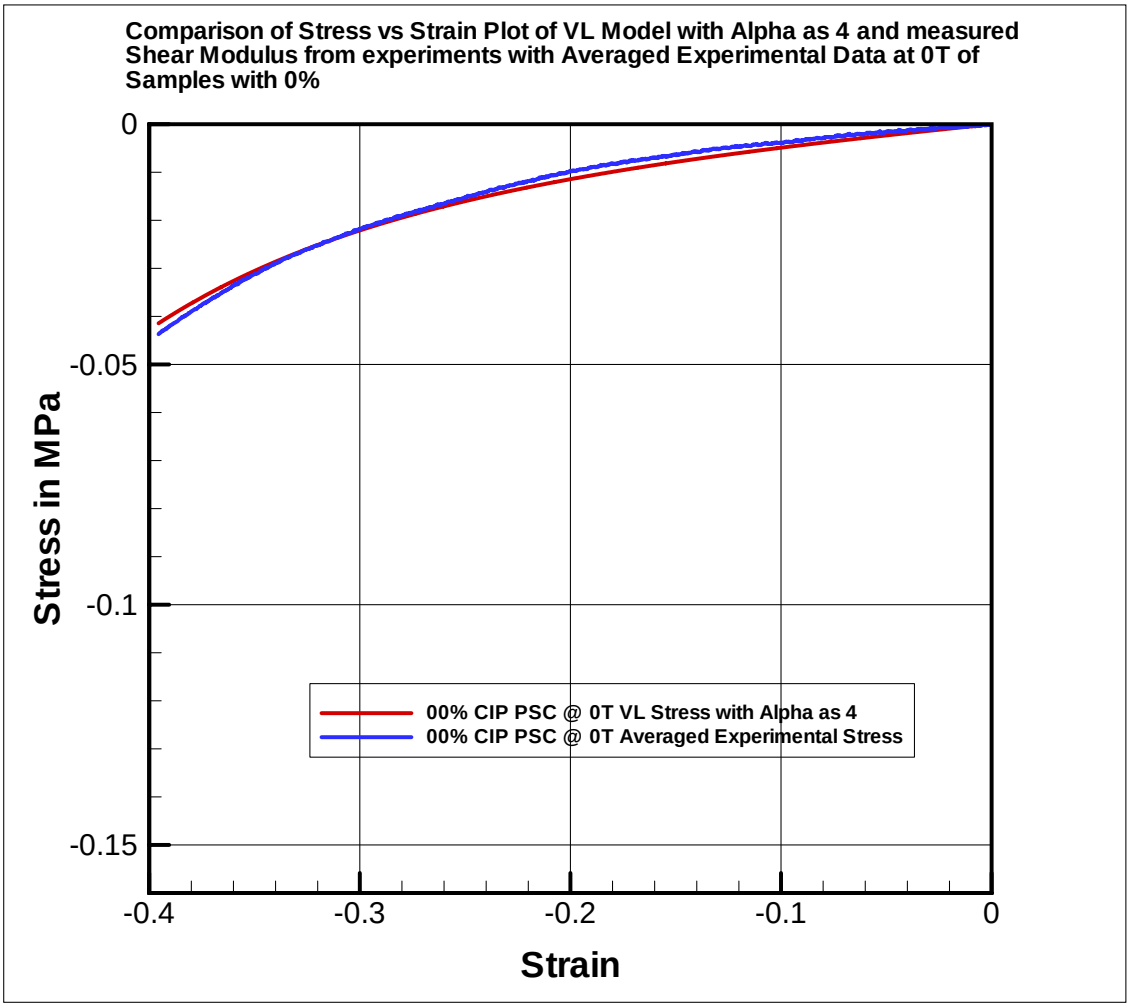

Fig. 69. Comparison of VL Model Plot with Alpha as 4 with Averaged Experimental Data for Sample with 0% CIP at 0T

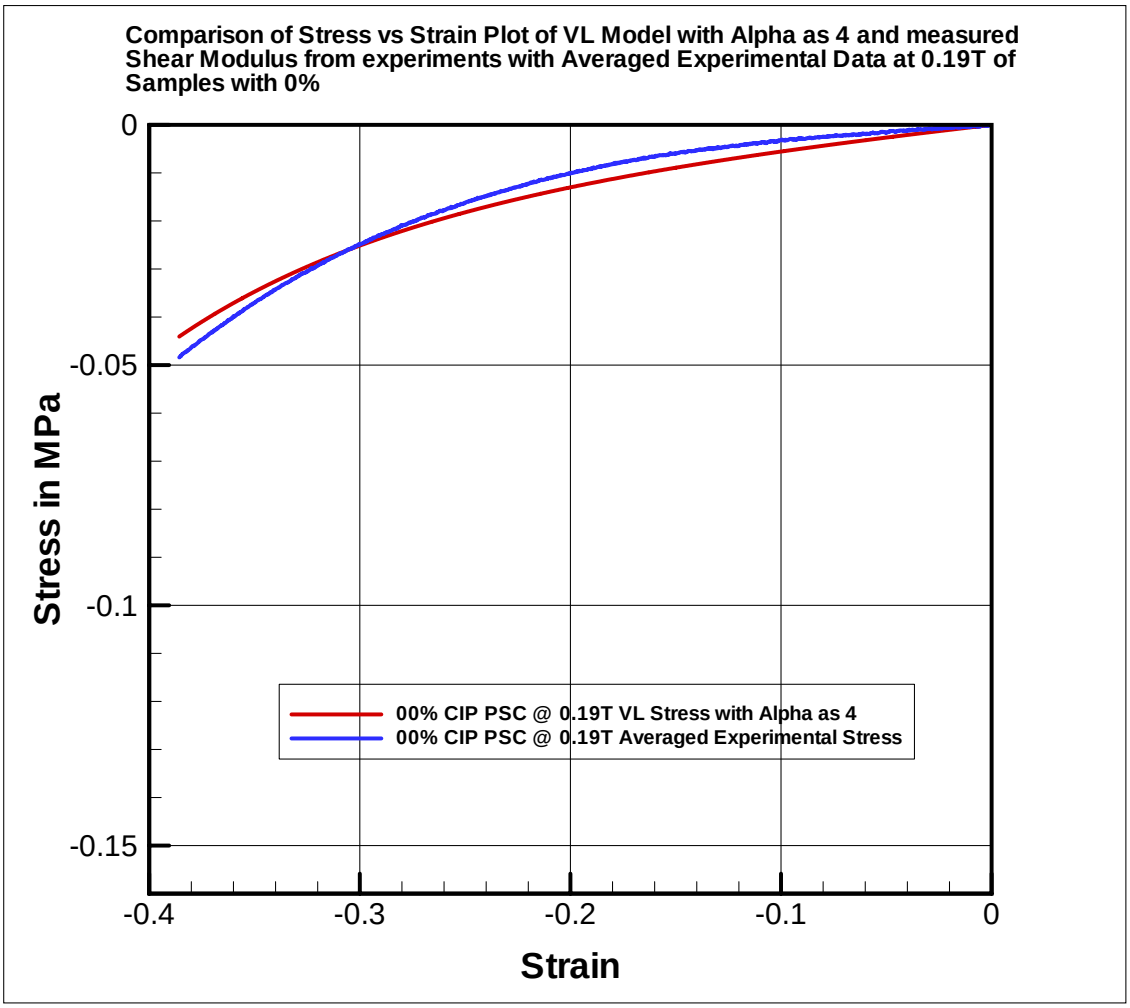

Fig. 70. Comparison of VL Model Plot with Alpha as 4 with Averaged Experimental Data for Sample with 0% CIP at 0.19T

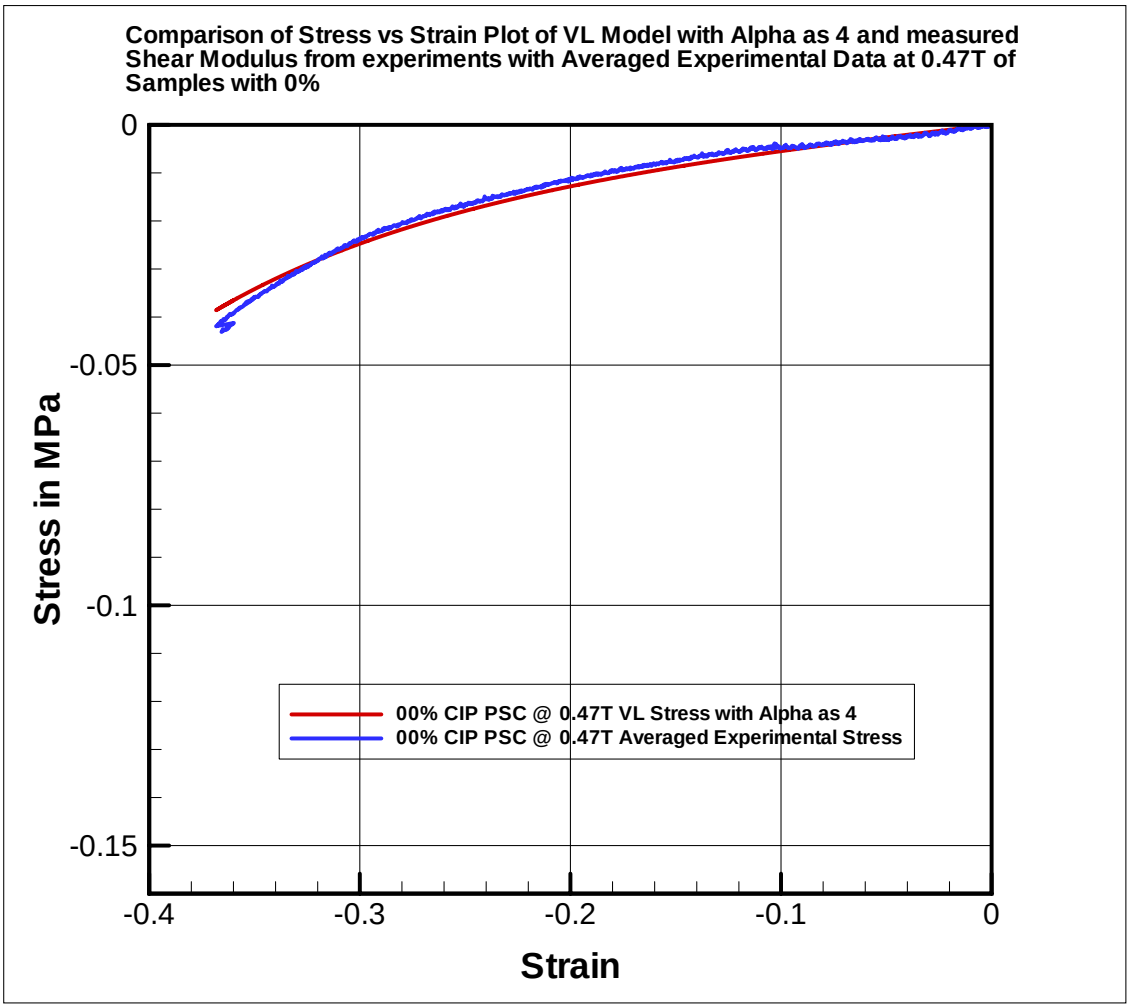

Fig. 71. Comparison of VL Model Plot with Alpha as 4 with Averaged Experimental Data for Sample with 0% CIP at 0.47T

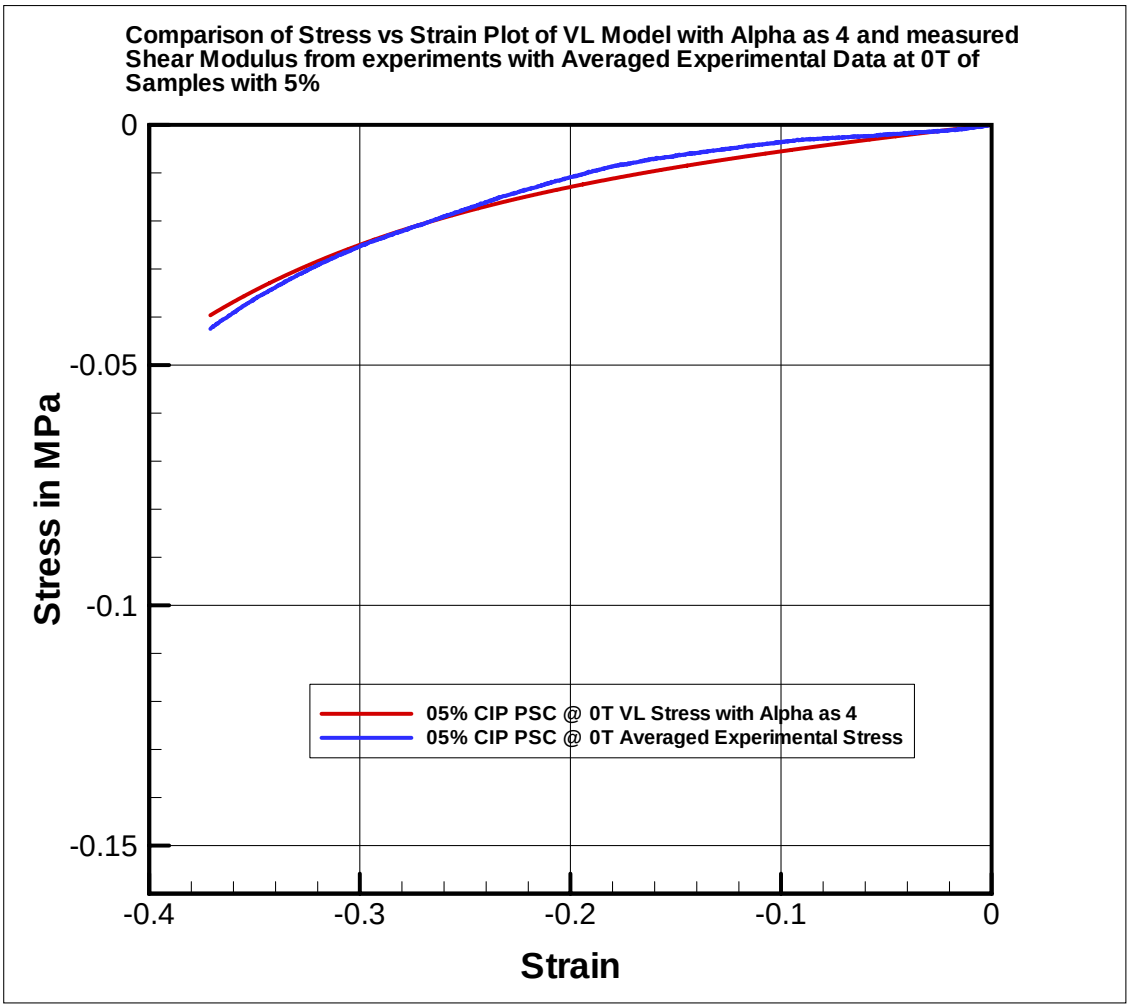

Fig. 72. Comparison of VL Model Plot with Alpha as 4 with Averaged Experimental Data for Sample with 5% CIP at 0T

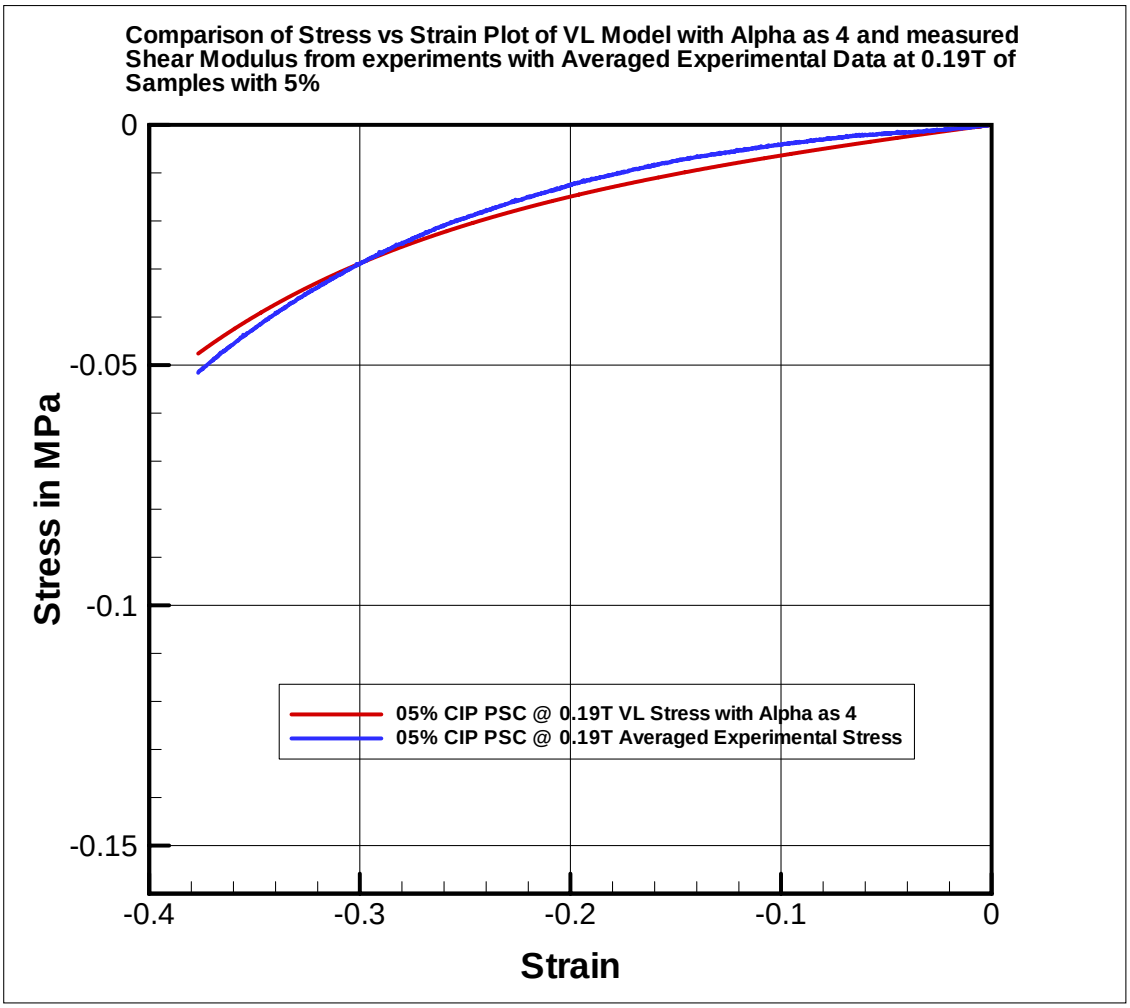

Fig. 73. Comparison of VL Model Plot with Alpha as 4 with Averaged Experimental Data for Sample with 5% CIP at 0.19T

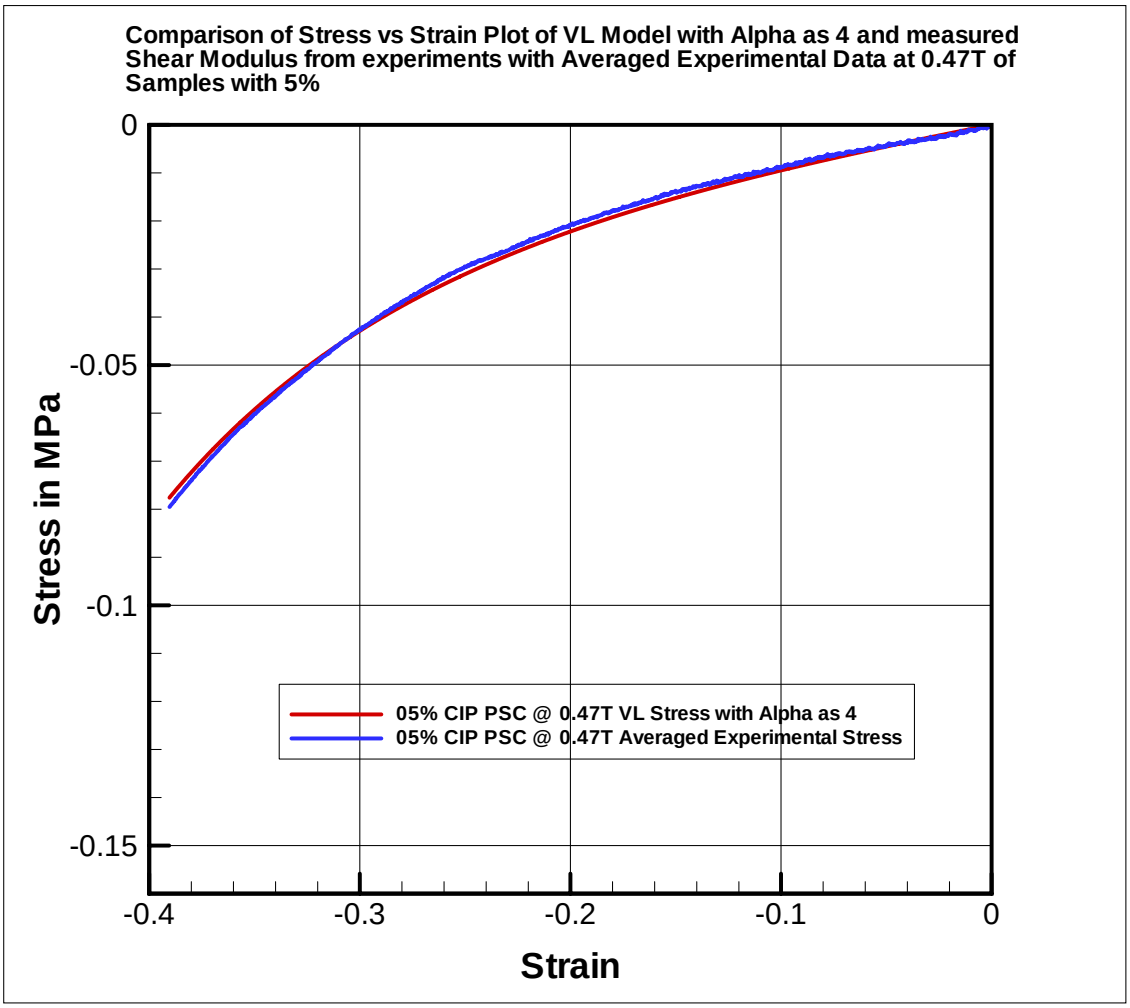

Fig. 74. Comparison of VL Model Plot with Alpha as 4 with Averaged Experimental Data for Sample with 5% CIP at 0.47T

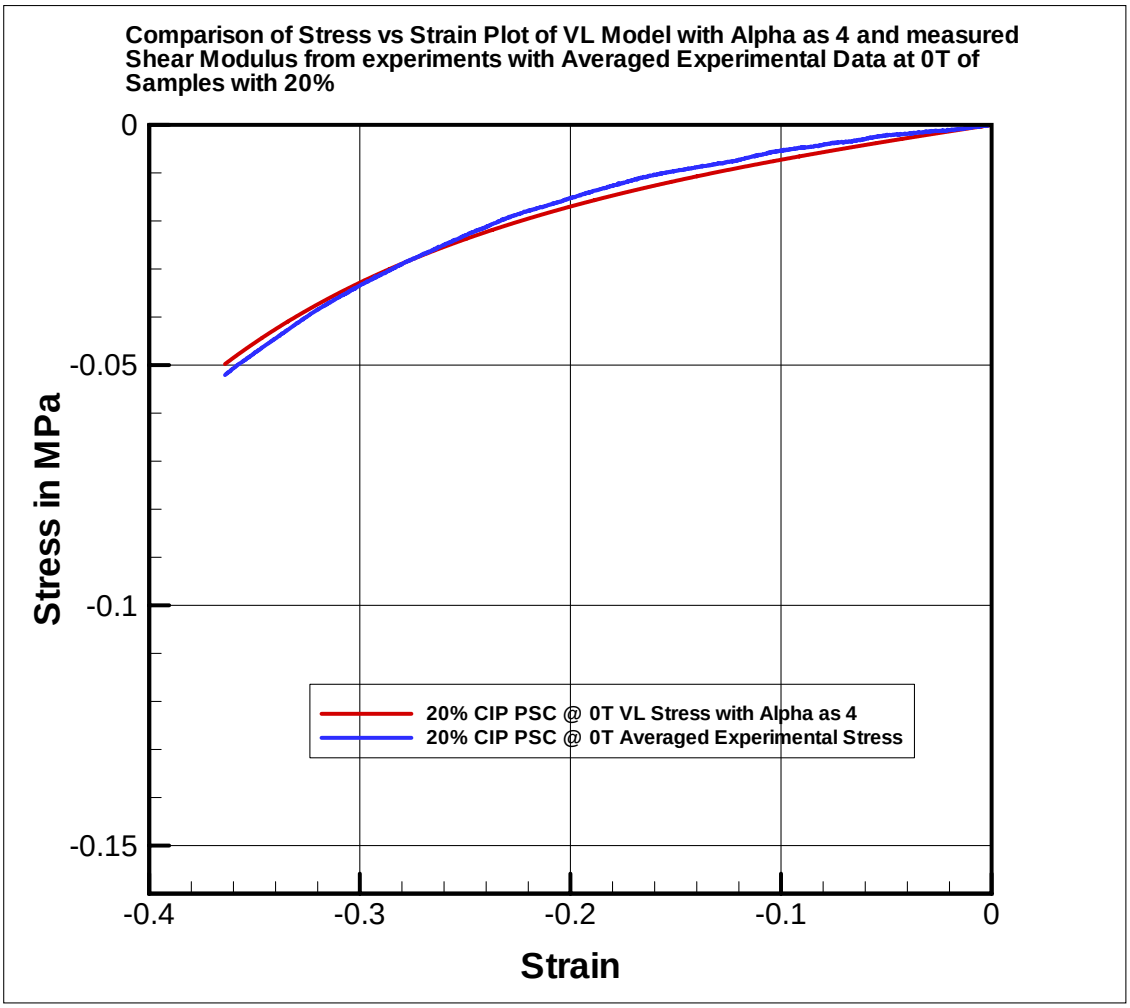

Fig. 75. Comparison of VL Model Plot with Alpha as 4 with Averaged Experimental Data for Sample with 20% CIP at 0T

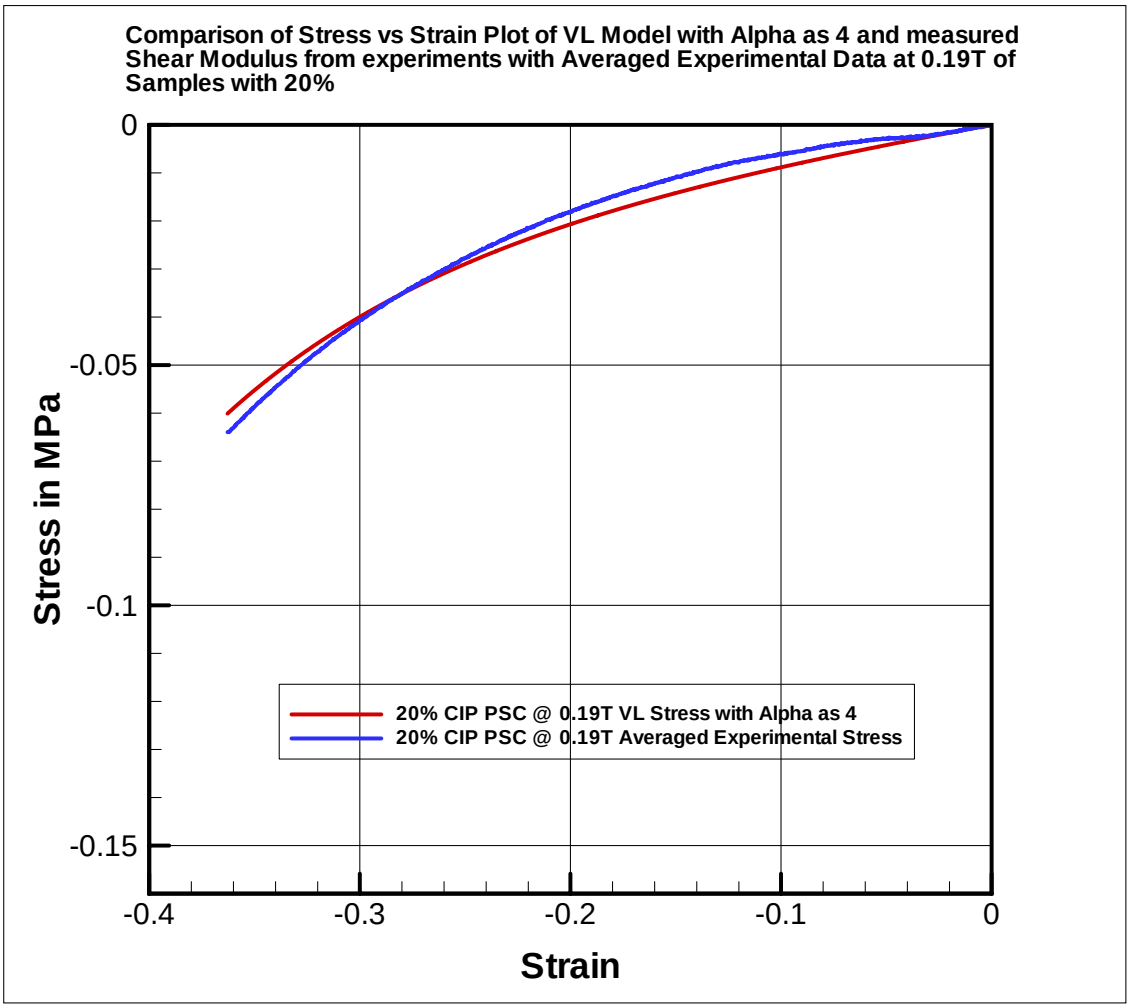

Fig. 76. Comparison of VL Model Plot with Alpha as 4 with Averaged Experimental Data for Sample with 20% CIP at 0.19T

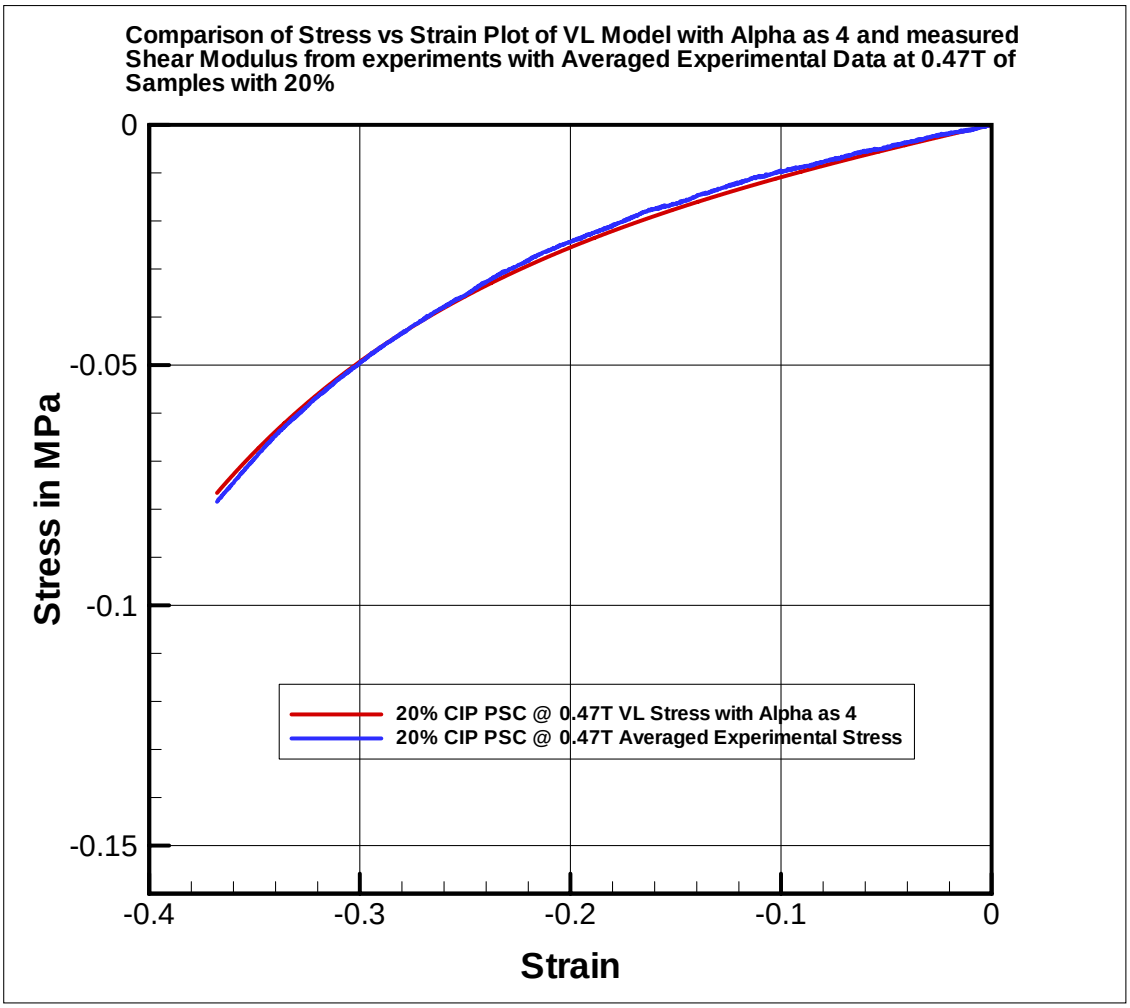

Fig. 77. Comparison of VL Model Plot with Alpha as 4 with Averaged Experimental Data for Sample with 20% CIP at 0.47T

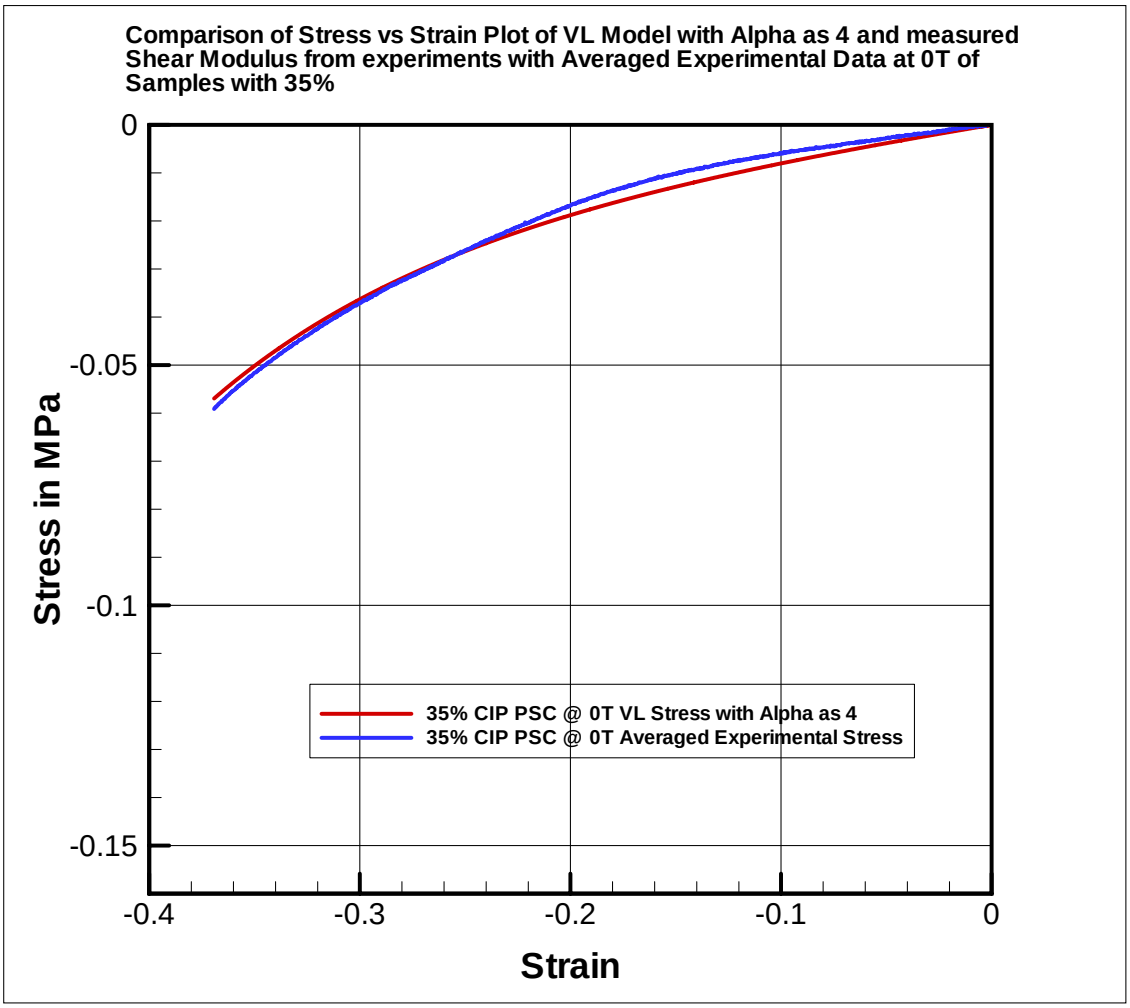

Fig. 78. Comparison of VL Model Plot with Alpha as 4 with Averaged Experimental Data for Sample with 35% CIP at 0T

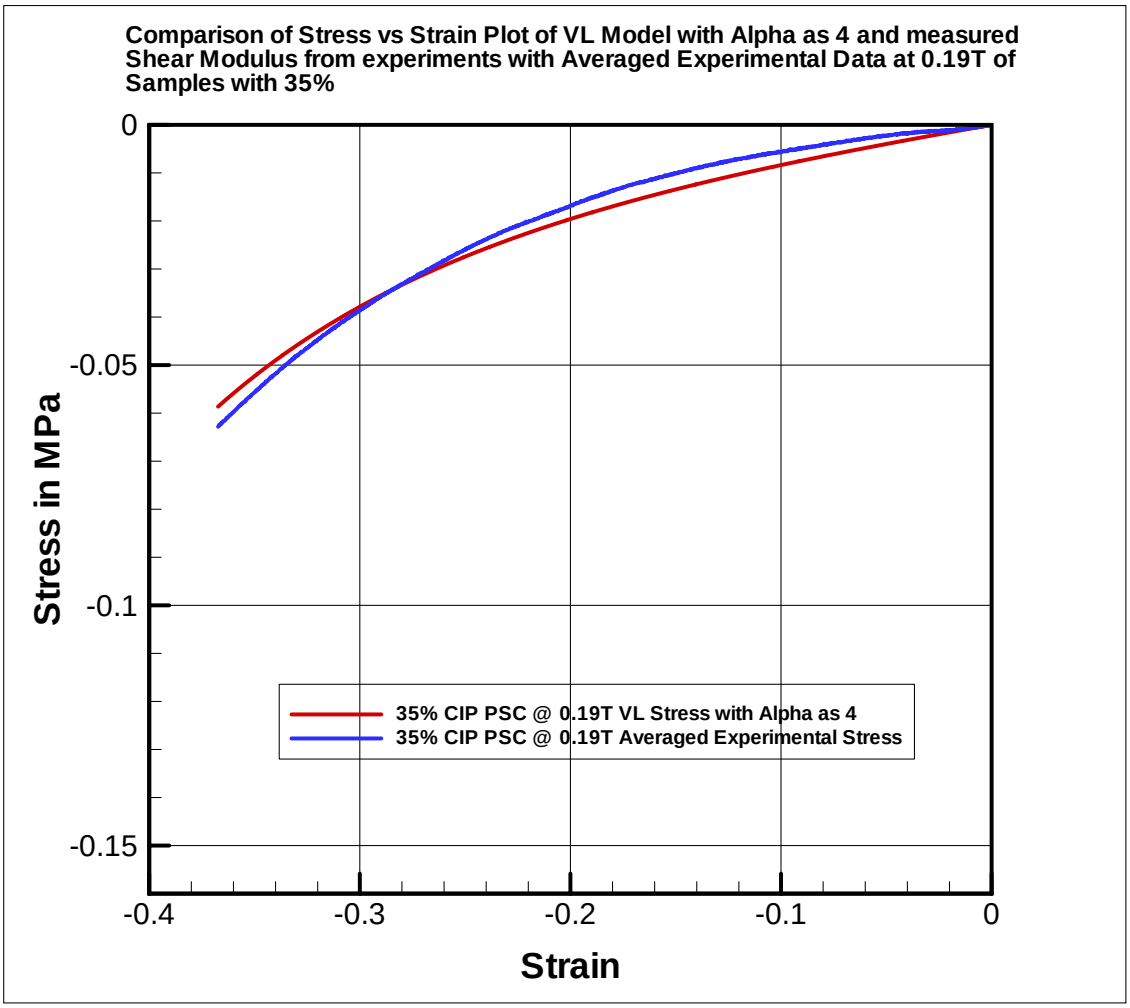

Fig. 79. Comparison of VL Model Plot with Alpha as 4 with Averaged Experimental Data for Sample with 35% CIP at 0.19T

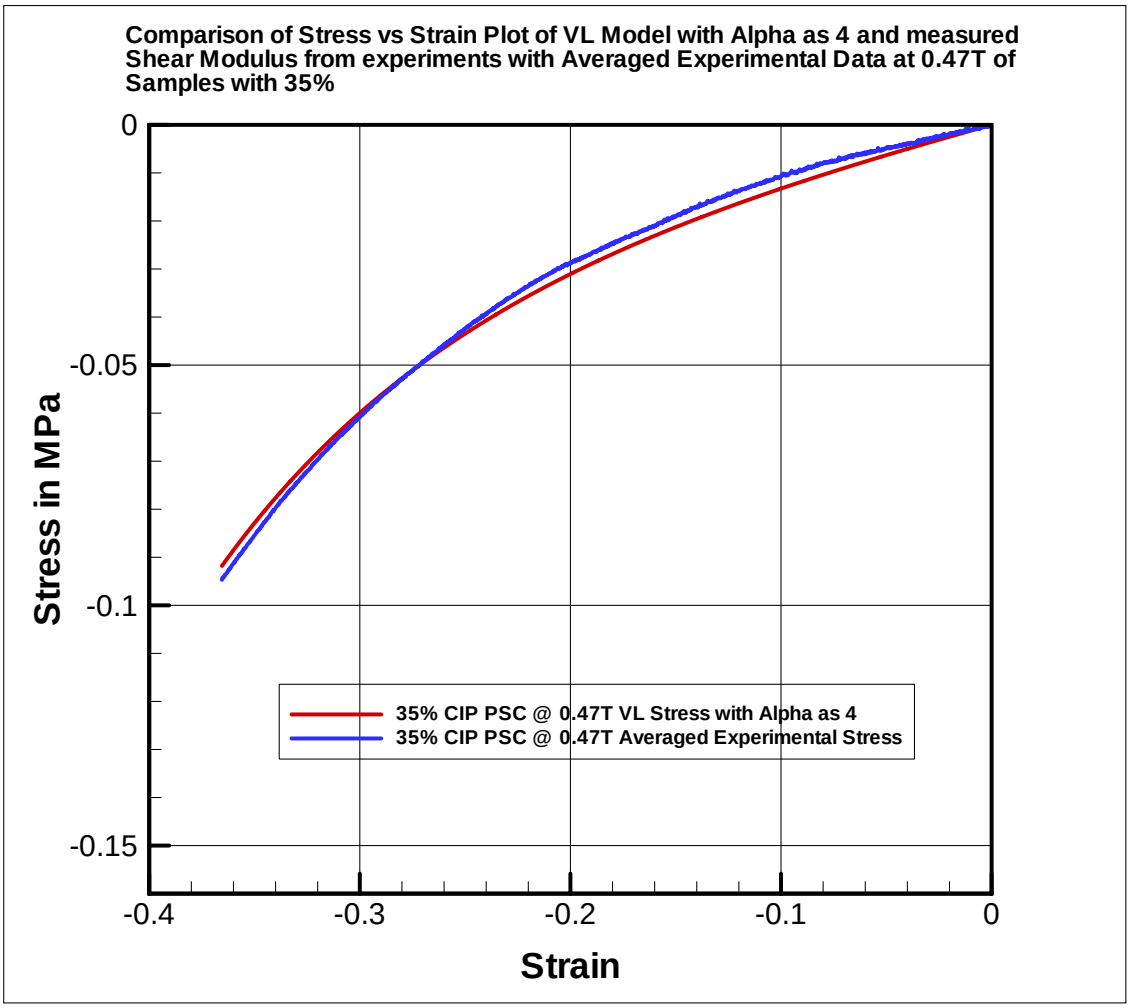

Fig. 80. Comparison of VL Model Plot with Alpha as 4 with Averaged Experimental Data for Sample with 35% CIP at 0.47T

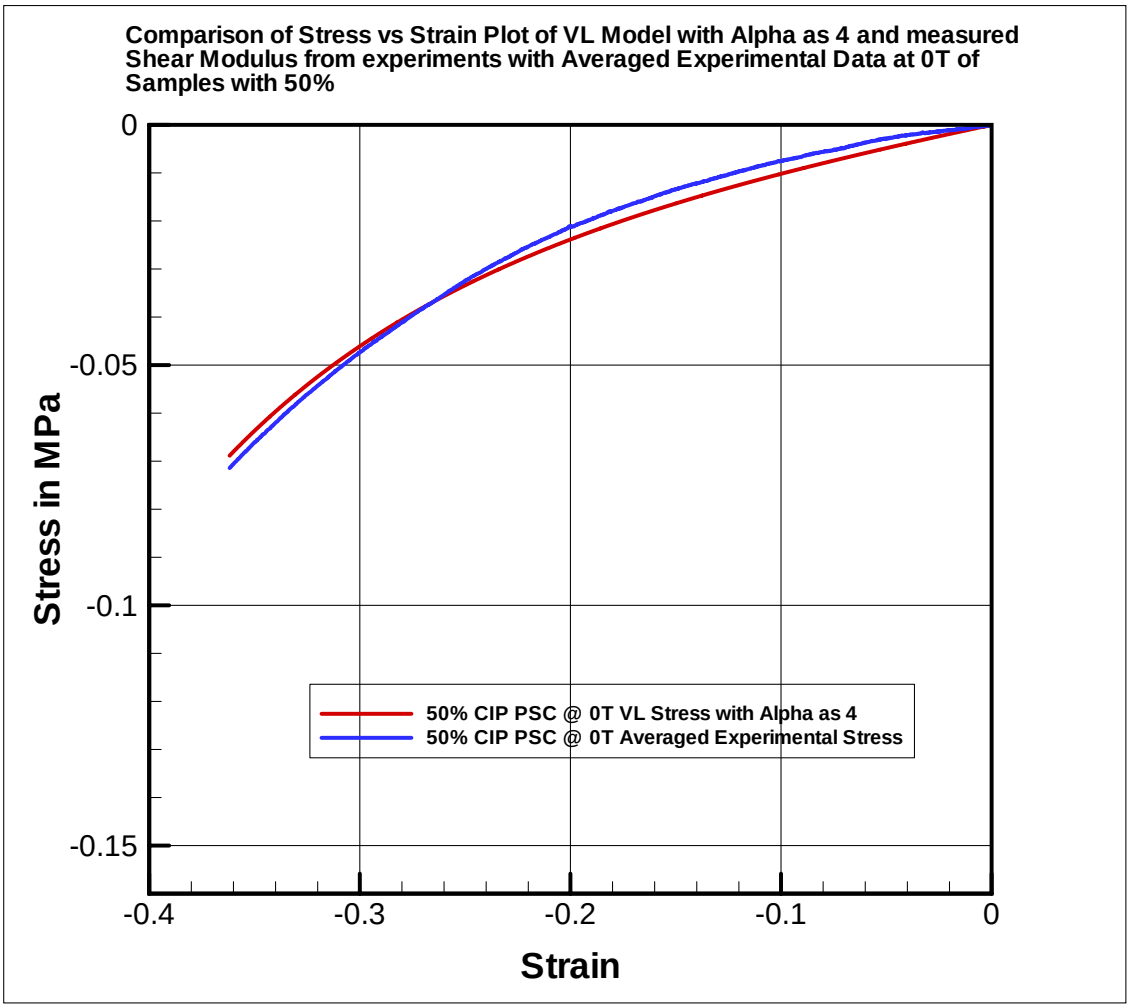

Fig. 81. Comparison of VL Model Plot with Alpha as 4 with Averaged Experimental Data for Sample with 50% CIP at 0T

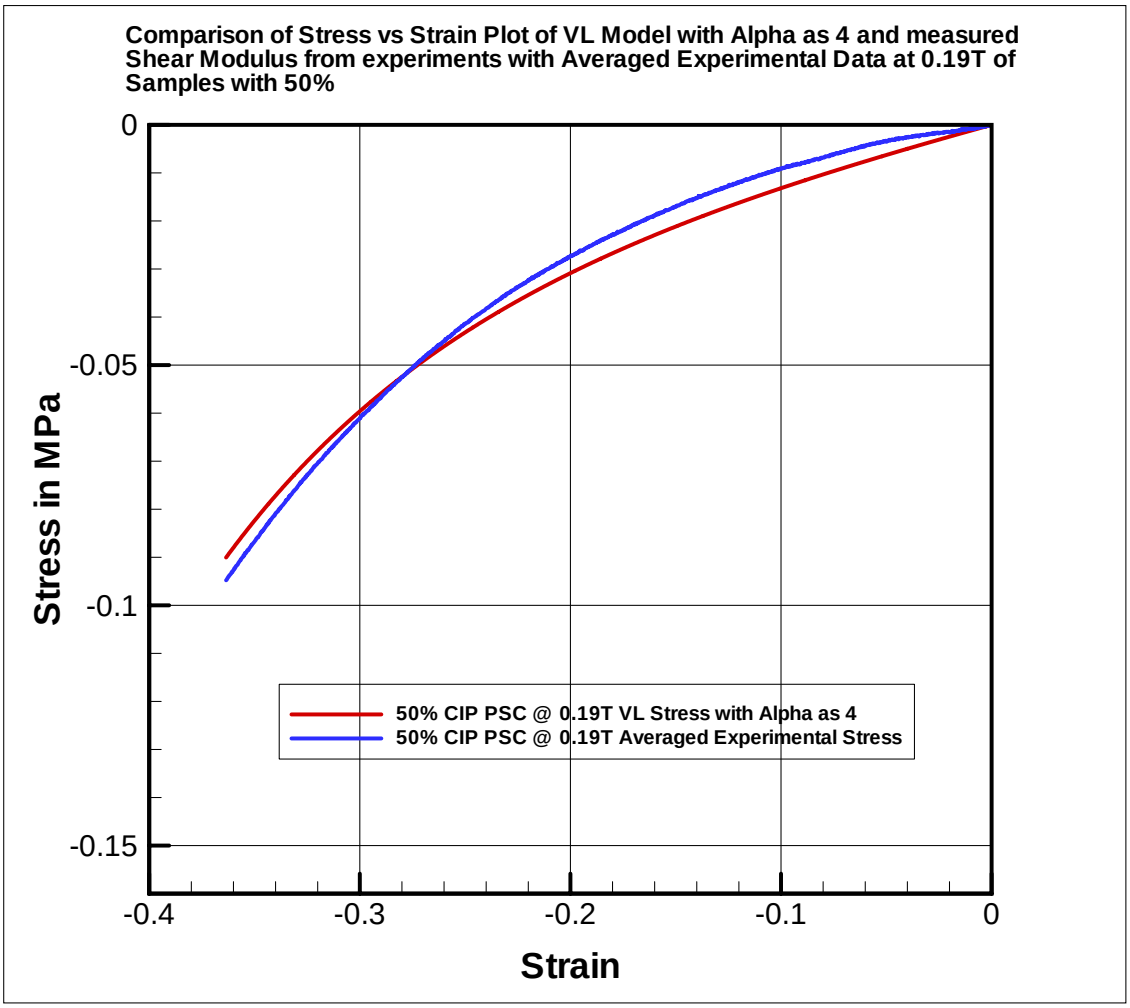

Fig. 82. Comparison of VL Model Plot with Alpha as 4 with Averaged Experimental Data for Sample with 50% CIP at 0.19T

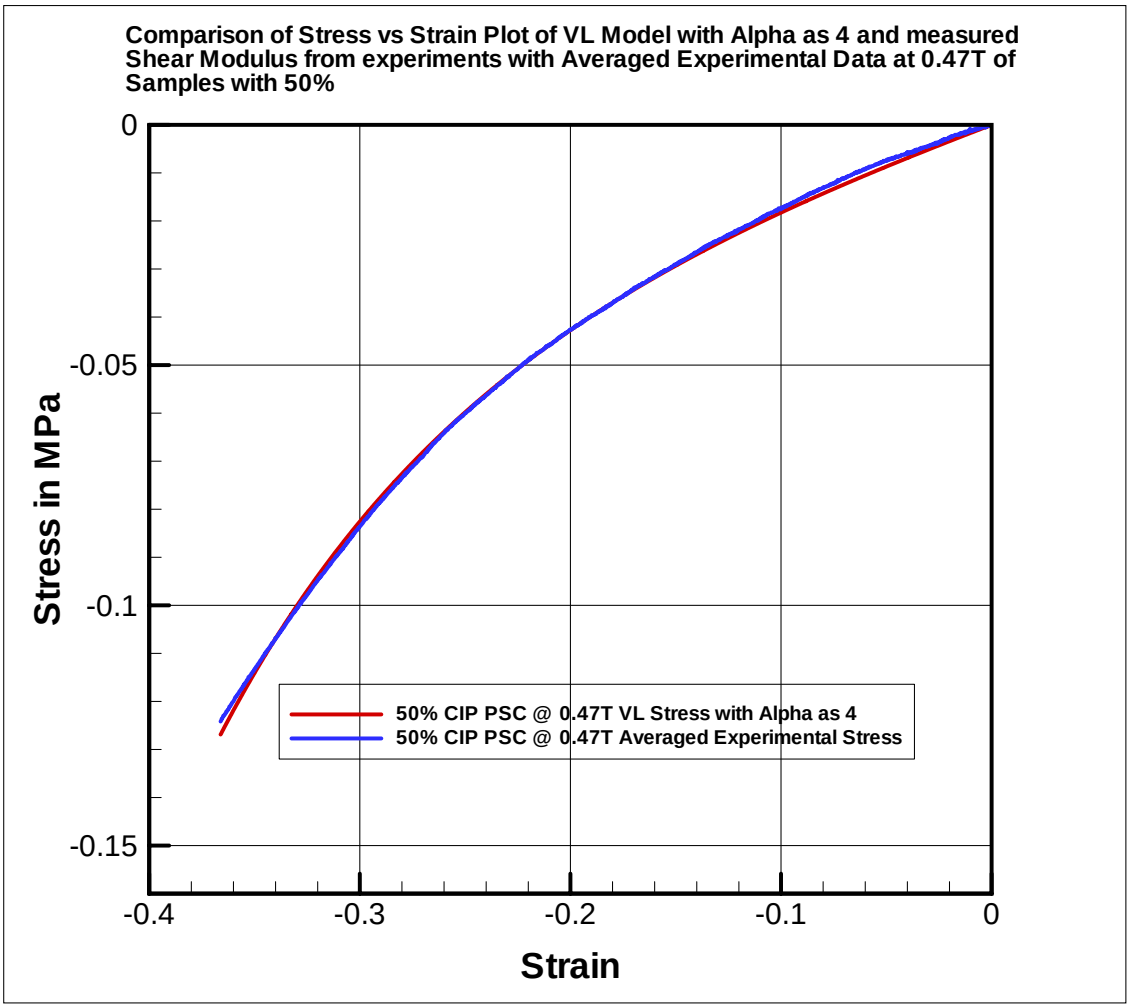

Fig. 83. Comparison of VL Model Plot with Alpha as 4 with Averaged Experimental Data for Sample with 50% CIP at 0.47T

APPENDIX I

COMPUTED SHEAR MODULUS PLOTS

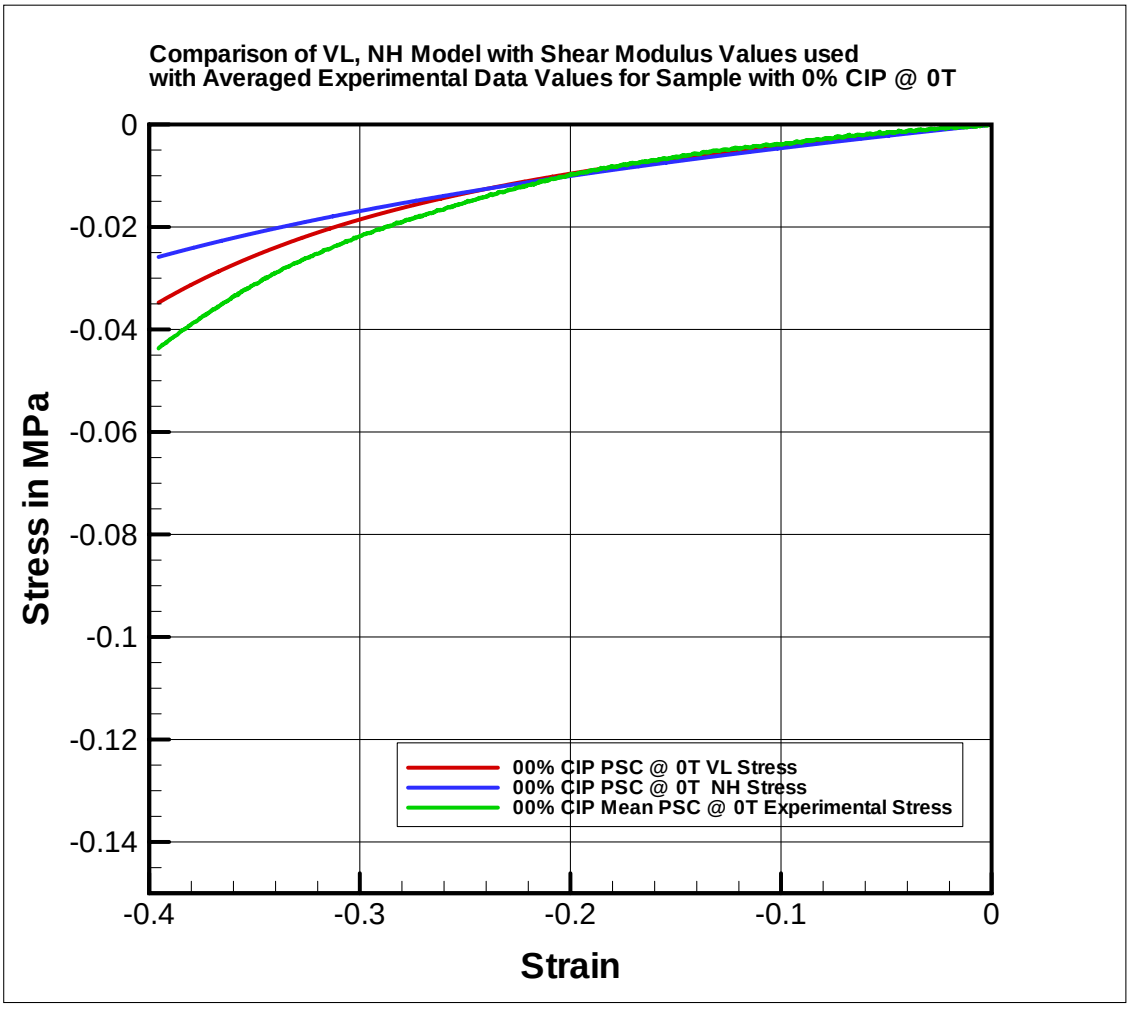

Fig. 84. Stress vs Strain Plot for Averaged Experimental Data, VL Model and NH Model Using Calculated Shear Modulus for Samples with 0% CIP at 0T

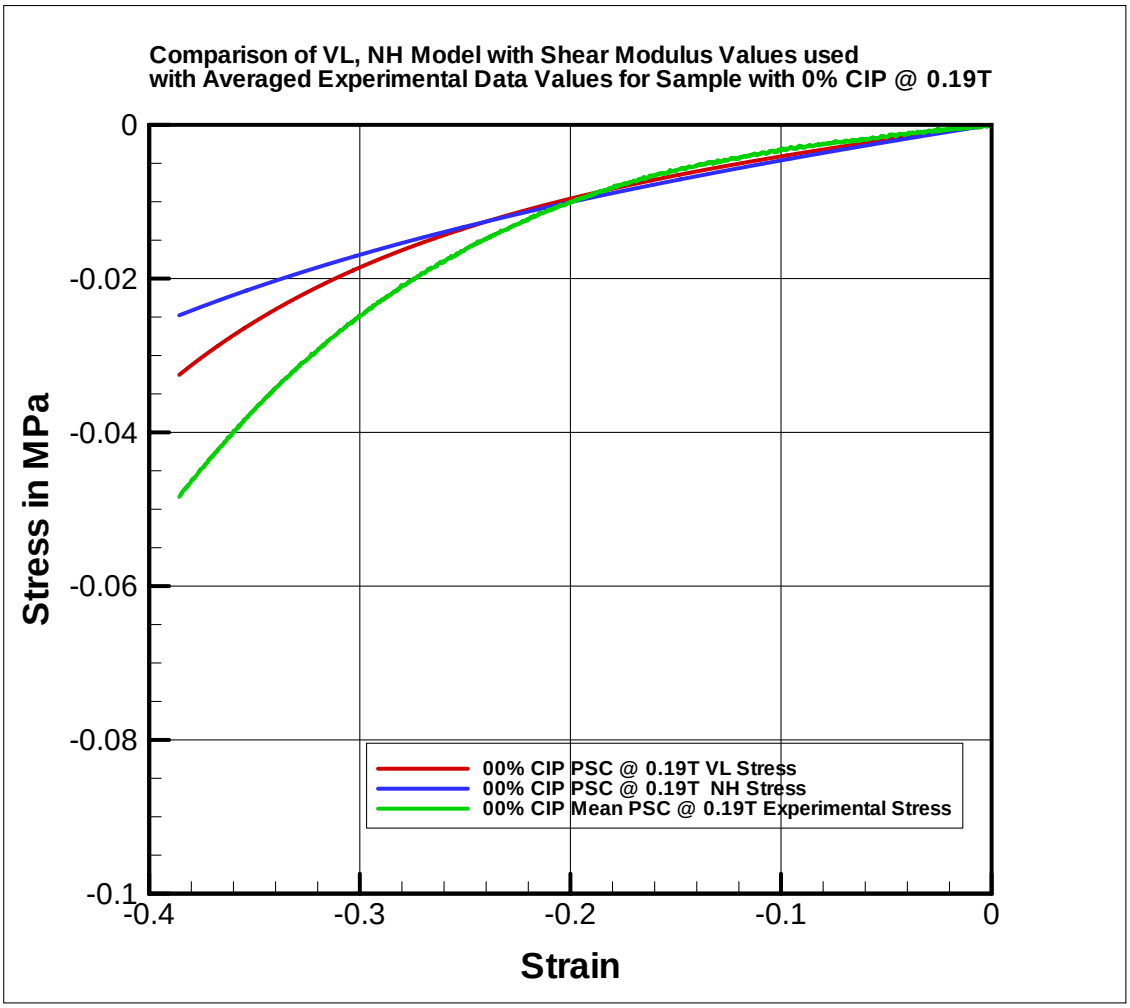

Fig. 85. Stress vs Strain Plot for Averaged Experimental Data, VL Model and NH Model Using Calculated Shear Modulus for Samples with 0% CIP at 0.19T

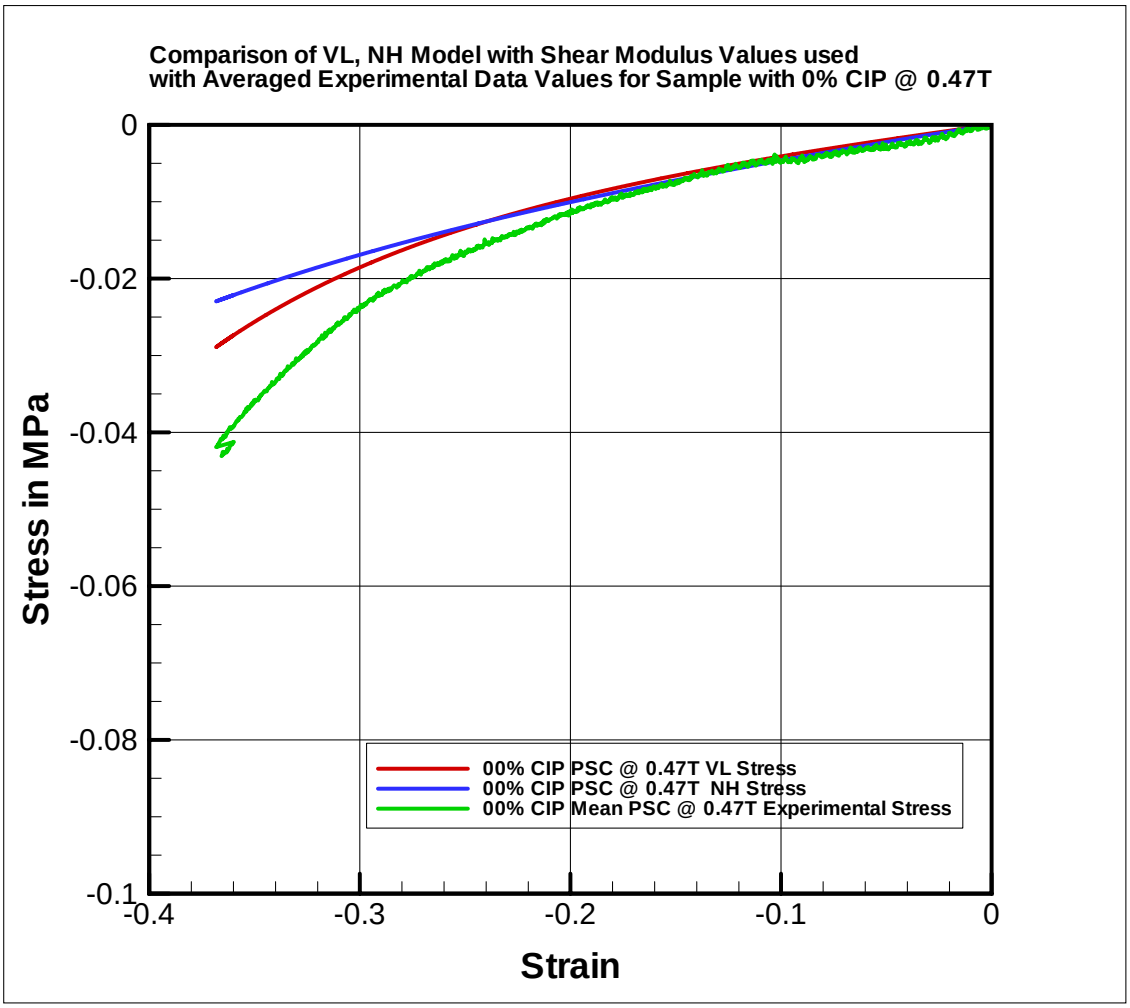

Fig. 86. Stress vs Strain Plot for Averaged Experimental Data, VL Model and NH Model Using Calculated Shear Modulus for Samples with 0% CIP at 0.47T

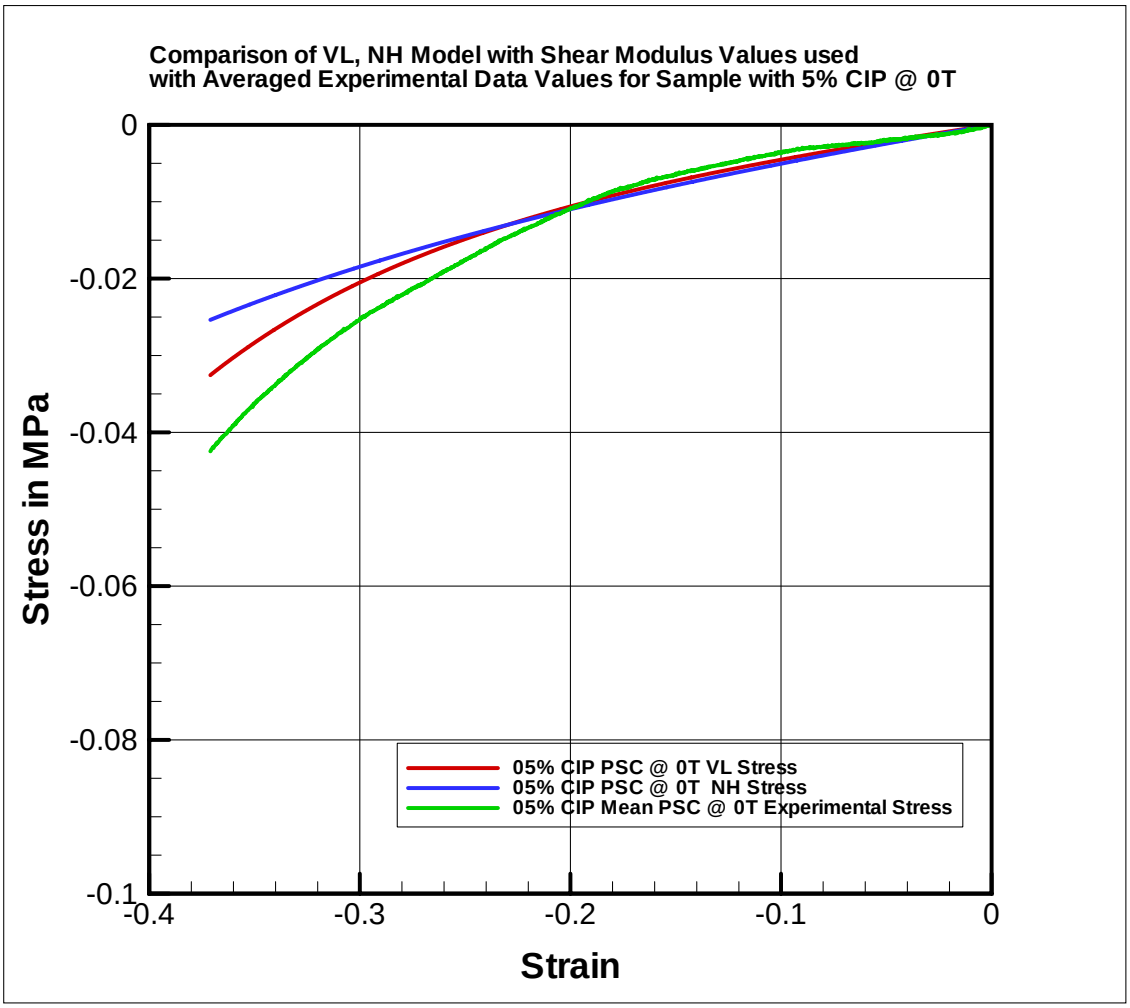

Fig. 87. Stress vs Strain Plot for Averaged Experimental Data, VL Model and NH Model Using Calculated Shear Modulus for Samples with 5% CIP at 0T

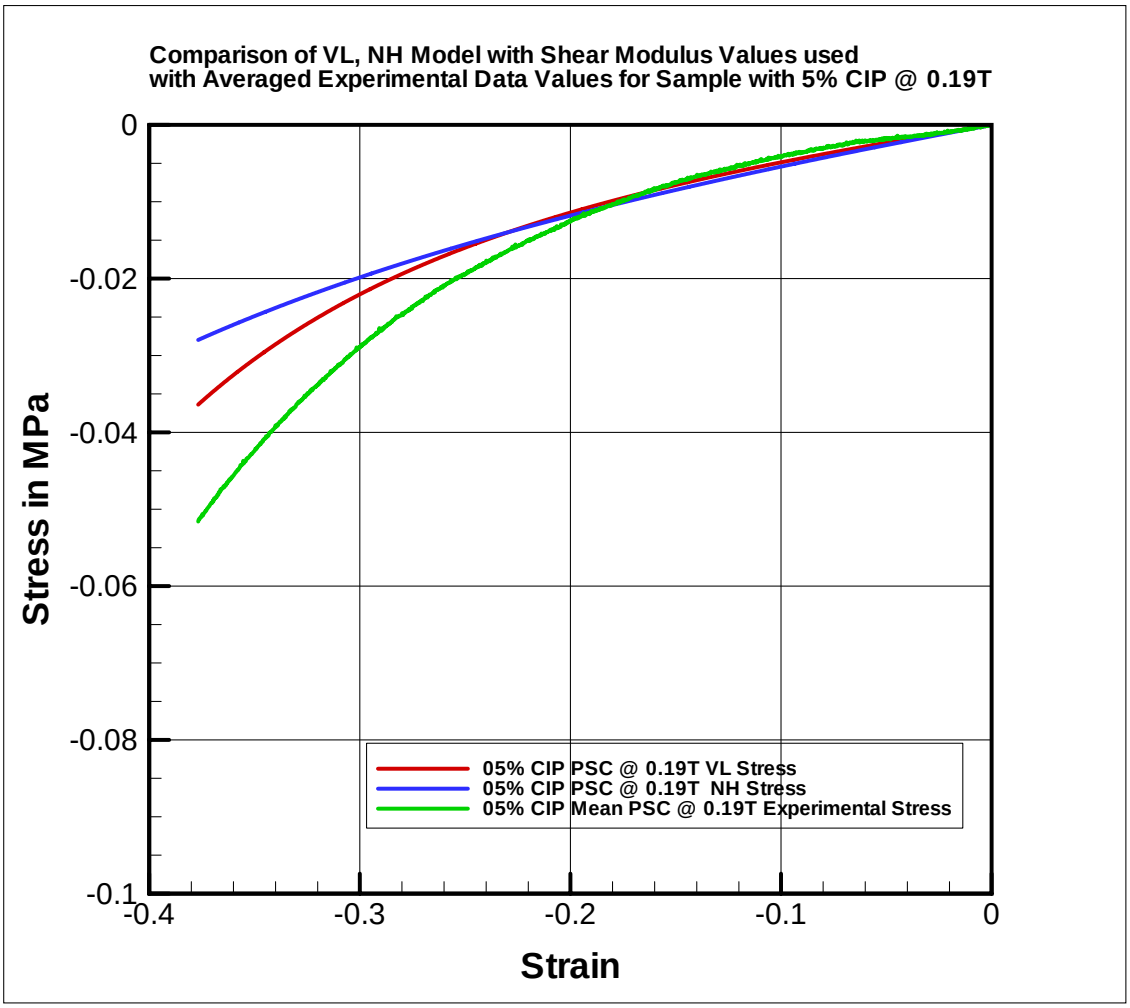

Fig. 88. Stress vs Strain Plot for Averaged Experimental Data, VL Model and NH Model Using Calculated Shear Modulus for Samples with 5% CIP at 0.19T

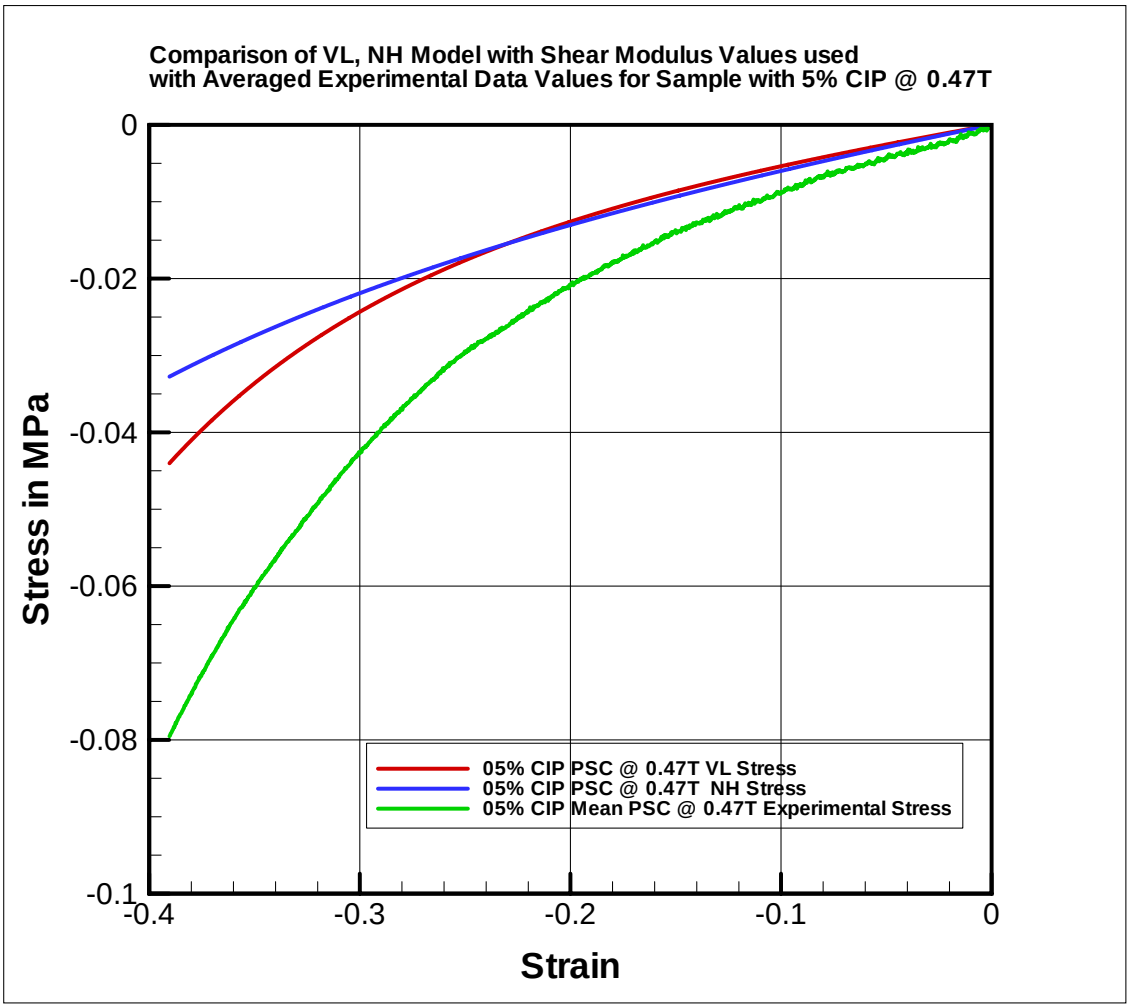

Fig. 89. Stress vs Strain Plot for Averaged Experimental Data, VL Model and NH Model Using Calculated Shear Modulus for Samples with 5% CIP at 0.47T

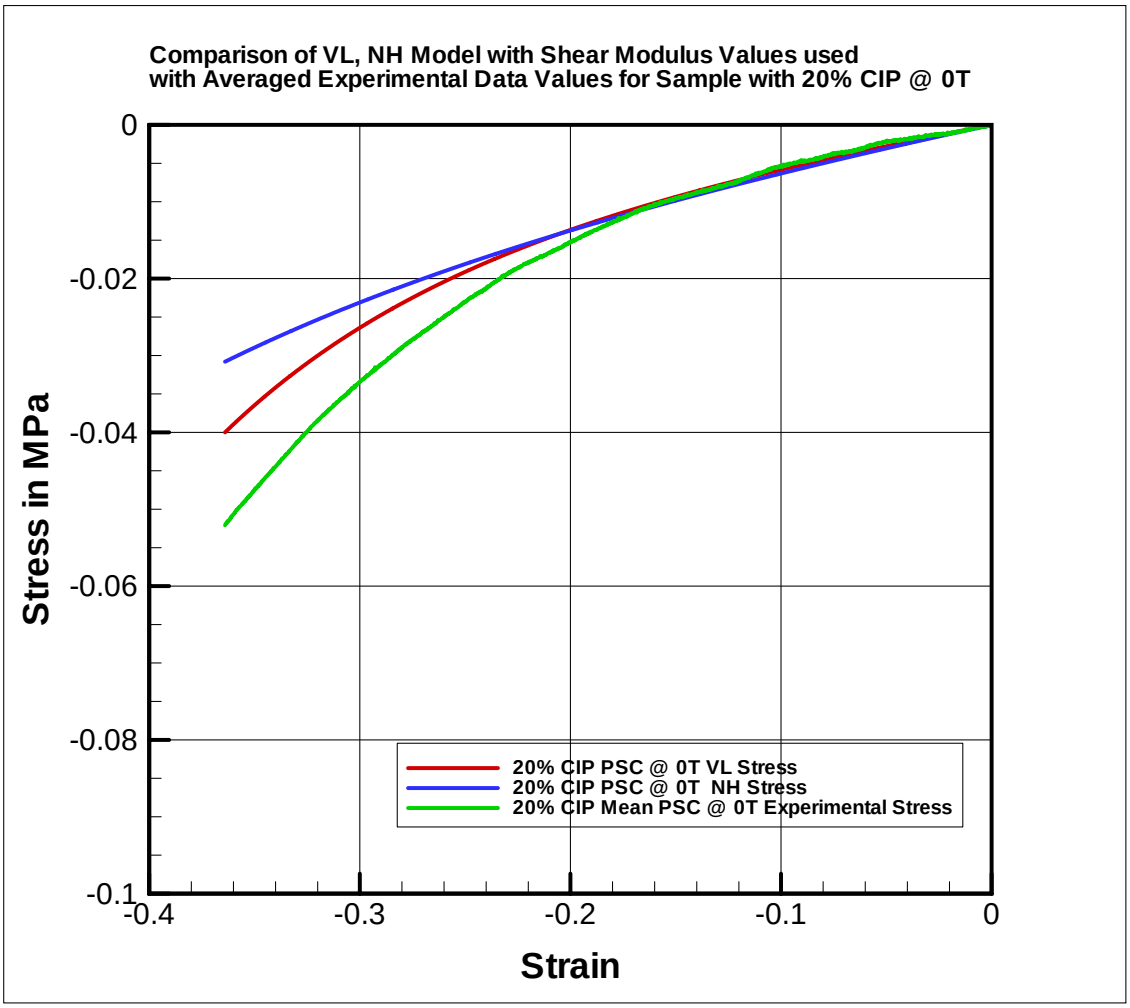

Fig. 90. Stress vs Strain Plot for Averaged Experimental Data, VL Model and NH Model Using Calculated Shear Modulus for Samples with 20% CIP at 0T

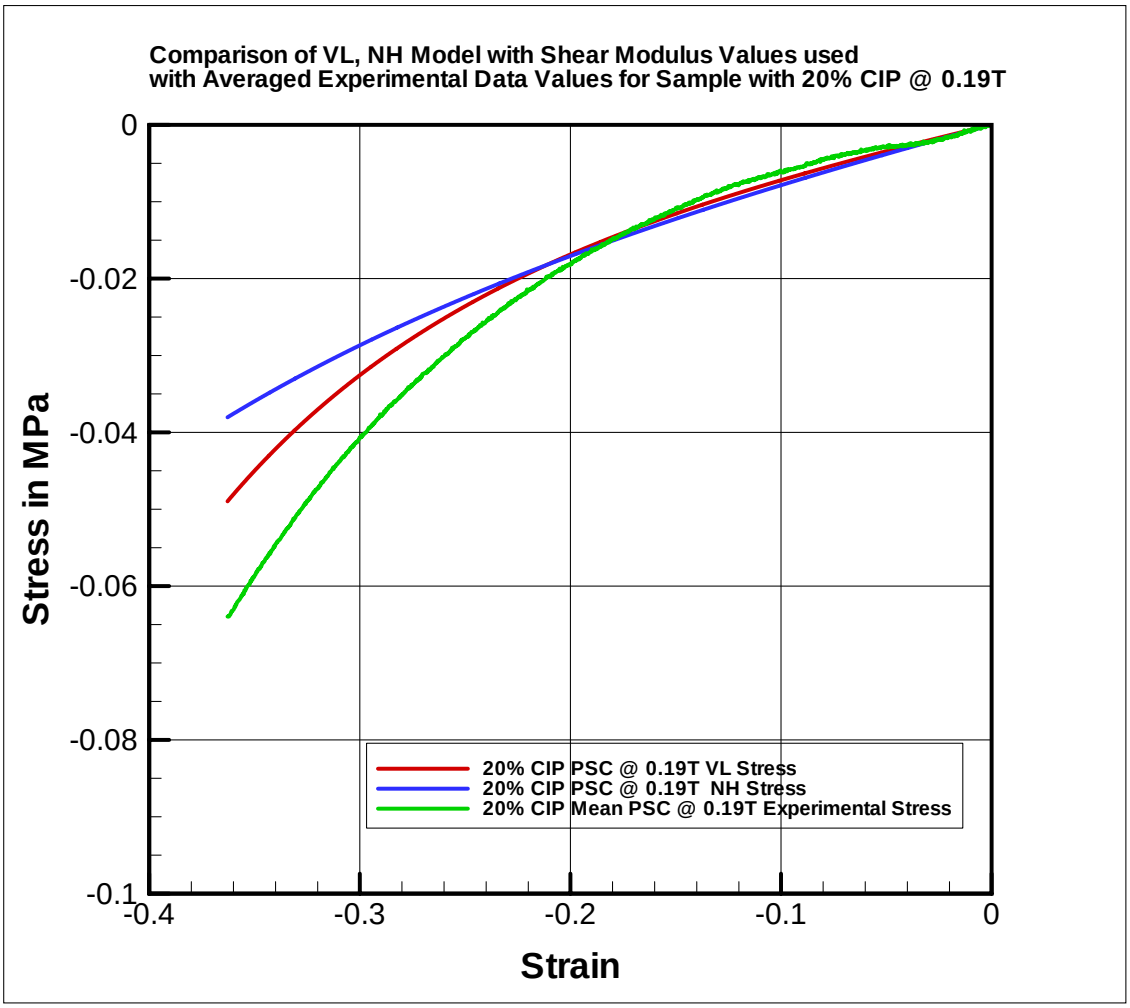

Fig. 91. Stress vs Strain Plot for Averaged Experimental Data, VL Model and NH Model Using Calculated Shear Modulus for Samples with 20% CIP at 0.19T

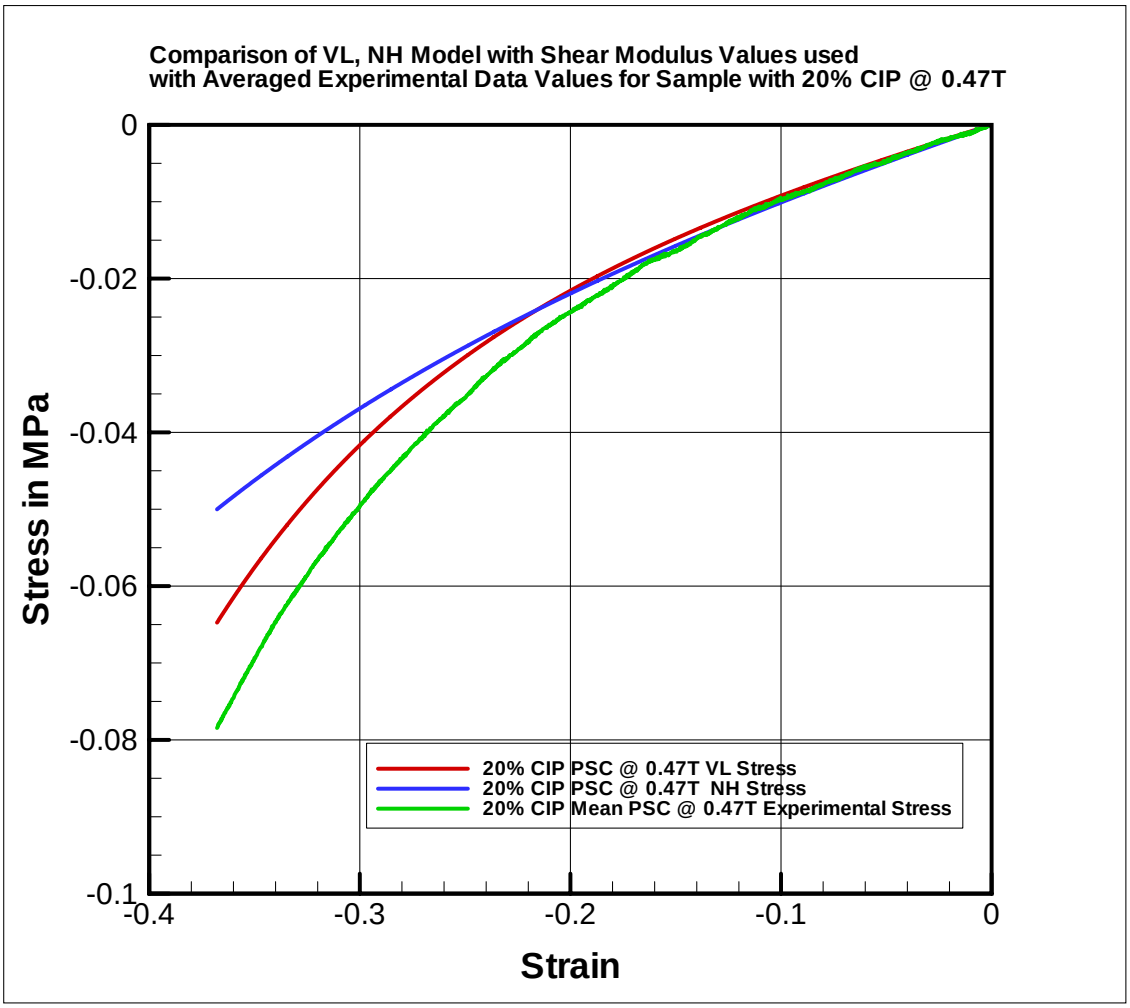

Fig. 92. Stress vs Strain Plot for Averaged Experimental Data, VL Model and NH Model Using Calculated Shear Modulus for Samples with 20% CIP at 0.47T

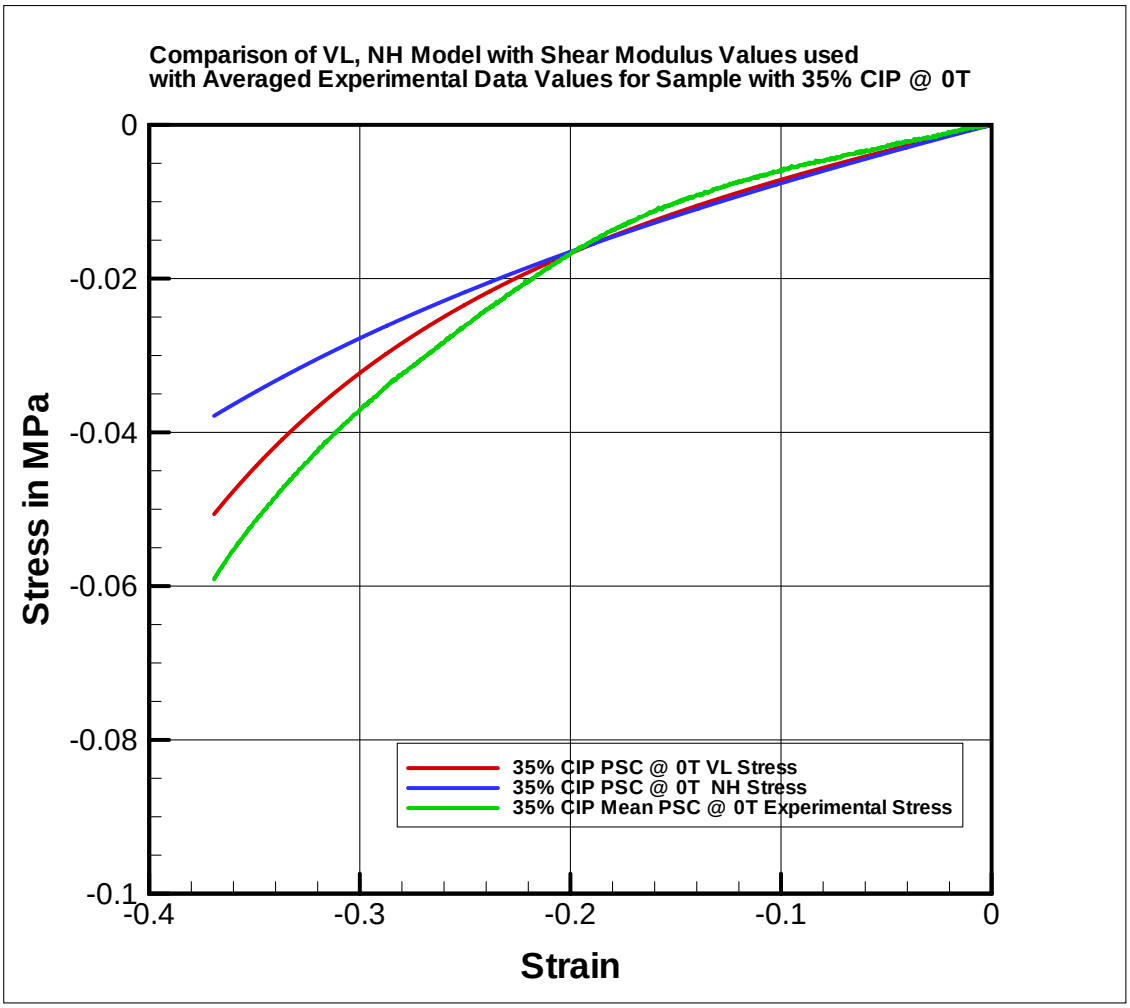

Fig. 93. Stress vs Strain Plot for Averaged Experimental Data, VL Model and NH Model Using Calculated Shear Modulus for Samples with 35% CIP at 0T

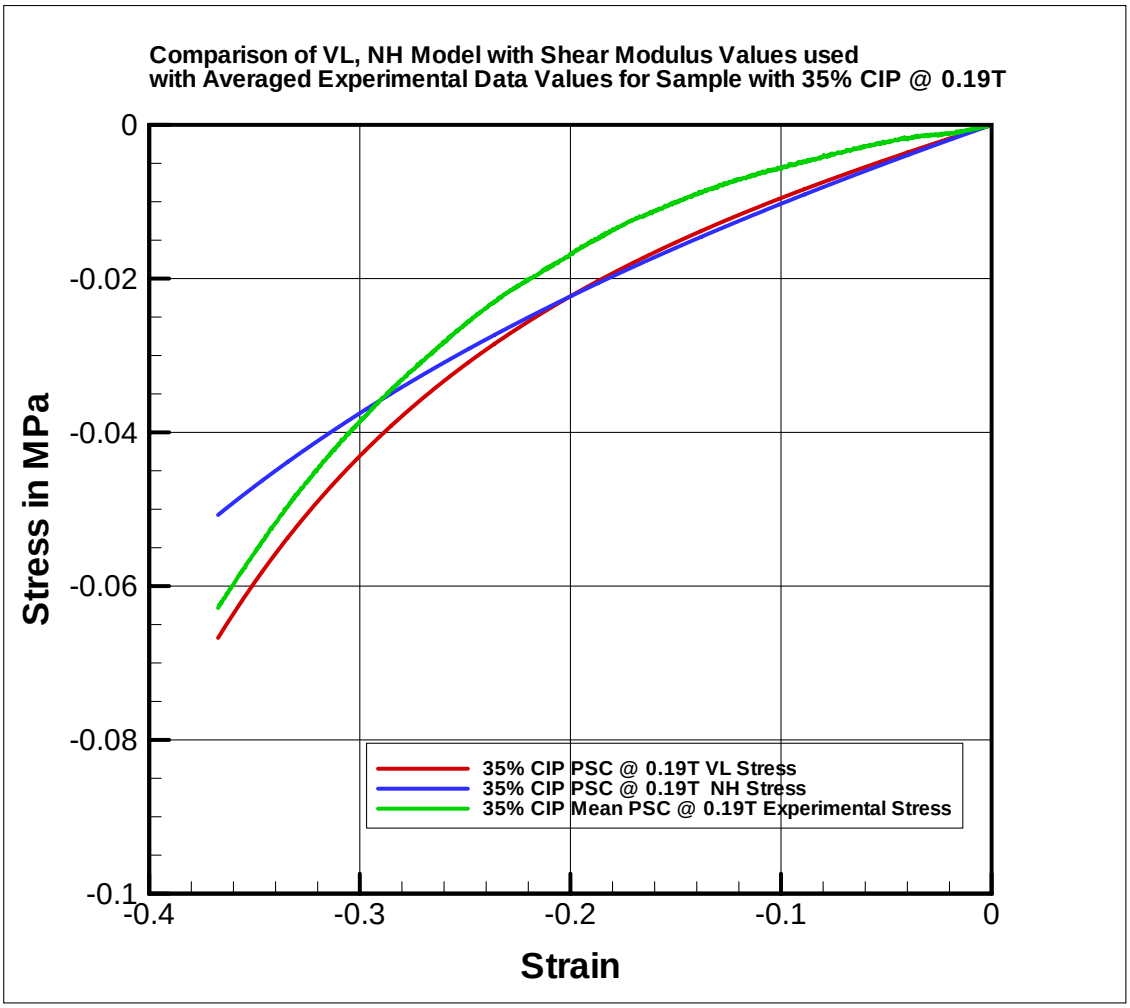

Fig. 94. Stress vs Strain Plot for Averaged Experimental Data, VL Model and NH Model Using Calculated Shear Modulus for Samples with 35% CIP at 0.19T

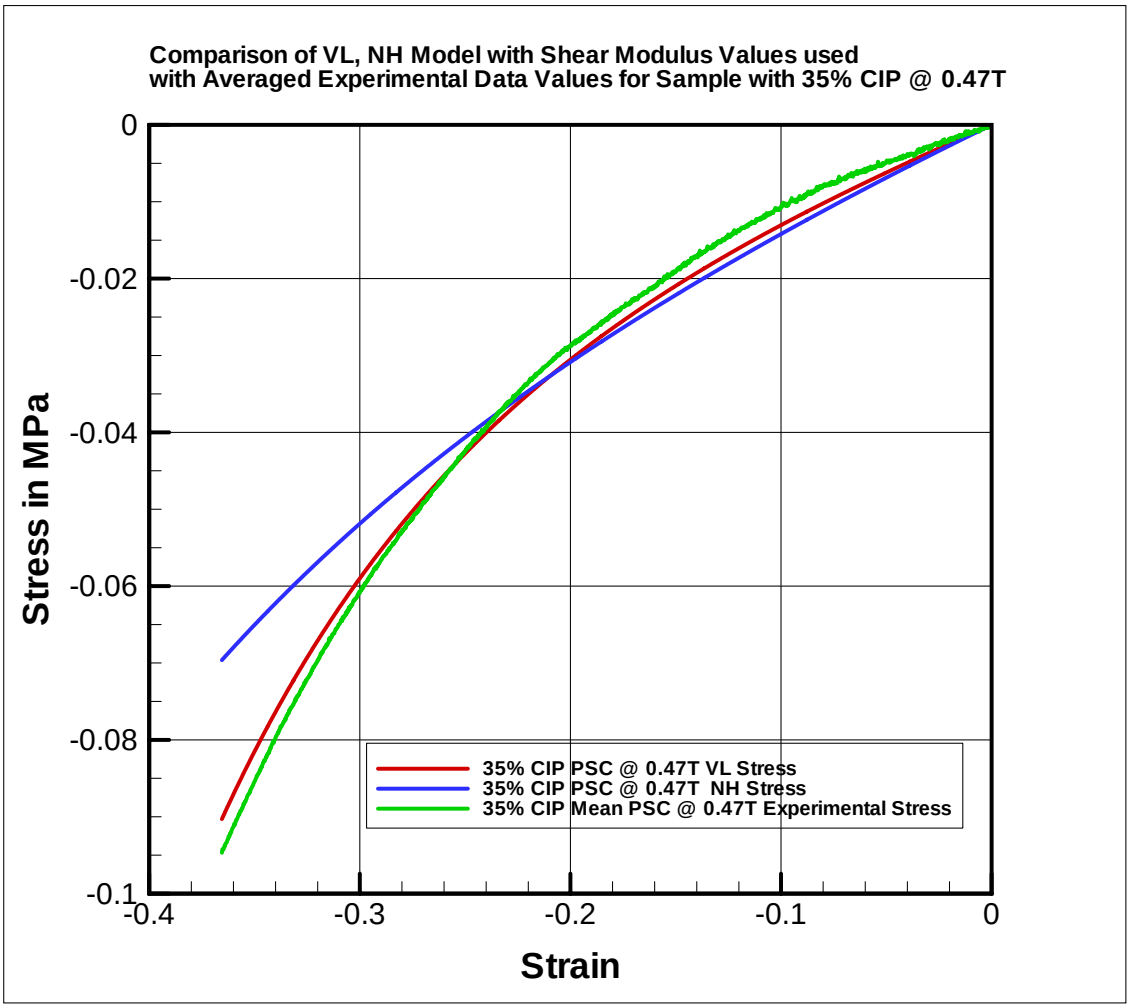

Fig. 95. Stress vs Strain Plot for Averaged Experimental Data, VL Model and NH Model Using Calculated Shear Modulus for Samples with 35% CIP at 0.47T

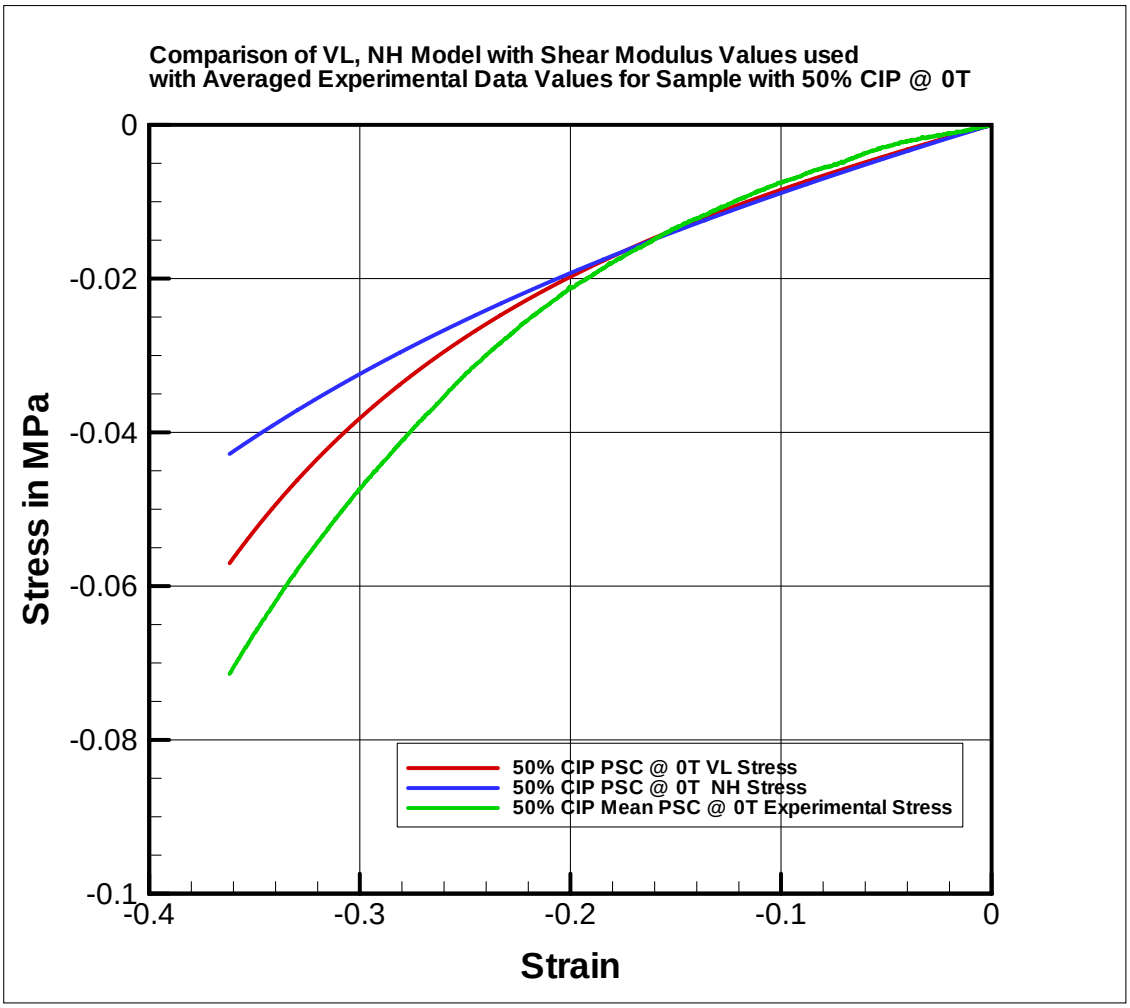

Fig. 96. Stress vs Strain Plot for Averaged Experimental Data, VL Model and NH Model Using Calculated Shear Modulus for Samples with 50% CIP at 0T

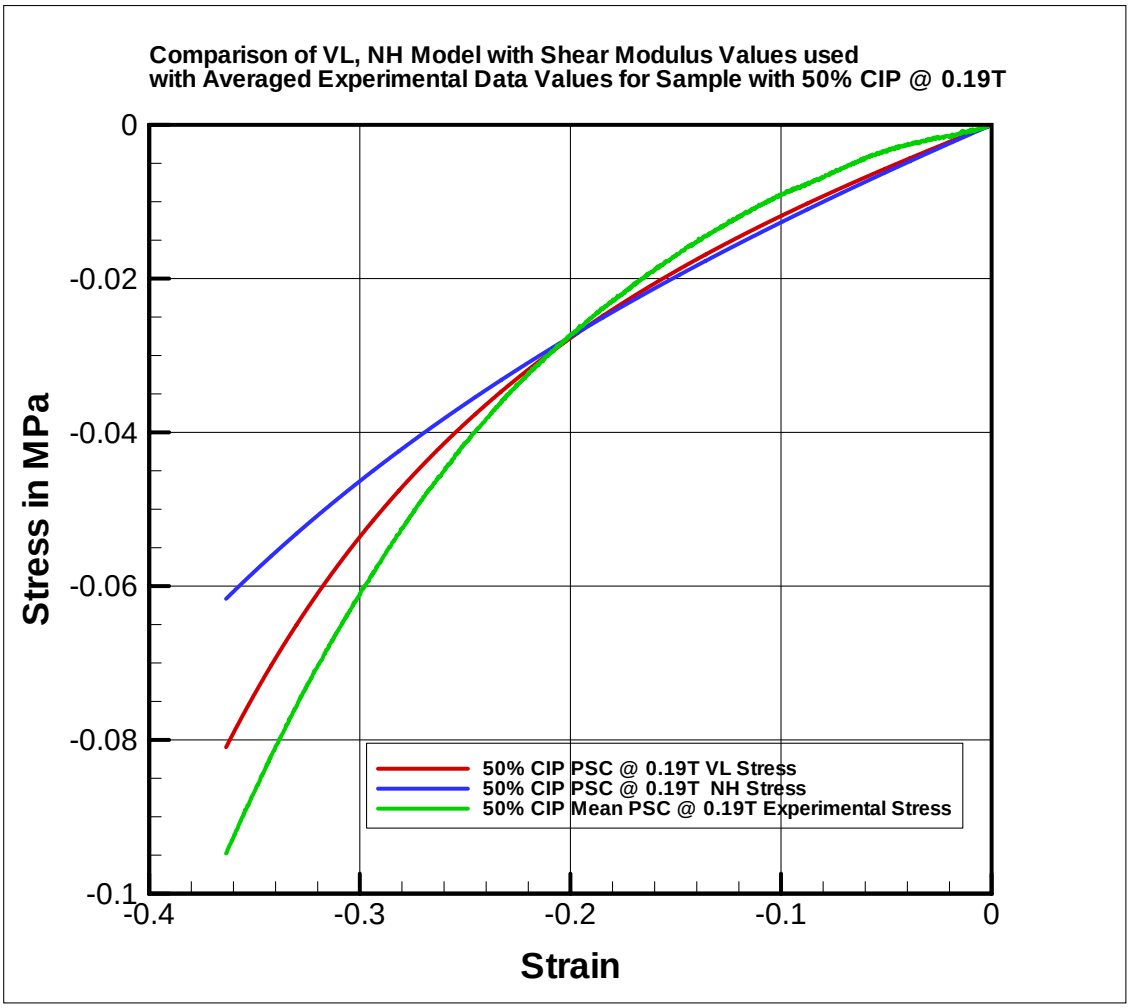

Fig. 97. Stress vs Strain Plot for Averaged Experimental Data, VL Model and NH Model Using Calculated Shear Modulus for Samples with 50% CIP at 0.19T

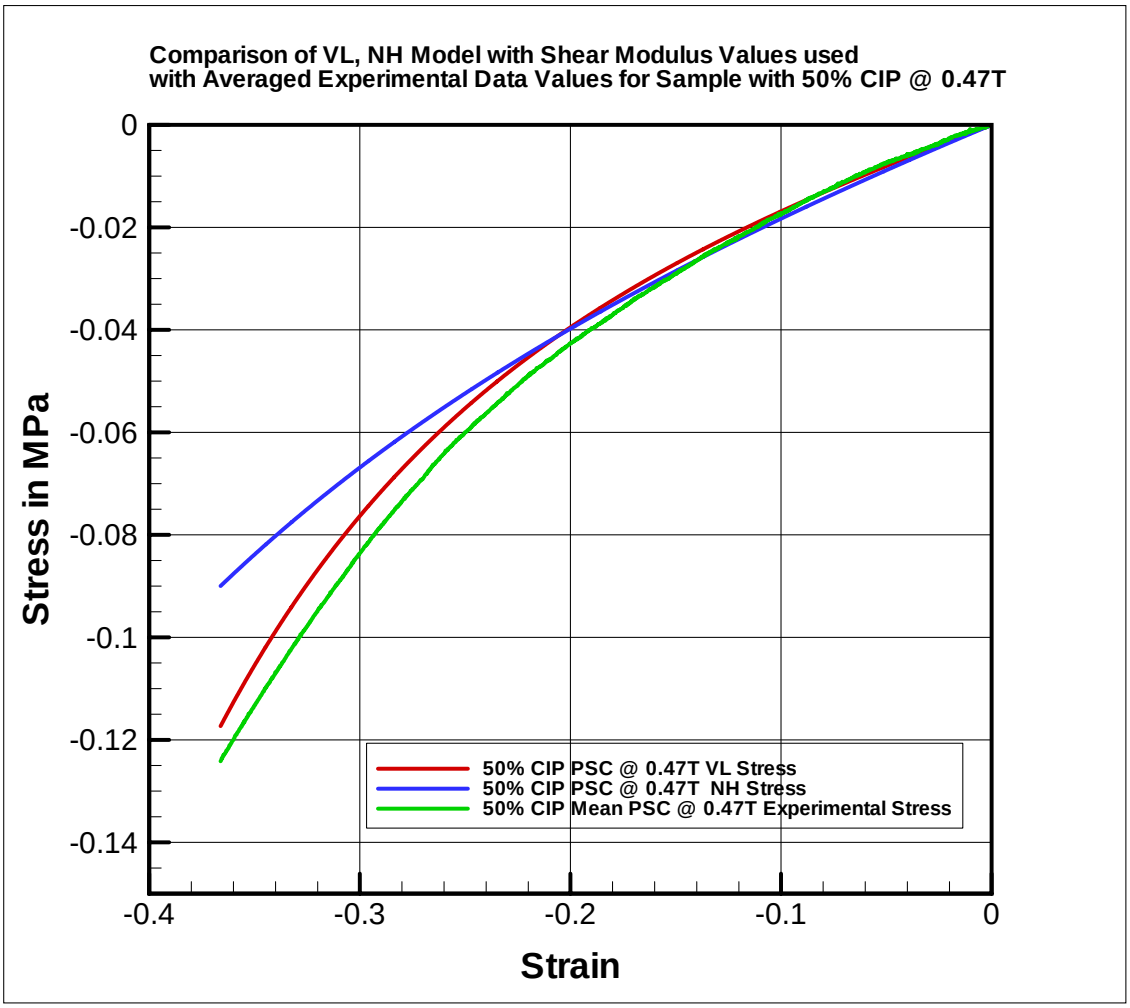

Fig. 98. Stress vs Strain Plot for Averaged Experimental Data, VL Model and NH Model Using Calculated Shear Modulus for Samples with 50% CIP at 0.47T

VITA

Jayadurga Iyer Ganapathi

Department of Mechanical Engineering,3123 TAMU

College Station TX 77843-3123

- **Email** jayadurga85@gmail.com

- **Education**
  - M.S, Mechanical Engineering, Texas A&M University, TX
  - B.Tech, Rubber and Plastics Technology, Anna University, India

The typist for this thesis was Jayadurga Iyer Ganapathi.